
Francisco Xavier Simões de Carvalho

# Immunometabolism modulation of $CD4^+$ T cells in Rheumatoid Arthritis

**Dissertação no âmbito do Mestrado em Biologia Celular e Molecular, orientada pela Doutora Maria Margarida Souto Carneiro e pelo Professor Doutor Rui de Albuquerque Carvalho e apresentada ao Departamento de Ciências da Vida da Faculdade de Ciências e Tecnologia da Universidade de Coimbra.**

Junho de 2020

# *Immunometabolism Modulation of $CD4^+$ T Cells in Rheumatoid Arthritis*

**Francisco Xavier Simões de Carvalho**

**Mestrado em Biologia Celular e Molecular**
Faculdade de Ciências e Tecnologia
Universidade de Coimbra


Junho de 2020

*"Em qualquer aventura,*
*O que importa é partir, não é chegar."*
**Miguel Torga, in 'Viagem'**
**'Câmara Ardente', 1962**

## Funding

The work and the consequent results analyses developed for this dissertation were performed under the supervision of Doctor Margarida Souto-Carneiro (OMZ, UH) and Professor Rui Carvalho (DCV, UC) at the Otto-Meyherhof Zentrum, in the laboratory of Professor Hanns-Martin Lorenz research group, Department of Internal Medicine V, Rheumatology, Universitätsklinikum Heidelberg, Germany.

The work presented here was funded by Deutsche Forschungsgemeinschaft under research grant SO 1402/1-1.

The Erasmus$^{+}$ mobility program has provided personal financial support for the project established period.




## Agradecimentos

Findo este ano trabalhoso, no qual não faltaram desafios e momentos de superação, venho deste breve modo agradecer a quem contribuiu de forma direta ou indireta para que o presente projeto possa ter sido concluído com sucesso.

À minha mãe, ao meu pai e ao meu irmão, tudo aquilo que poderia escrever nestas linhas seria escasso para lhes agradecer o apoio, a confiança e a dedicação que devotaram em mim não só neste ano que agora termina, mas também no meu restante percurso académico universitário que teve início há 5 anos. Obrigado por tudo.

À Gabriela, nunca será possível deixar materialmente escrito um justo agradecimento pelo amor e apoio demonstrados nos já longos anos nos quais partilhamos a nossa ainda jovem vida. Por toda a ajuda e confiança, por todos os esforços e conselhos dados, estarei eternamente grato. Obrigado por tudo.

À restante família e amigos que não se deixaram de preocupar e incentivar nesta particular aventura vivida no presente ano o meu sincero obrigado.

A nível científico, mas também pessoal, gostaria de expressar o meu especial agradecimento ao Professor Doutor Rui de Albuquerque Carvalho por me ter proporcionado as oportunidades que pude agarrar na minha ainda precoce vida académica e científica. O seu esforço e empenho, mas também o seu forte caráter e personalidade ficarão, sem qualquer dúvida, marcados para sempre na pessoa que sou e serei.

À Doutora Margarida Souto-Carneiro estarei sempre agradecido pela oportunidade que me proporcionou de trabalhar em Heidelberg de modo a desenvolver da melhor forma possível o presente trabalho. Obrigado por todos os ensinamentos, não apenas os científicos, mas também os pessoais e toda a disponibilidade e ajuda demonstrados em todo este período particularmente desafiante. Um agradecimento também especial ao Professor Doutor Hanns-Martin Lorenz por me ter aceitado no seu grupo de investigação em Heidelberg e pela simpatia sempre demonstrada.

Não poderia deixar de mencionar os colegas que colaboraram ativamente para que o trabalho desenvolvido no laboratório corresse da melhor forma. Um obrigado à Bárbara, à Franziska e à Katja por toda a ajuda proporcionada.

Indubitavelmente este trabalho não estaria de pé se o único a contribuir para ele tivesse sido eu. Obrigado a todos.

# Contents

## Acronyms and Abbreviations

| | |
|---|---|
| 2-NBDG | 2-(N-(7-Nitrobenz-2-oxa-1,3-diazol-4-yl)Amino)-2-Deoxyglucose |
| 2-DG | 2-Deoxyglucose |
| Ace | Acetate |
| Acetyl-CoA | Acetyl-Coenzyme A |
| ACPA | Anti-Citrullinated Protein Antibody |
| ADP | Adenosine DiPhosphate |
| AMP | Adenosine MonoPhosphate |
| ATM | Ataxia Telangiectasia Mutated kinase |
| ATP | Adenosine TriPhosphate |
| BCR | B Cell Receptor |
| C | Carbon |
| CFSE | Carboxyfluorescein Diacetate Succinimidyl Ester |
| CM | Central Memory |
| CNT | Control (healthy individuals) |
| $CO_2$ | Carbon dioxide |
| $D_2O$ | Deuterium Oxide |
| DAMP | Damage-Associated Molecular Pattern |
| DMSO | Dimethyl Sulfoxide |
| DNA | Deoxyribonucleic Acid |
| EDTA | Ethylene Diamine Tetra-acetic Acid |
| EM | Effector Memory |
| ETC | Electron Transport Chain |
| F2,6BP | fructose 2,6-biphosphate |
| FACS | Fluorescence-Assisted Cell Sorting |
| FCS | Fetal Calf Serum |
| Foxp3 | Forkhead box protein 3 |
| G6PD | glucose-6-phosphate dehydrogenase |
| GDH | Glutamate Dehydrogenase |
| Glc | Glucose |
| Gln | Glutamine |
| H | Hydrogen |
| IFN-γ | Interferon γ |
| IgA | Immunoglobulin A |
| IgD | Immunoglobulin D |
| IgE | Immunoglobulin E |
| IgG | Immunoglobulin G |
| IgM | Immunoglobulin M |
| IL-10 | Interleukin 10 |
| IL-13 | Interleukin 13 |
| IL-17A | Interleukin 17A |
| IL-17F | Interleukin 17F |
| IL-2 | Interleukin 2 |
| IL-21 | Interleukin 21 |
| IL-22 | Interleukin 22 |
| IL-26 | Interleukin 26 |
| IL-4 | Interleukin 4 |
| IL-5 | Interleukin 5 |
| IL-6 | Interleukin 6 |

| | |
|---|---|
| IL-9 | Interleukin 9 |
| JAK3 | Janus Kinase 3 |
| JC-1 | Tetraethylbenzimidazolylcarbocyanine Iodide |
| JIA | Juvenile Idiopathic Arthritis |
| Lac | Lactate |
| LDH | Lactate Dehydrogenase |
| MACS | Magnetic-Activated Cell Sorting |
| MHC | Major Histocompability complex |
| MS | Multiple Sclerosis |
| NADH | Nicotinamide Adenine Dinucleotide, reduced |
| NADPH | Nicotinamide Adenine Dinucleotide Phosphate, reduced |
| NK | Natural Killer |
| NMR | Nuclear Magnetic Resonance |
| Nstim | Non-stimulated |
| OAA | Oxaloacetate Acid |
| Oct | Octanoate |
| OXPHOS | Oxidative Phosphorylation |
| PAD | Peptidyl-Arginine-Deiminase |
| PAMP | Pathogen-Associated Molecular Pattern |
| PBMC | Peripheral Blood Mononuclear Cell |
| PBS | Phosphate-Buffered Saline |
| PD-1 | Programmed Death-1 |
| PDH | Pyruvate Dehydrogenase |
| Pen-Strep | Penicillin-Streptomycin |
| PEP | Phosphoenolpyruvate |
| PFK1 | 6-phosphofructo-1-kinase |
| PFKFB3 | 6-phosphofructo-2-kinase/fructose-2,6-biphosphatase 3 |
| PIKK | phosphatidylinositol-3-kinase-related kinase |
| PPP | Pentose Phosphate Pathway |
| PsA | Psoriatic Arthritis |
| RA | Rheumatoid Arthritis |
| RNA | Ribonucleic Acid |
| ROS | Reactive Oxygen Species |
| SDHA | Succinate Dehydrogenase A |
| SpA | Spondyloarthritis |
| Stim | Stimulated |
| T1DM | Type 1 *Diabetes Mellitus* |
| Tc | T cytolytic |
| TCA | Tricarboxylic Acid |
| TCR | T Cell Receptor |
| Tfh | Follicular Helper |
| Th | T helper |
| TNF-α | Tumor Necrosis Factor α |
| Treg | T regulatory |
| USA | United States of America |
| WHO | World Health Organisation |

## Abstract

The deeply characterization of the cells and components that mainly contribute to trigger and maintain the most undesirable pathologic states is of utmost importance to tackle those diseases towards total remission states and overcome patients suffering. Concerning Rheumatoid Arthritis (RA), an autoimmune chronic inflammatory disease, although the last few years have shown that our knowledge of this pathology is steadily increasing, our full dominance is far from being a reality.

One of the areas that has seen the most considerable advances in the recent years is the one of immunometabolism, which joins together both immunology and metabolism subjects, begin the ultimate aim the full characterization of our immune cells in a metabolic perspective towards being able to control these cells effector functions and, consequently, the pathologic states of the patients, using metabolic targets and metabolically driven therapeutic approaches.

Our study focuses its attentions in the capability of RA $CD4^+$ T cells to adapt their metabolism to distinct conditions available, ranging from normal glucose concentrations to low glucose availability, and tries to understand if these cells are capable of utilize fatty acids in the latter case, both to fulfil their energetic needs and to exert their cytotoxic functions.

The results suggest that $CD4^+$ T cells are not prone to utilize fatty acids, in scarce glucose availability, to fulfil their bioenergetic and cytotoxic functions, being that their viability and proliferation were also affected in these conditions. On the other hand, we could observe that the utilization of glucose by $CD4^+$ T cells is crucial to sustain their energetic requirements via aerobic glycolysis, being that their cytokine production was not affect in a certain range of glucose concentrations (down to 2 mM). Unexpectedly, concerning the $CD4^+$ T cells behaviour, we found just lesser differences when comparing healthy donors and RA patients.

Our findings could help to reformulate the current accepted paradigm about RA $CD4^+$ T cells metabolism, which states that these cells could be sustained by consuming only fatty acids and that glucose utilization is mainly done by a pentose phosphate pathway depend way. Overall, our results will contribute to the already crescent interest in $CD4^+$ T cells role, especially in the context of RA, and give scientific motivation to further characterize these cells immunometabolism.



**Keywords:** Immunometabolism; Autoimmunity; Rheumatoid Arthritis; $CD4^+$ T cells.

## Resumo

A caracterização detalhada das células e componentes que contribuem para despoletar e suster os estados patológicos mais indesejados é crucial para atingir a total remissão de doenças e suplantar o sofrimento dos pacientes. No que diz respeito à Artrite Reumatóide (AR), uma doença crónica inflamatória autoimune, apesar de nos últimos anos termos assistido a um crescimento considerável no conhecimento acerca dessa patologia, o nosso domínio da mesma está ainda longe de ser uma realidade.

Uma das áreas científicas que mais avanços teve nos últimos anos, nesta área do saber, foi o imunometabolismo, que congrega as disciplinas da imunologia e do metabolismo, sendo o seu objetivo primordial caraterizar as células imunes numa perspetiva metabólica de modo a permitir o controlo das suas funções efetoras e, consequentemente, do estado patológico dos pacientes, recorrendo a abordagens terapêuticas baseadas no metabolismo.

O presente estudo foca a sua atenção na capacidade das células $CD4^+$ T de pacientes com AR adaptarem o seu metabolismo às diferentes condições providenciadas, que vão desde concentrações normais de glucose até à escassa disponibilidade da mesma, tentando perceber se, no último caso, estas células são capazes de utilizar ácidos gordos, quer para suster as suas necessidades energéticas, quer para exercer as suas funções citotóxicas.

Os resultados obtidos sugerem que, em situações de baixa disponibilidade de glucose, as células $CD4^+$ T não estão propensas a utilizar os ácidos gordos para suprir as suas necessidades bioenergéticas e citotóxicas, sendo que a sua viabilidade e proliferação são também significativamente afetadas nessas condições. Por outro lado, foi observado que a utilização de glucose pelas células $CD4^+$ T é crucial para suster os seus requisitos energéticos por via da glicólise aeróbica, sendo que a sua produção de citoquinas não foi afetada dentro de um certo limite de concentração de glucose (até 2 mM). Inesperadamente, no que respeita ao comportamento das células CD4+ T, as diferenças observadas entre o grupo dos indivíduos saudáveis e o dos pacientes com AR foram mínimas.

As nossas descobertas podem ajudar a reformular o atual paradigma atribuído ao metabolismo das células T $CD4^+$ na AR, que sugere que estas células se podem sustentar recorrendo apenas a ácidos gordos e que a utilização de glucose é feita principalmente pela via das pentoses-fosfato. Em suma, os nossos resultados contribuem para o já

crescente interesse no papel das células $CD4^+$ T, especialmente no contexto da AR, e dar motivação científica para caraterizar ainda mais detalhadamente o imunometabolismo destas células.

**Palavras-chave:** Imunometabolismo; Autoimunidade; Artrite Reumatóide; Células T $CD4^+$.

# 1 Introduction

Since ever the humankind is fascinated by the creation and destruction of matter and energy, which is patent from the time humans managed to create fire to the most recent chemical industry. About 2500 years ago, in the ancient Greece, there was already the idea that nothing could be created or destroyed and, since then, two new concepts started to be widespread through the scientific/philosophic community: there was a mix of pre-existing things instead of pure creation and there was a separation in components instead of total destruction of something. These notions, attributed to Anaxagoras (c. 510 – c. 428 BC) and then worked over the years by philosophers and natural philosophers, nowadays entitled scientists, were eternalized by Antoine Laurent Lavoisier (1743 – 1794) in the so-called Law of Conservation of Mass that enunciates that "in a chemical reaction, matter is neither created or destroyed" (Lavoisier, 1785). In the same way, the Law of Conservation of Energy, normally associated with the First Law of Thermodynamics, which first most complete enunciation is attributed to Rudolf Clausius in 1879 postulates that "energy can neither be created nor destroyed - only converted from one form of energy to another" (Campbell *et al.*, 2018). It is based in this constant dynamism between the chemical substances and compounds and energy that Nature works, thus being the Biology totally grounded by Chemistry, being this latter one supported by Physics which have his plausibility founded in Mathematics. This intimate relationship between the biological and chemical fields lead to the creation… excuse me… to the birth of Biochemistry and, more specifically, to the insurgence of Metabolism.

Metabolism (from the Greek *metabole*, "a change") is a notion that was firstly developed and used in the late 19$^{th}$ century in the physiology field (https://www.etymonline.com/word/metabolism) and it is improbable to find another concept that reflects better the idea expressed in the laws of Conservation of Mass and Conservation of Energy. Biologically, we are constantly observing a symphonic molecular dynamism inside the cells that is the reflection of intermolecular conversion and energy emission and absorption routines. Ranging from the most primordial and basic unicellular organisms, such as bacteria, to the eukaryotic cells that form the most complete organisms (*Homo sapiens* included), it is inevitable to notice the communication network established between the different cellular organelles. Without access to Wi-Fi connection, these cooperative cellular interactions were established

through the production of molecules and ions that, all together, orchestrate the cell functions and adapt the organism to the constant energetic disequilibrium, the fundamental trigger to the metabolic engine. Thus, the ultimate goal of this archaic combustion system called metabolism is to regulate and control the biochemical machinery that, in a constant imperfect symbiosis, and form the organisms as we know them.

In the human organism, as well as in other vertebrates, one of the components of this machinery is the immune system. This system is ultimately linked to the response and defense of our organism against external agents' threats (e.g. bacteria or viruses) and, in recent decades, has been extensively studied due to the increasing frequency of autoimmune diseases. In this perspective, it is of utmost importance to know how this system works and, not less important, to understand how we can shape and conduct the immune responses in our favor, boosting a rapid and strong action when talking about viruses infections or, in reverse, to stop the unwished reactions that occur in the autoimmune pathologies or in allergic reactions. The best way to do so, is to focus our attention in each specific components and participants of these responses, mainly the immune cells like B and T cells or macrophages. And, after knowing the cellular agents that are involved in these unwanted procedures, how can we control their actions and interactions? Probably by managing their energetic fluxes, by promoting changings in their intermolecular conversions and communication systems, and most probably by modulating their metabolism. It is based in these assumptions and in the desire of metabolic modulation of the immune system that a new field of research has recently emerged, the immunometabolism.

The present work focuses in the immunometabolism of $CD4^+$ T cells in the specific context of an autoimmune chronic disease: Rheumatoid Arthritis (RA). But, before making a deep diving in the $CD4^+$ T cells immunometabolism modulation, some basic and succinct concepts need to be provided, starting with those associated with metabolism.

## 1.1 Metabolism and energy

All the processes that occur in the universe in one way or another are, with no exception, intrinsically connected to energy. Chemical reactions could be divided in two major groups when talking about the energetic balance: the exergonic reactions, that liberate free energy, and the endergonic reactions, that are energy-requiring processes

(Nelson and Cox, 2009). In biological reactions the molecule that is usually linked to energy is ATP (Adenosine TriPhosphate), whose breakage of phosphoanhydride bonds leads to the formation of ADP (Adenosine DiPhosphate) and then AMP (Adenosine MonoPhosphate) and to the release of free energy. ATP, ADP and AMP molecular structures are represented in **Figure 1**. These ATP molecules, and also GTP (Guanine TriPhosphate), could be considered the main sources of energy of the cells and so, one of the major players in cellular bioenergetics. In metabolism, exergonic reactions are usually referred as catabolic, that is, processes that lead to degradation of molecules and liberation of energy, being this type of reactions also connected to the release of the so-called reducing equivalents such as NADH and NADPH. These molecules can function as electron donors in processes associated with the production of ATP (such as the Mitochondrial Electron Transport Chain) or be a fundamental part in reductive steps in biosynthetic pathways (Nelson and Cox, 2009). This latter referred processes were considered anabolic reactions, usually consuming ATP and, in this way, are endergonic reactions. Metabolism is no more and no less than a fluent and dynamic interplay between this energy releasing reactions (catabolism) and energy demanding reactions (anabolism). It is the tentative of reaching the impossible state of equilibrium between these two types of processes that fuels our cells cooperative behavior and makes our body work.

But how, in more detail, the energy is extracted and used by the cells?

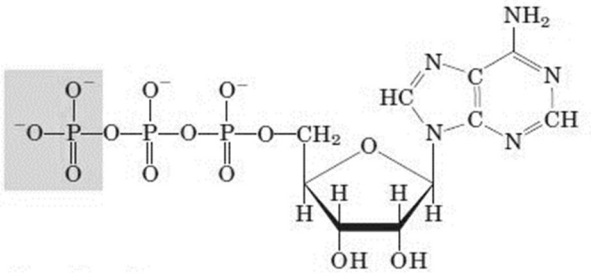

**Figure 1** - Representation of the chemical structure of ATP molecule (Adapted from Nelson and Cox, 2009).

### 1.1.1 Fundamental metabolic pathways

When talking about nutrients, the first thing that comes into our mind is carbohydrates. It is true that Glucose, for most types of cells, is a major energy-yielding nutrient (Nelson and Cox, 2009), but our cells are also capable of generating energy using other types of substrates including amino acids (e.g., glutamine) or fatty acids (e.g., palmitic acid). Cells are capable of driving each of these energy sources through various

metabolic pathways that will fulfill their bioenergetic and biosynthetic needs. In this way, glucose could be driven to either glycolytic pathway or pentose phosphate pathway (PPP), being the first one utilized, in basic terms, to provide energy and reducing equivalents, and the latter one normally utilized to provide new bio-materials (eg., NADPH and (deoxi)ribose phosphate) that support cell growth and proliferation. The glycolytic pathway could then end in the so-called aerobic glycolysis, a process known as Warburg Effect, were lactate is produced even in the presence of normal oxygen levels, or follow through the production of Acetyl-CoA from Pyruvate, feeding the Tricarboxylic Acid Cycle (TCA Cycle, also known as Krebs Cycle). **Figure 2** provides a schematic representation of these metabolic processes. In a first analysis it could launch a brain-storming feeling at our minds, but we should focus on how interesting it is to see the molecular dynamism in cellular metabolism, being quite similar to a big metropole road-map: confusing, but functional and objective, especially to the daily users.

As aforementioned, glucose could be metabolized to pyruvate, via glycolysis, and this pyruvate could divert for both Krebs cycle, by the production of Acetyl-CoA (reaction catalyzed by Pyruvate Dehydrogenase) or, instead, be converted to lactate with the catalytic help of Lactate Dehydrogenase (LDH) enzyme. Both catabolic pathways generate energy, but the utilization of the TCA Cycle, followed by the respective Mitochondrial Respiratory Chain utilization of the generated reducing equivalents, produce extra ATP molecules, being a much more efficient process when talking about energy generation, having a total net yield of (30)32 ATP molecules per molecule of glucose (Lunt and Vander Heiden, 2011). On the other way, the lactate production from glucose, via aerobic glycolysis, has a total net yield of 2 ATP molecules per molecule of glucose (Vander Heiden et al., 2009; Lunt and Vander Heiden, 2011). Taking this into account, we have a (15)16-fold difference, regarding the net ATP production, in favor of TCA Cycle/Mitochondrial Respiration. So, what makes possible that such an apparent most efficient flux is in reality, in some occasions, belittled in favor of Aerobic Glycolysis? As it will be explained in the next sub-section, it may be just a matter of velocity… and something else.

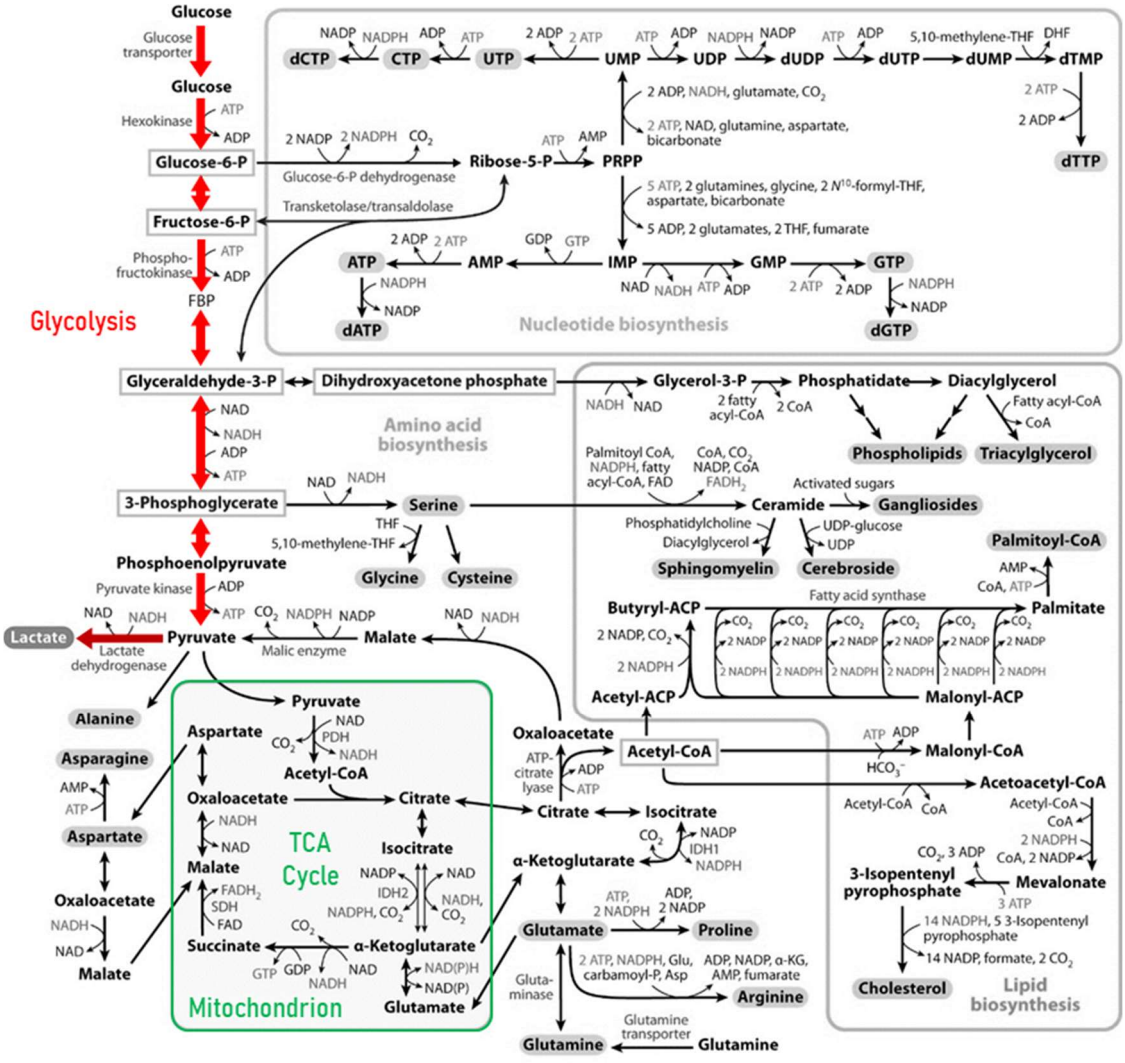


**Figure 2** - Representation of the principal cellular metabolic fluxes: an overpopulate dynamic organization. Particular emphasis is given to glycolytic pathway and TCA cycle. (Adapted from Lunt and Vander Heiden, 2011). Abbreviations: ACP (Acyl carrier protein); ADP (Adenosine diphosphate); Asp (Aspartate); ATP (Adenosine triphosphate); CoA (Coenzyme A); CTP (Cytidine triphosphate); dATP (Deoxyadenosine triphosphate); dCTP (Deoxycytidine triphosphate); dGTP (Deoxyguanosine triphosphate); DHF (Dihydrofolate); dTMP (Deoxythymidine monophosphate); dTTP (Deoxythymidine triphosphate); dUDP (Deoxyuridine diphosphate); dUMP (Deoxyuridine monophosphate); dUTP (Deoxyuridine triphosphate); FAD (Flavin adenine dinucleotide); $FADH_2$ (Flavin adenine dinucleotide, reduced; Glu (Glutamate); GMP (Guanosine monophosphate); GTP (Guanosine triphosphate); IDH1 (Isocitrate dehydrogenase 1); IDH2 (Isocitrate dehydrogenase 2); IMP (Inosine monophosphate); NAD (Nicotinamide adenine dinucleotide); NADH (Nicotinamide adenine dinucleotide, reduced); NADP (Nicotinamide adenine dinucleotide phosphate); NADPH (Nicotinamide adenine dinucleotide phosphate, reduced); P (phosphate); PDH (Pyruvate Dehydrogenase); PRPP (Phosphoribosyl pyrophosphate); SDH (Succinate dehydrogenase); THF (Tetrahydrofolate); UDP (Uridine diphosphate); UMP (Uridine monophosphate); UTP (Uridine triphosphate); α-KG (α-Ketoglutarate).

### 1.1.2 High-proliferative cells' metabolism

High-proliferative cells, that is, cells with a greatly activated metabolism, is almost synonym of signifying cancer cells, although, they are not exclusive members of this group and we could also be talking about immune cells in a specific context such as immune response. But for now we could center our attention in the most famous members of high-proliferative cells, since it was in cancer cells that aerobic glycolysis was firstly described in 1926 by Otto Warburg and his colleagues (Warburg *et al*., 1926), being the process named as Warburg Effect, as aforementioned. Until that time the production of lactate was only admitted to exists in hypoxic environments, that is in low-oxygen conditions, being known to occur both in yeast and in mammals' muscle cells, being the process named lactic fermentation.

Warburg discoveries launched the suspicion that lactate production was more than just a last opportunity energy resource, especially in cells that, due to the presence of oxygen, could easily utilize other metabolic fluxes, such as TCA cycle coupled with oxidative phosphorylation, that were more interesting in a purely bioenergetic perspective. In last decades the interest in aerobic glycolysis increased, certainly in accordance with the also exacerbated awareness about the cancer pathological development and its negative impact in our society. Some plausible theories about the reasons that lead the cells to utilize aerobic glycolysis were raised, but not all proved their veracity. One example, that was actually also proposed and supported by Otto Warburg, was the idea that cancer cells increase their lactate production because their mitochondrial machinery was somehow defected and dysfunctional or even partially or totally depleted, being the mitochondrial metabolism impaired (Gogvadze *et al*., 2010). Although being an attractive theory and in some specific cancer cells has actually been observed by the down-regulation of the catalytic subunit of mitochondrial ATP synthase (Gogvadze *et al*., 2010), it was proven wrong in the vast majority of cancers and other high-proliferative cell types, since the mitochondrial structures from these cells were found not to be defective and totally functional (Gogvadze *et al*., 2010; Lunt and Vander Heiden, 2011). Thus, the utilization of aerobic glycolysis seems to be an objective and a non-forced choice of high-proliferative cells.

One of the principal reasons that support the increased glycolytic flux in these cells may be, without doubt, the velocity of development of this pathway, being 10-100 fold-times faster than the full oxidation of glucose through TCA cycle and consequent Mitochondrial Respiratory Chain (Liberti and Locasale, 2016). So, despite being a lower

efficiency process in terms of ATP production, aerobic glycolysis is a highly valid energy-obtaining flux due the velocity at which it could occur, providing there is no shortage in substrate supply.

Although, it should be stated that highly proliferative cells do not shut-down the mitochondrial metabolism, quite the contrary. TCA cycle and oxidative phosphorylation are also exacerbated, being in a significant number of cases the major cell's ATP provider (Lunt and Vander Heiden, 2011). It has been shown that, in plenty cancer cell lines and tissues, the glycolytic contribution for the total ATP production is in average 17%, with a variable range that is highly dependent on the cell context (Zu and Guppy, 2004). Thus, oxidation phosphorylation remains the main contributor for the energetic production in proliferative cells and so the ATP production is not, for sure, the main objective when they exacerbate the aerobic glycolysis flux. Hence, the question is: why maintain the glycolytic flux activated and even increased in such a large scale in proliferative and replication situations if the cells do not depend on this pathway to be energetically proficient? The answer to this question will most probably be linked to the exacerbated biosynthetic needs of these proliferative cells.

Cell proliferation and division requires not only energy, but also macromolecular synthesis for replication of the cell contents of DNA, RNA, proteins and lipids molecules (Lunt and Vander Heiden, 2011) that will enable a single cell to form two daughter cells. These macromolecules are constituted by small blocks such as nucleotides (for DNA and RNA) or amino acids (for proteins) that are mainly produced using precursors provided by the glucose molecule when it is metabolized in the glycolytic pathway (glycolytic intermediates), or through the Pentose Phosphate Pathway (PPP). In this way, maintaining a high glycolytic flux will provide the material needed for cell proliferation and duplication, being possible at the same time some energy production *(Vander Heiden et al*., 2009). For a comprehensive understanding an analogy between the glycolytic flux and the stream of a river could be made. When in the flood season, the river will have his maximum amount of water running into its riverbed and the brooks that derive from this river to feed agricultural cultivations will be completely full, enhancing the productivity of the peasants. On the contrary, when the stream in the river is low, the referred brooks will run out of water and will dry, being the cultures affected. This is what happens with the glycolytic flux and the biosynthetic pathways associated with it: when the cells have an exacerbated glycolysis, there will be an increased production of glycolytic intermediates that are used in biosynthetic pathways, thus supporting cell proliferation.

For the biosynthesis of main structural lipids in cell membranes such as phospholipids and triacylglycerols it could be used the glycolytic intermediate glycerol-3-phosphate (Lunt and Vander Heiden, 2011). Glucose, in addition to glutamine, could be used as a carbon source to form both purine and pyrimidine nucleotides in the PPP, central components of nucleic acids, and some glycolytic intermediates, like pyruvate and 3-phosphoglycerate, are potential precursors of some amino acids such as alanine and serine plus glycine, respectively (Lunt and Vander Heiden, 2011). In addition to this, the higher glycolytic flux also contributes to higher PPP activity, leading to the generation of high quantities of NADPH, a very important element in several biosynthetic routines, including *de novo* lipid synthesis (Liberti and Locasale, 2016). Altogether, we can conclude that an exacerbated aerobic glycolysis constitutes in fact a high-efficiency mechanism to support cell proliferation.

Following glucose, or even at the same level of importance for cell proliferation, we have glutamine. This amino acid, the most abundant in human plasma, is also a major contributor to produce biomass precursors and, at some point, it could be defined as more essential for cells than glucose due to the presence in this substrate of an amino group, and more specifically of nitrogen atoms, that support the production of nucleotides, amino acids and hexoamines (used in the glycosylation of proteins and as lipid precursors) (Vander Heiden, Cantley and Thompson, 2009; Lunt and Vander Heiden, 2011). In addition to contributing to fatty acid biosynthesis through the generation of acetyl-CoA or by the reductive carboxylation of derived α-ketoglutarate, glutamine could also be converted to glutamate, through deamination reactions, providing amino groups required in the synthesis of non-essential amino acids.

The utilization of glutamine goes further more than just providing biomass precursors as it can also be metabolized to produce energy and reducing equivalents as well as glutathione that protects cells against oxidative stress (Lunt and Vander Heiden, 2011). Since it could easily fuel the TCA cycle, glutamine is an important contributor to fuel the oxidative phosphorylation, supporting the cellular ATP production by generating TCA cycle intermediates (Lunt and Vander Heiden, 2011). In addition, glutamine could be also metabolized to form lactate, being this process known as glutaminolysis (see **Figure 2**). In this process, beyond producing a net value of up to 6,5 ATP per molecule of glutamine (if coupled with mitochondrial oxidative chain), the conversion of malate to pyruvate by the malic enzyme, that is one the glutaminolysis steps, produces 1 molecule

of NADPH and, as aforementioned, this reducing equivalent is extremely important to support the biosynthetic needs of proliferative cells (Lunt and Vander Heiden, 2011).

Overall, glucose and glutamine are the main contributors to the sustenance of high-proliferative cells, not only when speaking about energy needs but also as carbon sources to biosynthesis purposes (**Figure 3** summarizes this idea).

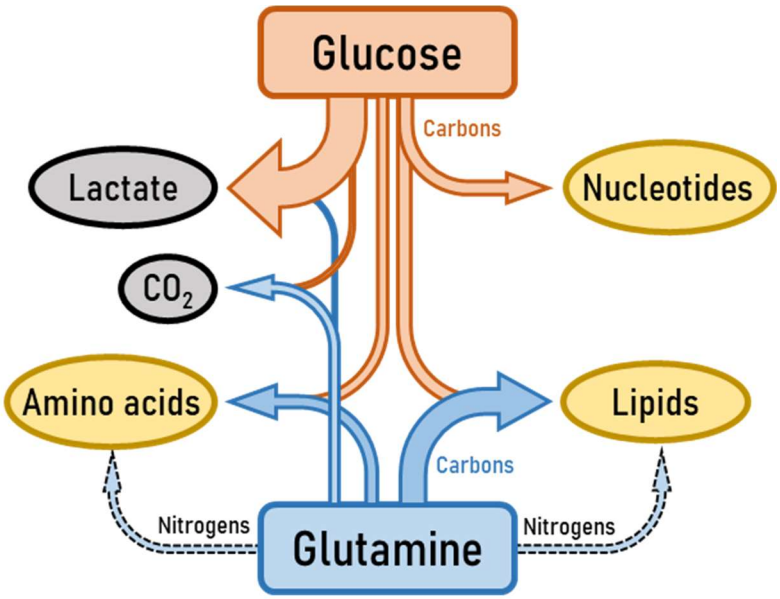


**Figure 3** - Representation of the contributions of glucose and glutamine to cells sustenance and proliferation (Adapted from Lunt and Vander Heiden, 2011).

In the context of an immune system response, both $CD4^+$ and $CD8^+$ T cells could be regarded as high-proliferative cells since they are engaged in an intensive replication, known as clonal expansion, and effector mechanisms that sustain the immunological response. These cells, in specific $CD4^+$ T cells, the major players in this research work, share some metabolic characteristics with cancer cells, being highly metabolic activated cells, but also represent some specific peculiarities. Before looking in more detail to the $CD4^+$ T cells metabolism, it is of the utmost importance to provide or remind the reader about some basic concepts of Immunology that will ground the future discussion. Let's talk about the immune system and its main components and dynamics.

## 1.2 The immune system

In our organism the immune system is responsible to combat the infectious agents and their respective actions, recovering the homeostasis that was lost in the time of invasion (Parkin and Cohen, 2001; Owen *et al.*, 2012). The designation of this incredibly complex system, derives from the Latin word *immunitas* (means "freedom from"), and comprises a complex array of molecules, cells and tissues that lead to the recognition and elimination of infectious agents, as well as tumor and apoptotic cells (Reuschenbach, *et al.*, 2009; Owen *et al.*, 2012; Quintin *et al.*, 2014). This system, in vertebrates, could be divided in two major parts with distinct but integrated and balanced strategies: the innate and the adaptive immune system (Parkin and Cohen, 2001; Owen *et al.*, 2012; Yatim and Lakkis, 2015).

Before specifying the rules of these complementary instruments, it is of utmost importance to remember that our first lines of defense against infectious agents are constituted by the skin or mucus, which compose the so-called external barriers. The immune system cellular elements just act after the unwanted agents cross these barriers, and that is the reason why it is so important to disinfect the region of a cut or a wound after it happens in the skin, that is, after one of the barriers has been damaged for some reason. These external barriers could be considered the first line of defense of the innate immune system and after an infectious agent crosses the skin or the mucous, the second line of defense takes the lead, that is, the leukocytes cells population of the innate immune system begin their action (Parkin and Cohen, 2001; Owen *et al.*, 2012; Delves *et al.*, 2017).

### 1.2.1 The innate immune system

As mentioned above, as the pathogen gets into our organism, the innate immune system is the first to come into action, being the responsible for triggering the activation of the adaptive immune system, especially when an unknown agent is introduced in to the organism (Quintin *et al.*, 2014; Delves *et al.*, 2017). The second line of defense (being the external barriers considered the first ones) is composed of soluble factors such as bactericidal enzymes and cells like macrophages or neutrophils, having as major objective kill the infiltrated infectious agent as soon as possible by destruction or phagocytosis, respectively, avoiding any negative impact to the organism. This action is triggered by the recognition of some invariant structures like PAMPs (pathogen-associated molecular pattern) or DAMPs (damage-associated molecular pattern) done due to the presence in

these innate cells of conserved PAMP receptors (PRRs) capable of recognizing highly conserved features presented by the common pathogens (Owen *et al.*, 2012; Quintin *et al.*, 2014).

More specifically, the referred second line of innate immune system is composed by cells derived by myeloid progenitor (macrophages, mast cells, neutrophils, eosinophils and basophils), being the natural killer (NK) cells the only lymphoid derived cells of this group of innate immune system agents (Parkin and Cohen, 2001; Owen *et al.*, 2012). The bridge between the two immunity contexts, innate and adaptive, is mainly established by another type of myeloid-derived cells called dendritic cells, being this relationship represented in **Figure 4** (Owen *et al.*, 2012; Carvalheiro, 2014). Although being part of the innate immune response, NK cells are also recognized as a bridge between both immunity contexts by inducing B cells activation (Parkin and Cohen, 2001; Owen *et al.*, 2012). Both lymphoid and myeloid progenitor cells derive from the pluripotent hematopoietic stem cells localized in the blood marrow, being the adaptive agents, B and T cells, beside the already referred innate NK cells, originated by the lymphoid progenitors (Owen *et al.*, 2012). The myeloid progenitors are also predecessors of other crucial blood components: erythrocytes and platelets, derived from megakaryocytes and erythrocytes progenitors, respectively (Parkin and Cohen, 2001; Owen *et al.*, 2012).

As depicted before, cells like macrophages, mast cells and dendritic cells act as a first intervention team and could counter-attack the infectious agent using processes such as phagocytosis (by macrophages and neutrophils). They can also influence and mediate further immune responses through the releasing of soluble factors such as cytokines, chemokines and vasoactive amines that will demand additional help to the site of infection (namely the adaptive immunity elements) (Parkin and Cohen, 2001; Owen *et al.*, 2012). These innate immune responses are rapid, being done in the space of minutes after the infectious agent enters the organism, what contrasts with the response done by the adaptive system that could hold up to a few days after infection. This delayed action is the reflection of the specificity inherent to the latter one, where a variety of membrane receptors highly specific to recognize a certain pathogen are produced in the cells that composed the adaptive response. The presentation of the antigen to the adaptive immune system cells is done by some innate cells called antigen-presenting cells (usually dendritic cells or macrophages) (Owen *et al.*, 2012; Delves *et al.*, 2017) being this process represented in **Figure 5**.

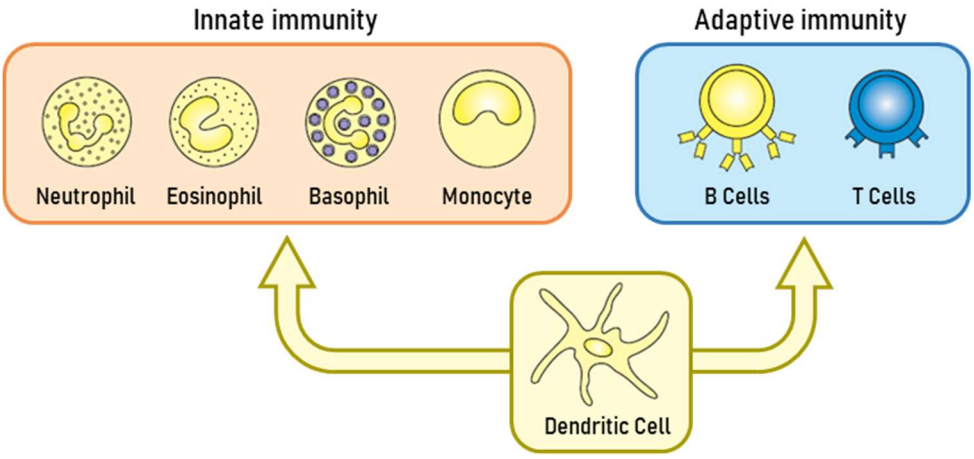


**Figure 4 -** Representation of the innate and adaptive immune cells. The dendritic cells function as a bridge between both immune contexts (Adapted from Murphy and Weaver, 2017).

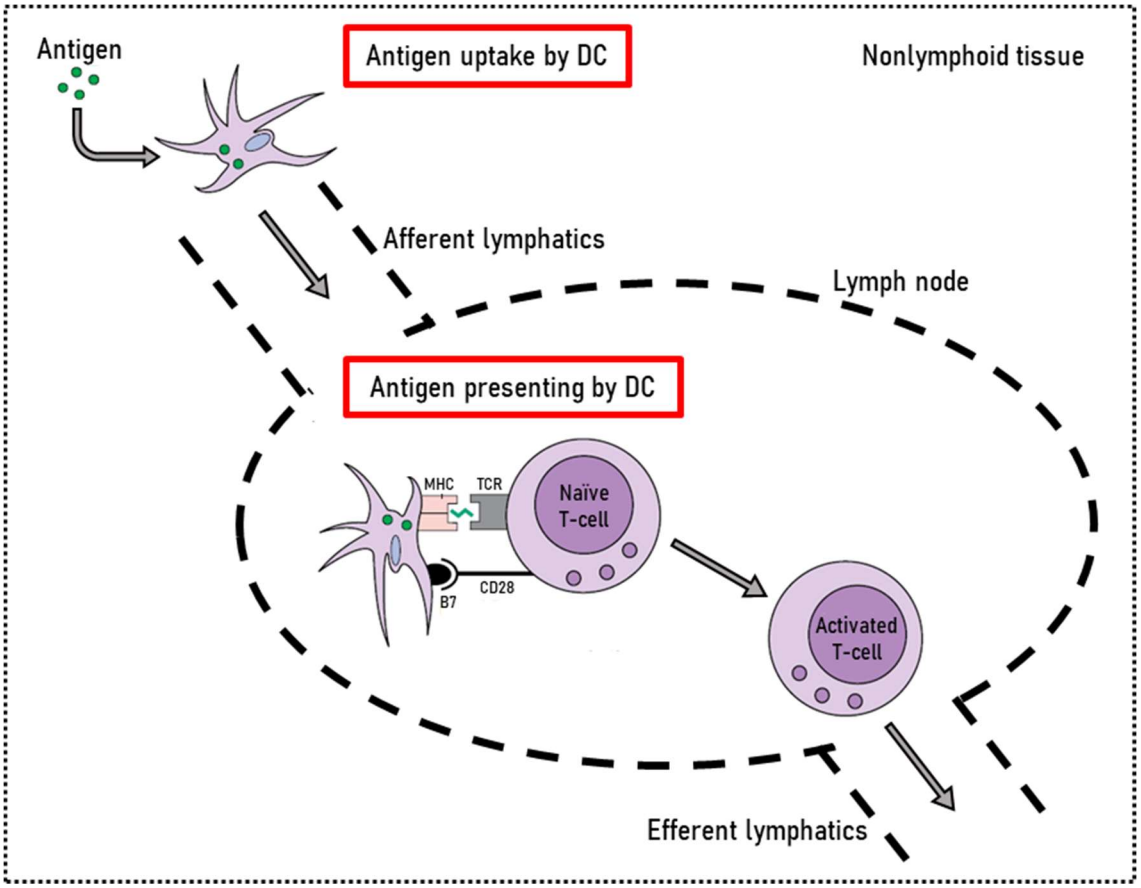


**Figure 5 -** Representation of a possible way of antigen presentation to T cells by dendritic cells (Adapted from Delves *et al*., 2017). Abbreviations: DC (Dendritic cells).

### 1.2.2 The adaptive immune system

The adaptive immune system is composed by T- and B-lymphocytes, being that both of these cells are derived from lymphoid progenitors. The lymphocytes represent approximately 20-30% of the leukocyte population, that is, of the total immune cells in the organism. These cells have the special ability to generate highly specific surface receptors by a process of genetic recombination based on particular molecular structures that, in this case, are the antigens (Delves *et al.*, 2017). As mentioned before, these antigenic structures are presented to the adaptive elements by the antigen-presenting cells. The receptors produced by T cells (T-cell receptors, TCRs) and B cells (B-cell receptors, BCRs) could, due to the randomization inherent to genetic recombination process, be specific for both non-self or self-antigens which in the latter case will guide the immune system to attack our own tissues, a negative impact mechanism called autoimmunity. For this purpose, an efficient regulation has to be done to exclude all the lymphocytes that could recognize self-antigens and therefore induce autoimmune processes. In addition to the receptors making process, the lymphocytes have also the ability to multiply themselves, that is, undergo a clonal expansion process that will permit an amplification of the specific (adaptive) immune response up to 7 days after the initiation of the immune response, conducting to the already mentioned delay in the adaptive response (Owen *et al.*, 2012; Delves *et al.*, 2017). There is also the possibility that B and T lymphocytes, produced with specific receptors to the antigen, stay stored until a new reencounter with the pathogen, being called the B and T memory cells, respectively. These cells will permit a faster and more efficient response in the case of a repeated exposure to a certain pathogen due to the absence of the delayed preparation of the adaptive context that occurs in the first antigen contact (Parkin and Cohen, 2001; Owen *et al.*, 2012). In latter sections this memory mechanism will be discussed in more detail.

Giving the different tasks performed by B and T cells, the adaptive response could be divided in two subtypes: the humoral and cell-based immune responses (Reuschenbach *et al.*, 2009; Carvalheiro, 2014).

### 1.2.3 B lymphocytes

The humoral immune response is predominantly dominated by B lymphocytes due to their production of antibodies against the invasive antigen. When the receptors of these cells, the already referred BCRs, bind to their target antigen, an intracellular signaling process starts, leading to the activation, differentiation and generation of plasma

and memory B cells (Parkin and Cohen, 2001; Tobón *et al.*, 2013). There are different subsets of B-cells presenting a specific function depending on their origin, function and localization (Tobón *et al*., 2013).

The B cells development begins in the bone marrow, being derived from lymphoid progenitors with assistance of stromal cells. There is an initial differentiation upon pro-B cells that undergo somatic recombination (or V(D)J recombination) to generate functional BCRs with IgM antibody isotype. This is followed by a negative selection process where the autoreactive cells (the ones that recognize the self-antigens) are eliminated (Parkin and Cohen, 2001; Owen *et al.*, 2012; Carvalheiro, 2014). Being in an immature state, B cells leave the bone marrow and migrate to the secondary lymphoid tissues where they will start to express IgD in addition to the already expressed IgM, developing into naïve and mature B cells (Tobón *et al*., 2013). After the B cells reach the spleen, type-1 (T1) and type-2 (T2) transitional B cells are produced. T1 cells are a short-lived subset that require BCR stimulation to develop into T2 B cells. These latter group will differentiate into two distinct subsets: mature circulating lymphocytes that will generate germinal centers or non-circulating lymphocytes that will settle in the marginal zone (Tobón *et al*., 2013; Parkin and Cohen, 2001). Later on, when cells encounter the antigens that bind to their BCRs, the activated B cells undergo proliferative expansion and differentiation in the germinal center which leads to the development of either antibody producing plasmablasts or memory cells after a somatic hypermutation, driving to high-affinity antigen receptors production and immunoglobulin class switch processes (antibodies class can change between IgA, IgD, IgE, IgG or IgM upon encountering with the cognate antigen) (Owen *et al.*, 2012; Tobón *et al*., 2013).

### 1.2.4 T lymphocytes

T cells are subdivided into three main subsets: helper (Th), cytotoxic (Tc) and regulatory (Treg), which in basic words, respectively, help B-cells to make antibodies (Th), kill virally-infected cells (Tc) and control the actions of other T-cells (Treg) (Parkin and Cohen, 2001; Owen *et al.*, 2012; Delves *et al.*, 2017). The Th (namely Th1, Th2, Th9, Th17 and Th22) and Treg cells are part of the $CD4^+$ subtype, while Tc cells constitute the $CD8^+$ domain. These two T cell subtypes could be defined by the presence of two distinct membrane proteins: CD4 and CD8, respectively (Owen *et al.*, 2012). Both proteins act as co-receptors for MHC molecules but, structurally, CD4 is a surface located single-chain polypeptide containing four Ig-like domains whose cytosolic tail is crucial for TCR

signaling as it interacts with *Lck*, a protein tyrosine kinase that initiates the signal transduction cascade fired when the T cells recognize an antigen (Parkin and Cohen, 2001; Owen *et al.*, 2012). The CD8 protein has a similar intracellular function but it has a different structure: CD8 is a disulfide-linked heterodimer of α and β chains, which binds to a glycosylated polypeptide projecting from the T cell surface by Ig-like domains (Owen *et al.*, 2012). These structural differences dictate distinct patterns in the antigen recognition by $CD4^+$ and $CD8^+$ T cells, defining the MHC molecules and, consequently, the antigen that these cells will recognize. The $CD8^+$ T cells become activated upon encounter with antigen presented within MHC class I molecules and act as cytotoxic T cells. The $CD4^+$ T cells are activated when the peptides are presented by MHC class II molecules and become helper or regulatory T cells (Owen *et al.*, 2012; Delves *et al.*, 2017). In both subtypes the TCR are also intimately linked, even though non-covalently, to a complex of transmembrane polypeptides called CD3 that is crucial in the propagation of activation signals into the lymphocyte (Parkin and Cohen, 2001; Delves *et al.*, 2017). The TCR complex for both $CD4^+$ and $CD8^+$ are represented in **Figure 6**.

In terms of development, both $CD4^+$ and $CD8^+$ T cells are generated in the thymus, being derived from lymphoid progenitors that leave the bone marrow and migrate to that organ to finish their differentiation. This is different from what occurs in the case of B-cells that, as aforementioned, are fully developed in the bone marrow (Parkin and Cohen, 2001; Owen *et al.*, 2012).

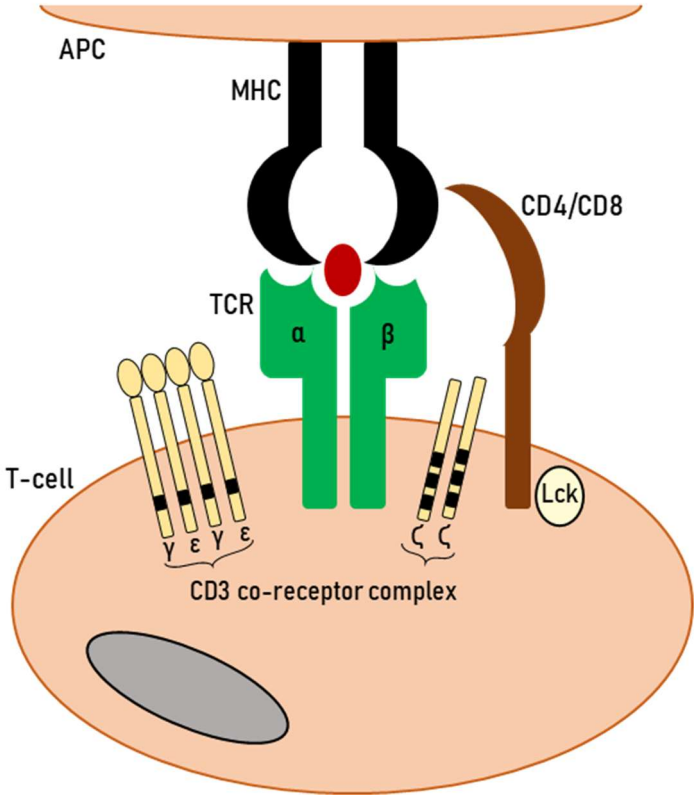


**Figure 6 -** Representation of T cell receptor complex with CD4 or CD8 proteins that define a $CD4^+$ or $CD8^+$ T cell, respectively (Adapted from Delves *et al.*, 2017). Abbreviations: APC (Antigen-Presenting Cell); MHC (Major Histocompability Complex); TCR (T Cell Receptor).

#### 1.2.4.1 $CD4^+$ T cells

As stated above, after stimulation by APCs, naïve $CD4^+$ T cells undergo a proliferation and differentiation process and two major subsets could be distinguished: T helper (Th) and T regulatory (Treg) (Parkin and Cohen, 2001; Owen *et al.*, 2012). The first ones attracted almost all the attentions from a research point of view due to their capacity of cytokine production that enable them to interact with other immunological agents and mediate the immune response, reflecting the high impact of these cells in this process.

T helper cells are divided in distinct and specific subtypes that includes, for example, Th1, Th2 or Th17 (Parkin and Cohen, 2001). Th1 cells are responsible by production of interferon- γ (IFN-γ) and tumor necrosis factor-α (TNFα), both conducing to phagocyte activation and production of opsonizing and complement-fixing antibodies, having a big impact in the fight against intracellular pathogens such as viruses or intracellular bacteria (Parkin and Cohen, 2001; MacLeod *et al.*, 2009). However, in

contrast to these protective roles, these cells were shown to help promoting inflammation in autoimmune diseases (Annunziato and Romagnani, 2009). Th2 cells, due to their production of IL-4, IL-5 and IL-13, are involved in anti-parasite immune reactions being that they also have a major role in allergic responses and asthma (MacLeod *et al.*, 2009). Th17 cells produce mainly IL-17, IL-22 and IL-26 cytokines and are involved in protection against extracellular bacteria and fungi (MacLeod *et al.*, 2009; Zhu and Paul, 2009), being a clear example of these processes the immune actions against intestinal bacteria. In other way, they also have a strong impact in autoimmune diseases progression like rheumatoid arthritis (RA) (Lubberts, 2010). Th17 cells have the capacity to self-convert into Th1 cells, acquiring the ability to produce the IFN- γ, being the other way round also possible (Geginat *et al.*, 2016). Both types of cells (Th1 and Th17) have a high probability to play a major role in chronic inflammatory disorders.

The Treg subset main function is to control the activity of Th cells and maintain the immune homeostasis which could avoid the excessive immune responses. This latter unbalanced process could lead, for example, to triggering autoimmune responses, which one of the main characteristics is the hyper activation of Th1 or Th17 cells (Sun *et al.*, 2017). Treg cells could be divided in natural Treg (nTreg), if generated in the thymus, and in induced Treg (iTreg) when originated in peripheral organs and tissues. Treg cells are mastered by Forkhead box P3 (Foxp3) transcription factor that control their capacity to suppress the immune functions of T helper cells (Sakaguchi *et al.*, 2010; Sun *et al.*, 2017). An abnormal activity of Treg cells is not only associated with autoimmune disorders (when these cells activity is at low levels) but also with cancer incidence (when Treg cells activity is exacerbated, suppressing much of the immunity protective responses of Th cells) (Sun *et al.*, 2017).

#### 1.2.4.2 $CD8^+$ T cells

The $CD8^+$ T cells, also known as cytotoxic T lymphocytes (Tc or CTLs), participate actively in the protection against infectious agents and pathogens and also in the eradication of malignant cells (Parkin and Cohen, 2001; Andersen *et al.*, 2006; Owen *et al.*, 2012). The naïve $CD8^+$ T cells develop and differentiate into effector subtypes that induce and promote the inflammatory process by the secretion of proinflammatory cytokines and proteolytic enzymes, being this an excellent reason to focus autoimmunity studies in the action and functions of these cells. They could also have a suppressive effect against the immune responses by anti-inflammatory cytokines production (Parkin and Cohen, 2001; Owen *et al.*, 2012). As aforementioned in the case of $CD4^+$ T cells, the immunological equilibrium is an essential role in an organism. Thus, a predominance of pro- or anti-inflammatory signals will generate an imbalance that, in case of persistence of a pro-inflammatory signal could generate the awful conditions that lead to autoimmune disorders. In this way the existence of anti-inflammatory signals is required for the maintenance of tolerance against self-antigens, avoiding autoimmunity problems. The activity of these cells could be regulated by $CD4^+$ T cells action, namely by the cytokines and chemokines produced by these cells (Owen *et al.*, 2012).

#### 1.2.4.3 Memory T cells

As mentioned above, both $CD4^+$ and $CD8^+$ T cells could, beside developing their effector actors, give rise to cells that are similar to naïve cells when one looks to their activation state but already have been differentiated and present some receptors that react against specific pathogens. These cells are called memory cells and are generated from both T and B lymphocytes (Owen *et al.*, 2012; Natoli and Ostuni, 2019). They are generated during the contraction process that occurs when the pathogen, that initiated the immune response, had been cleared and therefore our protection system could relax and reduce its activity. In this way, and speaking specifically about the T cells, the majority of Th and Tc cells are destroyed, being that some of them are simply modified and give rise to these memory type cells. As the name indicates, this subset of cells will be of extreme importance when and if the immune system gets contact with the same pathogen again, a proceed called re-exposure (Owen *et al.*, 2012). This specific immune reaction upon re-exposure is called secondary response, in accordance with the primary response that happens when the antigen is totally new to the organism (Owen *et al.*, 2012; Delves *et al.*, 2017). The clearance of these invasive component much faster and efficient in the

secondary response since the organism already has in circulation cells that are specific for that agent (antigen-specific cells). In addition, memory cells were shown to produce effector cells more rapidly than their naïve counterparts (MacLeod *et al.*, 2009).

The differences in the immunological response induced by the existence of these memory subsets, that is, between the primary and the secondary responses are represented in **Figure 7**. Since the innate part of the immune system does not produce this memory phenotypes, its magnitude of response is the same between the primary and secondary responses (Owen *et al.*, 2012).

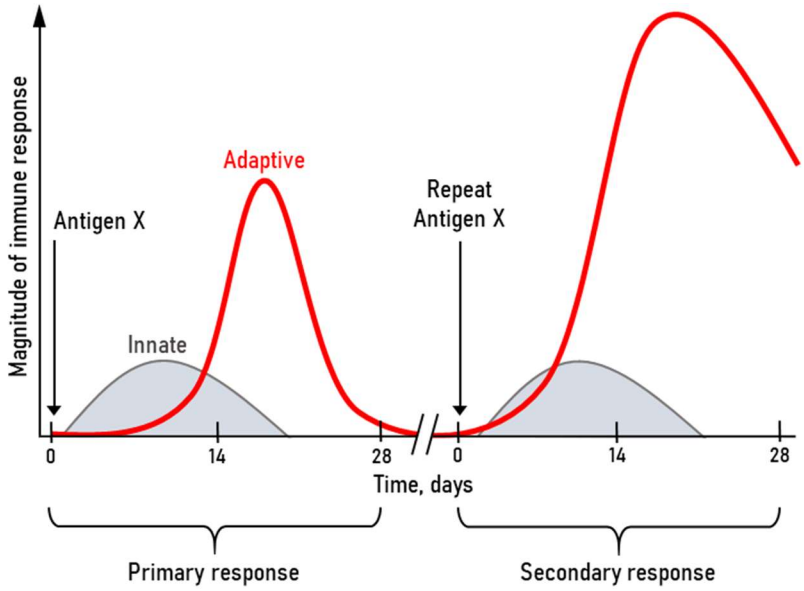


**Figure 7 -** Representation of the difference in the immunological magnitude between a primary and a secondary response to an antigen exposure (Adapted from Owen *et al.*, 2012).

The immunological memory mechanism is the basis of the vaccination procedures, since it enables the organism to produce memory cells based in a partial or total inoffensive agent that, when needed, could then react against a real invasive agent, avoiding is major negative impact in the organism. For the vaccination success contributes the fact that memory cells are able to remain in the organism for decades (Owen *et al.*, 2012). In latter sections the differences from a metabolic point of view between memory, naïve and effector cells will be discussed in more detail.

## 1.3 Autoimmune disorders

Although the immune response has, in the great majority of the cases, a beneficial effect in organism homeostasis by fighting infectious agents, there are moments when the immune system could be acting against antigens that are not supposed to be the target. This situation happens in allergic reactions where an environmental antigen is targeted or in the foreign tissue rejection after transplantation procedures. The principal reason that potentiates these adverse reactions is the antigen receptors flexibility present in immunity cells, resulting in hypersensitivity processes (Delves *et al.*, 2017). In a similar fashion, the events that lead to a self-antigen recognition by immunity cells could result in pathologies, the so-called autoimmune diseases. It is important to mention that even healthy individuals have auto-antibodies in circulation, which recognize self-antigens and function as house-keepers removing the debris that result from a cellular or tissue breakdown (Elkon and Casali, 2008). The pathological state is only recognized when the autoimmune responses became uncontrolled, being that these disorders are probably caused by failures of the self-tolerance processes that, in normal cases, protect the host organism from the exacerbated action of self-reactive lymphocytes and auto-antibodies. The action of auto-antibodies (produced by B cells) and/or self-reactive T cells result in deterioration of patient's life quality by destruction of self-proteins, cells and organs (Elkon and Casali, 2008; Owen *et al.*, 2012).

In the next section of this introduction, the arthritic autoimmune diseases will be discussed, being that in these disorders there are specific actions of self-reactive B and T lymphocytes in the joints region, leading to tissue destruction, as well as auto-antibodies and cytokines accumulation in the synovium and its peripheral regions. Other examples of diseases that could be caused by T cells-mediated autoimmunity are Type 1 *diabetes mellitus* (T1DM) and multiple sclerosis (MS). Hashimoto's thyroiditis, where the thyroid tissue is destroyed by self-reactive antibodies that recognize antigens in the thyroid, is driven by auto-antibodies, that is, by B cells activity (Owen *et al.*, 2012).

Overall, the autoimmunity diseases affect between 3% and 8% of the population in the so-called industrialized world, disturbing the patient's quality of life by increasing the morbidity and mortality (Cooper *et al*., 2009). In most of these disorders, the clinical disease aspects just appear years or even decades after the breakdown in the self-tolerance mechanism aforementioned, which makes the early diagnosis a major goal in the treatment of autoimmune diseases (Weyand *et al*., 2017). These disorders could be classified as organ-specific or systemic if the disease affects a single organ or multiple

systems in the organism, respectively (Owen *et al.*, 2012). As stated above, they can be also grouped having into account which immune components are involved: T cells or B cells-derived anti-bodies. The process that is responsible for the autoimmunity triggering is still unknown and under intensive study in the last years. The higher frequencies, in most of these disorders, in women than in men have been also an object of intensive study. In both cases, the genetics seems to have a preponderant influence. In the next sub-section, the discussion will be focused in the autoimmune arthritic diseases, more specifically on Rheumatoid arthritis (RA).

### 1.3.1 Arthritic autoimmune diseases

The autoimmune problems affect plenty of different tissues, generating a huge number of diseases. Inside this group of disorders one can find the arthritic autoimmune diseases that are characterized by inappropriate immune responses that leads mainly to joint destruction, which include Rheumatoid Arthritis (RA) but also Spondyloarthritis (SpA) and Psoriatic Arthritis (PsA). From now on, the attentions will be focused in RA: how this disease could be characterized, who are the main players in the disorder triggering and development and what could be done, if something, to retain its undesirable effects in patients.

#### 1.3.1.1 Rheumatoid arthritis

RA is an incurable, systemic, autoimmune disease characterized by chronic inflammation of the joints that leads to complications such as swelling and pain, cartilage damage, bone erosion, severe joint deformation, disability and premature mortality (Klein *et al*., 2018). According to World Health Organization (WHO) data, the disease tends to strike during the most productive years of adulthood, that is, between the ages of 20 and 40 and the prevalence varies between 0.3% and 1%, being more common is industrialized countries. Is it also stated that 50% of patients are unable to hold down a full-time job within 10 years on onset (World Health Organization, 2020). The frequency of appearance of this condition is two-to-three times higher in women than in men, being that the cause of this distinct disease gender prevalence could be originated by some factors linked to the X chromosome, as inactivation patterns, or the RA development and severity may be affected by the higher presence of female sex hormones (Klein *et al*., 2018). As aforementioned for the autoimmune diseases in general, RA patients present the main clinical disorder aspects such as pain and dysfunctional joint inflammation only years or decades after the immunological trigger point, that is, the moment when the

immune system starts to react against its own organism (Weyand *et al*., 2017). This aspect makes the battle against this disease a really difficult task, since at the point where the clinical signals are visible the cellular machinery that supports RA is almost impossible to stop.

In terms of pathogenesis, there are two major subtypes of RA that could be considered, being defined by the presence or absence of anti-citrullinated protein antibodies (ACPAs) (Guo *et al.*, 2018). Citrullination is a process that changes a positively charged arginine to a polar but neutral citrulline, being catalyzed by the calcium-dependent enzyme peptidyl-arginine-deiminase (PAD) and the result of post-translational modification. Although the exact events triggering RA are still unknown, the recognition of citrullinated proteins and immune complexes by autoantibodies is one of the strongest theories to explain the arise of activated osteoclasts that initiate the bone, and consequently, the joint damage (McInnes and Schett, 2017). Approximately 67% of RA patients have been detected with ACPAs in circulation and these indicators could serve as a useful diagnostic tool, especially in early and undifferentiated arthritis, and to provide information about the disease progression. It is stated that the ACPA-positive ($ACPA^+$) subtype of RA has a more aggressive clinical phenotype compared to ACPA-negative ($ACPA^-$) subset of RA (Guo *et al.*, 2018), being that $ACPA^+$ presents an estimated heritability ranging from 40% to 65% and $ACPA^-$ only presents 20% (Klein, Karouzakis and Gay, 2018). In addition to this genetic susceptibility, it is believed that some epigenetic alterations associated with environmental factors could lead to the immune dysregulation verified in the RA condition.

The aforementioned autoantibodies production, done by B cells, in conjugation with the reactiveness of T cells, namely $CD4^+$ and $CD8^+$ T cells, conduces to an exacerbated production of pro-inflammatory cytokines due to the failure of their regulatory machinery that was mentioned in early sections. These constitute the major cellular and molecular patterns of the disease (Klocke *et al*., 2017). This production of autoantibodies and pro-inflammatory cytokines will amplify the local and systemic inflammatory processes by recruiting and activating the innate immune cells and synovial fibroblasts. These linkages between cells and molecules function as a vicious cycle, leading to the continuous destruction of the proteins from the synovial membrane and subsequent joints destruction. The evolution of the pathogenesis of RA in the specific joint environment is represented in the **Figure 8**.

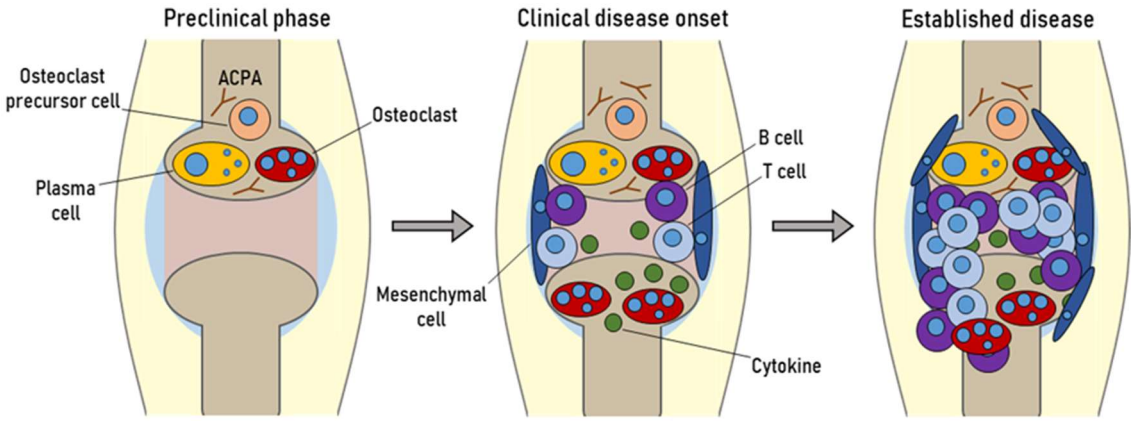


**Figure 8 -** Representation of the RA pathogenesis, showing the accumulation of T and B cells in the joint as the disease progresses (Adapted from Carvalheiro, 2014). Abbreviation: ACPA (Anti-citrullinated protein antibody).

## 1.4 T cells in rheumatoid arthritis

In the last few years it has been noticeable a growing interest in deciphering the roles of both $CD4^+$ and $CD8^+$ T cells in triggering and sustaining the joint damage in RA as well as their specific actions in the evolution of this disease. Without any doubt, this has conducted to a better understanding of the protagonist of these cells in this pathology, but yet not totally clear (Pearce *et al.*, 2013; Carvalheiro *et al.*, 2015).

These two cells subtypes, as aforementioned, differ in their role during immune responses. In a broad view, while the $CD4^+$ T cells act as main producers of immune mediators and work as helpers/regulators of the immune response, the $CD8^+$ T cells can produce both immune mediators, recruiting other cells, and release cytolytic molecules capable of destroying specific targeted cells. Both types of cells seem to present an altered behavior in RA patients when compared with healthy individuals, being the roles of $CD4^+$ and $CD8^+$ T cells in RA pathogenesis studied in plenty different point of views, including the metabolic one. This latter perspective could give us an idea of the activation state of these cells in different contexts, including the disease one, being this metabolic activity correlated with the disorder clinical effects. Thus, both T cells subsets are being metabolically characterized in order to understand how they act in the specific context of RA disease and, knowing that, how can we try to modulate these immune cells functions to minimize the disorder severity, improving patient's life quality standards. In the next sub-section, it will be exposed the current knowledge about $CD4^+$ T cells metabolism in RA and how it is known to affect these cells functions and, consequently, the disease state of activation.

### 1.4.1 $CD4^+$ T cells metabolism in rheumatoid arthritis

As aforementioned, $CD4^+$ T cells are one of the major players in autoimmune diseases' triggering and progression, due to their capacity of interaction with the other components of the immune system and, as a consequence, these cells gain substantial importance when one tries to understand these types of disorders. Thus, clarifying the role of $CD4^+$ in the autoimmunity specific context could lead to the development of new strategies to deal with diseases such as RA. One of the most interesting methods to do so is to study the way that $CD4^+$ T cells produce and consume energy and metabolites to sustain their functions, that is, studying their metabolism. With $CD4^+$ T cells' functions in RA deciphered, as well as the relationship between them and their metabolic machinery, researchers and clinicians could think on specific interventions to modulate these cells in order to stop or, at least, to soften these cells actions and raise the RA patients' quality of life.

Before their activation by antigen-presenting cells (APCs), as stated above, naïve $CD4^+$ T cells present a low activity profile and, thus, minor energy requirements. In this resting profile, $CD4^+$ T cells mainly use oxidative phosphorylation (OXPHOS) at low rates to meet their minimal energetic needs (Wahl *et al.*, 2010). As explained in early sections, this way of producing energy is highly dependent on mitochondrial activity, being the glucose available metabolized to pyruvate via glycolysis, entering in the mitochondrial matrix as acetyl-CoA and being then oxidized via TCA cycle coupled with mitochondrial respiratory chain (Lunt and Vander Heiden, 2011). This basal metabolic activity is in accordance with the low activity of these naïve cells.

In the moment when $CD4^+$ T cells are stimulated by an antigen presentation, they promptly wake-up from their basal state and become highly proliferative cells with an exacerbated replication and clonal expansion (Owen *et al.*, 2012; Pearce *et al.*, 2013). These actions, part of the adaptive immune response that leads to formation of effector cells, are highly reliant on energy and biosynthetic precursors to allow cell replication (though the synthesis of nucleic acids but also lipids and proteins) and effector synthesis ( Lunt and Vander Heiden, 2011; Weyand and Goronzy, 2017). As stated in early sections of this introduction, high proliferative cells swift their metabolism from the basal oxidative to the stimulated highly glycolytic, achieved by intensified rates of aerobic glycolysis, which lead to exacerbated lactate production, in order to fuel the secondary metabolic pathways that divert from glycolysis and warrant biosynthetic precursors production. The Pentose Phosphate Pathway (PPP) and serine and glycine synthesis from

3-phpsphoglycerate constitute principal example examples (Vander Heiden *et al*., 2009; Lunt and Vander Heiden, 2011).

This high commitment of glucose to lactate production to fulfill the bioenergetic purposes of $CD4^+$ T cells was shown to occur in acute stimulation conditions (Wahl *et al.*, 2010), which could be referred as normal immune responses that cease after some time. However, when considering chronically stimulated lymphocytes, cells that are in a permanent state of activation, the majority of research evidence states that the paradigm may change (Tsokos, 2016). This is the case in Rheumatoid Arthritis, an autoimmune chronic disorder where a chronical activation state sustains the clinically undesired proliferation and effector functions of $CD4^+$ T cells as well as the other T and B cells.

In RA, $CD4^+$ T cells purified from the peripheral blood had been associated, once stimulated, with a higher utilization of PPP in a direct way, being the captured glucose directly diverted to this pathway and the glycolytic flux not being necessarily exacerbated, quite the contrary, it is almost shut-down (Weyand and Goronzy, 2017; Weyand *et al.*, 2018). This shift towards PPP seems to be associated with the reduction of activity of the glycolytic enzyme 6-phosphofructo-2-kinase/fructose-2,6-biphosphatase 3 (PFKFB3) and also with the incapacity of these cells to obtain biosynthetic precursors via autophagy, a process of cellular self-degradation of internal components, such as proteins or even organelles, that could help cells responding to specific nutrient stress (Glick et al., 2010; Yang *et al.*, 2013).

PFKFB3 is a critical glycolytic regulator as a generator of fructose 2,6-biphosphate (F2,6BP), an allosteric activator of 6-phosphofructo-1-kinase (PFK1), the enzyme that catalyzes the phosphorylation of fructose-6-phosphate to fructose-1.6-biphosphate (Yang *et al.*, 2013). This step is an irreversible reaction in the process of glucose breakdown, committing the glucose to be irremediably oxidized via glycolysis. Thus, this apparent deficiency in the induction of PFKFB3 activity is believed to be one major contributor to the PPP exacerbation in RA $CD4^+$ T cells in consequence to the shut-down of glycolysis. This is corroborated by the fact that overexpression of PFKFB3 in these RA $CD4^+$ T cells reactivates both glycolytic pathway and autophagy (Yang *et al.*, 2013). This commitment through PPP enables RA $CD4^+$ T cells to fulfill their biomass requirements, namely the biosynthesis of precursors fundamental to the generation of nucleic acids, that will permit their clonal expansion in the context of a permanent immune response (Weyand and Goronzy, 2017). Associated with the production of pentose sugars, basic components of nucleotides, the PPP rate-limiting reaction catalyzed

by glucose-6-phosphate dehydrogenase (G6PD) also generates NADPH (reduced nicotinamide adenine dinucleotide phosphate): one molecule of glucose-6-P gives rise to one ribose-5-P and 2 NADPH molecules. This latter molecule, due to its electron donor function, is the cell's most abundant reductive agent and therefore is a crucial component in both regulation of cells' redox state, acting as an anti-oxidant, and production of biomass, providing reducing equivalents (Vander Heiden et al., 2009; Yang *et al.*, 2016; Weyand and Goronzy, 2017). NADPH exerts its antioxidant functions regenerating the reduced form of glutathione (GSH) by transferring electrons to the oxidized glutathione (GSSG), being this latter one formed when hydrogen peroxide is converted and reduced to water. In this way, the exacerbated PPP will result in an increased production of NADPH which, by interaction with glutathione and, consequently, scavenging the reactive oxygen species (ROS) such as hydrogen peroxide, will induce a reductive state in cells.

ROS molecules that are generated mainly during the mitochondrial oxidative phosphorylation process, were for many years linked to the worst side of the oxidative metabolism, being often connected to excessive oxidative stress and cells' malfunctions. However, the study of ROS impact in the immune responses lead to the unveil of their specific actions in controlling and regulating some $CD4^+$ T cells functions (Weyand and Goronzy, 2017; Weyand *et al*., 2018). One of the consequences of this highly reductive environment inside $CD4^+$ T cells is the defective function of ataxia telangiectasia mutated kinase (ATM) (Tsokos, 2016). ATM is a serine/threonine protein kinase, member of the phosphatidylinositol-3-kinase-related kinases (PIKKs) superfamily, and acts as a response to DNA double-strand damage, coordinating its repair or, if not possible, inducing the apoptotic cell death (Weyand et al., 2018). ROS have been shown to activate the dimerization required for ATM function and, therefore, low levels of ROS in $CD4^+$ T cells reduce the activity of this enzyme. The consequences are a hyper-proliferation state where the cells overtake the essential cell cycle checkpoints, dividing at higher rates and an higher conversion of these cells from naïve directly to memory state (Weyand *et al*., 2018). This hyper-proliferation associated with cell-cycle dysfunctions had a higher impact in Th1 and Th17 populations, which corroborates with the linkage between these cells, RA and this exacerbated PPP in $CD4^+$ T cells (Yang *et al.*, 2016). It is than plausible, due to this data, that RA $CD4^+$ T cells could rely their metabolism in a PPP dependent manner, being their clonal expansion potential supported by this higher reductive pathway.

In addition to RA $CD4^+$ T cells from peripheral blood having been associated with higher PPP utilization, $CD4^+$ T cells purified from the synovial fluid of patients with juvenile idiopathic arthritis (JIA) have shown a specific oxidative metabolism, having the capacity to rely exclusively on fatty acid oxidation for maintaining their actions (Hradilkova *et al.*, 2019). These chronically stimulated cells, more specifically Th1 cells that expressed the programmed death 1 (PD-1) protein, saw their survival blocked when the fatty acid oxidation was obstructed, namely by the transport inhibition of these macro-nutrients, the fatty-acyl molecules, from the cytoplasm to mitochondria by the action of the carnitine palmitoyltransfetase 1 inhibitor etomoxir (Hradilkova *et al.*, 2019). PD-1 protein has been reported as an important but not indispensable player in the process of controlling the extent of $CD4^+$ T cells accumulation in the immunological responses, (Konkel *et al.*, 2010). Although PD-1 expression seems to be connected to $CD4^+$ T cells that are in exacerbated clonal expansion, its specific role in the autoimmune diseases like RA are still only superficially known. In the study previously referred (Hradilkova *et al.*, 2019), it has been shown that Th1 cells from synovial fluid of arthritic patients had a high expression of *TWIST1*, a E-box-binding transcription factor that seems to control and regulate the metabolism and function of these cells, namely by forcing the utilization of fatty acid oxidation and inducing their proinflammatory activity which contributes to the chronicity of arthritic diseases (Hradilkova *et al.*, 2019).

Considering the information reported in the above paragraphs, the most recent research done in chronically stimulated $CD4^+$ T cells point towards a lower utilization of aerobic glycolysis pathway that is, as stated in early sections, a main metabolic characteristic of high-proliferative cells such as the cancer ones of even of T cells on their acute stimulated responses. Both utilization of PPP and fatty acids oxidation in chronically simulated T cells seems like a contradiction to what had been postulated in the last decades about high-proliferative cells metabolism, but it seems sustained in the specific context of immunological responses. Having this apparent contradiction in mind, we aim in this work to uncover the true metabolic phenotype of CD4+ T cells by applying a state-of-the-art methodology, $^{13}C$ Nuclear Magnetic Resonance (NMR) isotopomer analysis, for monitoring intermediary metabolic fluxes using stable $^{13}C$-isotope metabolic tracers.

## 1.5 $^{13}C$ isotopomer analysis by $^{1}H$-NMR

In this project, we will use proton ($^{1}H$) NMR spectroscopy to perform a $^{13}C$ isotopomer analysis of the metabolic intermediate lactate, which can provide important metabolic information concerning several metabolic pathways. The focus in this research was centered in the metabolic answers that the lactate molecule could give to our metabolic questions, and was grounded in the possibility of distinguishing the different lactate isotopomers. The concept of isotopomer, emerged from the fusion of the terms isotope and isomer, and portrays molecules that are composed by the same atomic species but have different mass and could be distinguished by optical or magnetic techniques such as NMR. In our approach, different $^{13}C$ lactate isotopomers will be generated by the utilization of known $^{13}C$-enriched substrates such as [U-$^{13}C$]glucose or [U-$^{13}C$]glutamine. Whether and how these substrates are metabolically transformed by the cells will influence the appearance of the distinct lactate isotopomers, that is, the $^{13}C$ enriched positions in the lactate molecule will be determined by the metabolic routes used by the cell to transform the nutrients provided.

Being the lactate molecule composed by 3 carbon atoms it is possible to identify 8 distinct lactate isotopomers when observing an $^{1}H$ NMR spectrum of the methyl group. The identification of these $^{13}C$ isotopomers molecules is possible not only because they have different spectral positions (chemical shifts) but also due to the appearance of distinct multiplets for each isotopomer due to direct and long-range heteronuclear coupling constants (Günther, 2013). **Figure 9** represents the 8 different Lactate isotopomers and their respective spectra obtained by $^{1}H$ NMR.

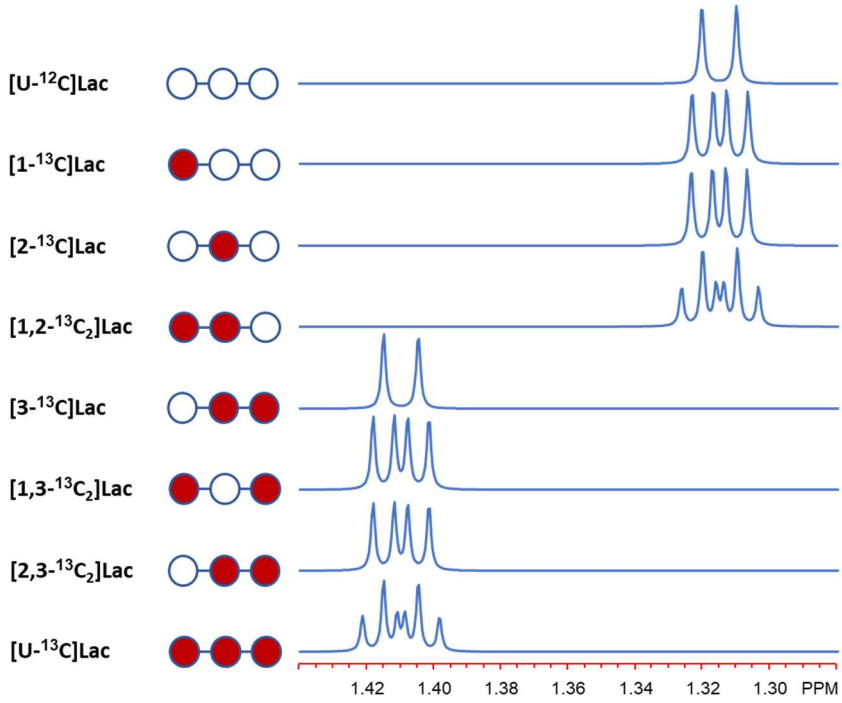


**Figure 9** - Schematic representation of the NMR resonances of the methyl protons due to each of the 8 possible lactate isotopomers. Filled circles represent $^{13}$C-enriched carbons while open circles denote unenriched carbons. From top to bottom: i) unenriched lactate – [U-$^{12}$C]Lac; ii) lactate $^{13}$C-enriched in carbon 1 – [1-$^{13}$C]Lac; iii) lactate $^{13}$C-enriched in carbon 2 – [2-$^{13}$C]Lac; iv) lactate $^{13}$C-enriched simultaneously in carbons 1 and 2 – [1,2-$^{13}C_2$]Lac; v) lactate $^{13}$C-enriched in carbon 3 – [3-$^{13}$C]Lac; vi) lactate $^{13}$C-enriched simultaneously in carbons 2 and 3 – [1,3-$^{13}C_2$]Lac; vii) lactate $^{13}$C-enriched simultaneously in carbons 1 and 3 – [2,3-$^{13}C_2$]Lac; viii) lactate uniformly $^{13}$C-enriched – [U-$^{13}$C]Lac. For isotopomers $^{13}$C enriched in carbon 3 only one of the two $^{13}$C satellites is presented. Abbreviations: Lac (Lactate).

In this work, the $^{13}$C source were the substrates given to the cells in the culture media, being the composition of the media specified in the Materials and Methods section.

## 1.6 Working hypothesis and study objectives

The activity of $CD4^+$ T cells is an important player in the development of an immune response, being its cytotoxic action highly dependent on metabolic adaptations. Our working hypothesis is that stimulated $CD4^+$ T cells withstand their pro-inflammatory phenotype providing that the substrates glucose and glutamine are present in the culture media in sizeable amounts and that the lowering of glucose has severe repercussions in $CD4^+$ T cells activity.

The alteration in substrate contents of culture media will be made to mimic the specific immunological environments of rheumatoid arthritis, and to be able to follow the metabolic adaptations of $CD4^+$ T cells to sustain their activity. This metabolic knowledge will impact in the design of metabolic-driven therapies capable of improving the quality of life of RA patients.

In accordance to the work that has been previously done in our research group regarding T cells metabolism in RA (Souto-Carneiro *et al.*, 2020), and considering the recent research developments in T cells metabolism, this work proposes a state-of-the-art experimental approach to study $CD4^+$ T cells metabolic activity and its impact in cells' functions in the specific context of RA.

To tackle the devised main objective, the following tasks will be executed using $CD4^+$ T cells isolated from the blood of RA patients of Heidelberg University Hospital:

i) Decipher the metabolic profile of RA $CD4^+$ T cells at rest (Nstim) and activated (Stim), when incubated in media with normal levels of glucose, using $^{13}C$ NMR isotopomer analysis.

ii) Evaluate the changes in $CD4^+$ T cells metabolic profile and function induced by ample changes in substrate availability capable of interfering with glycolytic and OXPHOS fluxes.

iii) Understand how the bioenergetic and biosynthetic metabolic machinery of RA $CD4^+$ T cells could eventually be manipulated in order to control their functions and moderate the immunological response against self-antigens in RA.

# 2 Materials and methods

## 2.1 Reagents and materials

**Table 1:** Reagents List.

| Reagent | Brand | Headquarters |
|---|---|---|
| (10x) Dulbecco's Phosphate Buffered Saline (DPBS) | Sigma-Aldrich | St. Louis, Missouri, USA |
| (1x) Dulbecco's Phosphate Buffered Saline (DPBS) | Sigma-Aldrich | St. Louis, Missouri, USA |
| [1,6-$^{13}C_2$]Glucose | Sigma-Aldrich | St. Louis, Missouri, USA |
| [2,4,6,8-$^{13}C_4$]Octanoate | Sigma-Aldrich | St. Louis, Missouri, USA |
| [U -$^{13}$C]Glutamine | Sigma-Aldrich | St. Louis, Missouri, USA |
| [U-$^{13}$C]Glucose | Sigma-Aldrich | St. Louis, Missouri, USA |
| 2-Deoxy-2-[(7-nitro-2,1,3-benzoxadiazol-4-yl)amino]-D-glucose (2-NBDG) | Thermo Fisher Scientific | Waltham, Massachusetts, USA |
| APC Annexin V | Biolegend | San Diego, California, USA |
| APC/Cyanine7 anti-human CD4 Antibody | Biolegend | San Diego, California, USA |
| BD Cytofix/Cytoperm™ Fixation/Permeabilization Solution Kit | Becton Dickinson & Company | Franklin Lakes, New Jersey, USA |
| Bodipy™ 493/503 | Thermo Fisher Scientific | Waltham, Massachussets, USA |
| Bovine Serum Albumin | Thermo Fisher Scientific | Waltham, Massachussets, USA |
| Brilliant Violet 510™ anti-human CD4 Antibody | Biolegend | San Diego, California, USA |
| Brilliant Violet 605™ anti-human CD45RO Antibody | Biolegend | San Diego, California, USA |
| Brilliant Violet 711™ anti-human CD45RA Antibody | Biolegend | San Diego, California, USA |
| Brilliant Violet 785™ anti-mouse CD4 Antibody | Biolegend | San Diego, California, USA |
| $CD4^+$ T Cell Isolation Kit | Miltenyi Biotec | Gladbach, Germany |
| CellROX® Deep Red Reagent | Thermo Fisher Scientific | Waltham, Massachusetts, USA |
| FX11 | Sigma-Aldrich | St. Louis, Missouri, USA |
| GDH 1/2 (D9F7P) Rabbit mAb | Cell Signaling Technology | Danvers, Massachusetts, USA |
| Gibco™ Fetal Bovine Serum | Thermo Fisher Scientific | Waltham, Massachusetts, USA |
| Goat Anti-Rabbit IgG H&L (Alexa Fluor® 488) | Abcam | Cambridge, UK |
| Invitrogen™ EDTA | Thermo Fisher Scientific | Waltham, Massachusetts, USA |
| JC-1 Dye (Mitochondrial Membrane Potential Probe) | Thermo Fisher Scientific | Waltham, Massachusetts, USA |
| LDHA (C4B5) Rabbit mAb | Cell Signaling Technology | Danvers, Massachusetts, USA |
| LEGENDplex™ Human Inflammation Panel 1 (13-plex) with V-bottom Plate | Biolegend | San Diego, California, USA |
| Pancoll Separing Solution | PAN-Biotech | Aidenbach, Germany |
| PDH (C54G1) Rabbit mAb | Cell Signaling Technology | Danvers, Massachusetts, USA |
| PE/Dazzle™ 594 anti-human CD279 (PD-1) Antibody | Biolegend | San Diego, California, USA |
| Penicillin-Streptomycin (Pen-Strep) | Thermo Fisher Scientific | Waltham, Massachusetts, USA |
| PerCP/Cyanine5.5 anti-human CD27 Antibody | Biolegend | San Diego, California, USA |
| Rotenone | Sigma-Aldrich | St. Louis, Missouri, USA |
| RPMI-1640 medium | Thermo Fisher Scientific | Waltham, Massachusetts, USA |
| SDHA (D6J9M) XP® Rabbit mAb | Cell Signaling Technology | Danvers, Massachusetts, USA |
| Sodium Fumarate dibasic | Sigma-Aldrich | St. Louis, Missouri, USA |
| Sodium phosphate dibasic | Sigma-Aldrich | St. Louis, Missouri, USA |
| Sodium phosphate monobasic monohydrate | Sigma-Aldrich | St. Louis, Missouri, USA |
| Zombie Aqua™ Fixable Viability Kit | Biolegend | San Diego, California, USA |
| Zombie Violet™ Fixable Viability Kit | Biolegend | San Diego, California, USA |

**Table 2:** Materials List.

| Material | Brand + Reference | Headquarters |
|---|---|---|
| 1 mL Pipette | Sigma-Aldrich | St. Louis, Missouri, USA |
| 10 µL Pipette | Sigma-Aldrich | St. Louis, Missouri, USA |
| 10 mL Pippettes | Sigma-Aldrich | St. Louis, Missouri, USA |
| 100 µL Pipette | Sigma-Aldrich | St. Louis, Missouri, USA |
| 15 mL CELLSTAR® Polypropylene Tube | Greiner Bio-One | Kremsmünster, Austria |
| 2 µL Pipette | Sigma-Aldrich | St. Louis, Missouri, USA |
| 200 µL Pipette | Sigma-Aldrich | St. Louis, Missouri, USA |
| 5 mL Corning® Costar® Stripette® serological pipettes | Corning Life Sciences | Amsterdam, Netherlands |
| 50 mL CELLSTAR® Polypropylene Tube | Greiner Bio-One | Kremsmünster, Austria |
| 50 mL Leucosep™ Tube | Greiner Bio-One | Kremsmünster, Austria |
| 96-Wells V-Bottom Plates | Thermo Fisher Scientific | Waltham, Massachussets, USA |
| BD FACSCelesta™ Flow Cytometer | Becton Dickinson & Company | Franklin Lakes, New Jersey, USA |
| BD LSR II™ Flow Cytometer | Becton Dickinson & Company | Franklin Lakes, New Jersey, USA |
| Greiner CELLSTAR® 24-well Culture Plates | Greiner Bio-One | Kremsmünster, Austria |
| Heracell 150i Incubator | Thermo Fisher Scientific | Waltham, Massachussets, USA |
| Heraceus™ Biofuge Pico™ Microcentrifuge | Thermo Fisher Scientific | Waltham, Massachussets, USA |
| MACS Multistand | Miltenyi Biotec | Gladbach, Germany |
| MidiMACS Separator | Miltenyi Biotec | Gladbach, Germany |
| NMR 1.5 mm Tubes | NORELL, Inc. | Morganton, North Carolina, USA |
| Rotofix 32 A | Andreas Hettich | Tuttlingen, Germany |
| Varian 600 MHz Spectrometer | Varian | Palo Alto, California, USA |

## 2.2 Patients

The peripheral blood samples were collected from 20 Rheumatoid Arthritis patients (disease group, RA) and 16 healthy donors (control group, CNT). The patients were recruited at the Internal Medicine V department of Heidelberg University Hospital (Im Neuenheimer Feld, Heidelberg, Germany). From the 16 healthy volunteers, we did not have access to the demographic data from 2 of them because these samples correspond to Buffy-Coats obtained by DRK Blutspendedienst and collect at Blutbank IKTZ in Heidelberg gGmbH (INF 305, 2. OG). The demographic data of both groups and the clinical parameters of RA group is indicated in **Table 3**.

The study was approved by the Institutional Ethics Committee (272/2006, S-374/2008 and S-096/2016). All subjects signed an informed written consent prior to any study procedure.

**Table 3**: Demographic data of both CNT and RA patients and clinical parameters of the disease group.

| Parameter | CNT (n=14) | RA (n=20) |
|---|---|---|
| Female: Male | 8:6 | 15:5 |
| Average Age (years) | 39,5 | 67,0 |
| (min-max in years) | 21-63 | 48-84 |

## 2.3 Methods

### 2.3.1 $CD4^+$ T cells isolation

Starting with the peripheral blood samples, the Peripheral Blood Mononuclear Cells (PBMCs) were isolated through centrifugation (2500 rpm, 10 minutes, room temperature, brakes off) using a 1.070 density separating solution (Biocoll). The supernatant obtained was transferred to a new tube, filled out with (1x)PBS (Sigma) and centrifuged (2000 rpm, 10 minutes, room temperature, brakes off). The supernatant was discarded and the PBMCs pellet was resuspend in MACS buffer being the $CD4^+$ T cells isolated using a human $CD4^+$ T cell isolation kit (Biolegend) through a magnetic separation protocol provided by the company (available at *www.biolegend.com*). After the isolation, $CD4^+$ T cells were counted in the microscope (Nikon, 10x amplification) using a Hemocytometer (Assistent), in the presence of Trypan-Blue to exclude dead ones, in order to, in future steps, do the normalization of the data obtained.

### 2.3.2 $CD4^+$ T cells stimulation and culturing

The $CD4^+$ T cells were cultured for 72 hours at 37 ˚C, 5% $CO_2$ in three different mediums supplemented with distinct combinations of $^{13}C$ enriched substrates and, for each medium, there were four conditions: non-stimulated, stimulated, stimulated in addition to FX11 inhibitor (60 μM) and stimulated in addition to Rotenone inhibitor (2 μM). Being the inhibitors originally diluted in DMSO, the non-stimulated and stimulated mediums had 1% DMSO (v/v). The composition of mediums were: a) RPMI medium with 5 mM [U-$^{13}C$]glucose, 2 mM non-labelled glutamine, 10 % FCS and 1 % Pen-Strep; b) RPMI medium (without glucose or glutamine) with 2 mM [1,6-$^{13}C_2$]glucose, 2 mM [U-$^{13}C$]glutamine, 10 % FCS and 1 % Pen-Strep; c) RPMI medium (without glutamine) with 1 mM non-labelled glucose, 2 mM [U-$^{13}C$]glutamine, 1 mM [2,4,6,8-$^{13}C_4$]octanoate

and 1% Pen-Strep. The enriched substrates are from Sigma. The stimulation was induced to the cells via anti-human CD28 and plate-bound anti-human CD3 (Biolegend).

### 2.3.3 Enzyme expression, oxidative stress and lipid levels measurement

After 72 hours of culturing, the media were collected to tubes and $CD4^+$ T cells were isolated by centrifugation at 7000 rpm, 5 minutes. The supernatant (medium), corresponding to each culture condition previously described, was saved to perform NMR analysis (described in a subsection below) and the cell pellet was resuspend in (1x)PBS (Sigma). Each cell suspension was then pipetted into 5 different wells in V-bottom 96-well plates (Thermo-Fisher). The $CD4^+$ T cells were incubated for 30 minutes with mouse anti-human antibody against Zombie (diluted 1:500 in (1x)PBS), room temperature, dark. Then the cells were incubated for 45 minutes with mouse anti-human CD27, CD45 RO, CD45 RA, CD4 and PD-1 antibodies diluted 2:100 in (1x)PBS, room temperature, dark. The wells destined to measure the oxidative stress and lipid levels were incubated for 15 minutes, 37 ˚C, dark, with Bodipy (Thermo Fisher Scientific) and CellRox (Thermo Fisher Scientific) diluted 1:1250 and 2,5:1250, respectively, in (1x)PBS. All the wells were incubated for 20 minutes, room temperature, dark with Fixation/Permeabilization buffer (BD Biosciences). The wells destined to quantify the enzyme expression were then incubated overnight, 4 ˚C, dark, with unconjugated polyclonal rabbit anti-human antibodies LDHA, PDH, GDH or SDHA, all of them diluted 2:100 in (1x)Perm/Wash buffer (BD Biosciences) and, after this proceed, goat anti-rabbit IgG Alexa Fluor 488 secondary antibody, diluted 1:500 in (1x)PBS, were added to the wells and incubated for 30 minutes, room temperature, dark.

The cells were resuspended in (1x)PBS and FACS was performed in a BD FACSCelesta™ flow cytometer and using the BD FACSDiva™ software provided. All the data obtained was processed and analyzed using FlowJo® v10.6.1 software (Becton Dickinson & Company, Franklin Lakes, New Jersey, USA).

### 2.3.4 Cytokine quantification

Citokine quantification was performed in cell-culture media isolated from the cells, after 72 hours of culturing, by centrifugation (as explained above). The cytokines (IL-2, IL-4, IL-5, IL-6, IL-9, IL-10, IL-13, IL-17A, IL-17F, IL-21, IL-22, IFN-γ and TNF-α) quantification was done using a custom-made LEGENDplex™ Multi-Analyte Flow Assay Kit (Biolegend) following manufacturer's instructions accessible at

*www.biolegend.com/legendplex*. The plates were read in a BD™ LSR II flow cytometer and using the BD FACSDiva™ software provided. All the data obtained were processed and analyzed in a CBA raw way using LEGENDplex™ Data Analysis Software v.8 (Biolegend). The concentrations obtained were normalized using the number of $CD4^+$ T cells counted before culturing, as explained above.

### 2.3.5 Metabolite quantification

Cell-culture media were separated of the cells by centrifugation (7000 rpm, 5 minutes). Proton ($^1H$) Nuclear Magnetic Resonance (NMR) Spectroscopy was used to quantify some target metabolites such as glucose, lactate and their respective isotopomers obtained by utilization of the $^{13}C$ enriched substrates.

The samples were composed by 180 µL of cell-culture medium and 45 µL of 10 mM sodium fumarate phosphate buffer in 99.9% $D_2O$, being the latter used for internal reference for quantification purposes. $^1H$ NMR spectra were acquired in a 14,1 Tesla spectrometer equipped with a 3-mm PFG triple resonance indirect detection probe (Varian). Each spectrum of media consisted of 64 averaged transients and typical acquisition parameters included a spectral width of 7183.9 Hz, a radiofrequency observation pulse of 30˚ and an interpulse delay of 10 seconds to ensure full relaxation of all $^1H$ nuclei in the sample, for quantification purposes. Solvent presaturation was applied before the radiofrequency excitation pulse. Spectral analyses and deconvolution (by line-fiting and integral-display sub-routines) were performed using NUTSpro™ NMR software (Acorn NMR Inc., Livermore, CA, USA).

### 2.3.6 $CD4^+$ T cells proliferation

After purification and prior to *in vitro* culturing in the three distinct mediums aforementioned in non-stimulated or stimulated conditions, $CD4^+$ T cells were incubated with 5 µM carboxyfluorescein diacetate succinimidyl ester (CFDA, SE) for 5 min at room temperature, dark, and washed twice with (1x)PBS with 5 % of heat-inactivated FBS. After 72h of *in vitro* culturing, the cells were additionally stained with antibodies against Annexin V, which allows to measure the apoptotic activation of the cells. Cell proliferation was then assessed by determining CFSE fluorescence decay and apoptotic indicators were measured by flow cytometry in a BD™ LSR II flow cytometer and using the BD FACSDiva™ software provided. All the data obtained were processed and

analyzed using FlowJo® v10.6.1 software (Becton Dickinson & Company, Franklin Lakes, New Jersey, USA).

### 2.3.7 Mitochondrial membrane potential and glucose and palmitate incorporation

Purified $CD4^+$ T cells were cultured *in vitro* for 72h at 37 ˚C, 5 % $CO_2$ in a RPMI medium containing 5 mM of Glucose and 2 mM of Glutamine in four different conditions: non-stimulated, stimulated, stimulated in addition to FX11 inhibitor (60 µM) and stimulated in addition to Rotenone inhibitor (2 µM). Being the inhibitors originally diluted in DMSO, the non-stimulated and stimulated mediums had 1% DMSO (v/v). The cells were then stained with antibodies against CD4 and also with the dead cell marker Zombie, being after that divided in 3 groups. Cells were stained with JC-1 (100 µL of (1x) PBS containing 2,12 µM of JC-1), which allows to follow de depolarization of the mitochondrial membrane, with 2-NBDG (100 µL of (1x)PBS with 0,2 µM of 2-NBDG), which allows to follow the cellular glucose incorporation), or with Bodipy-Palmitate (200 µL of (1x)PBS with 1 µM of Bodipy-Palmitate), which allows to follow the cellular palmitate incorporation. The cells were then immediately analyzed by flow cytometry in a BD™ LSR II flow cytometer and using the BD FACSDiva™ software provided. All data obtained was processed and analyzed using FlowJo® v10.6.1 software (Becton Dickinson & Company, Franklin Lakes, New Jersey, USA).

### 2.3.8 LDHA enzymatic activity

Purified $CD4^+$ T cells from healthy individuals were cultured *in vitro* for 72h at 37 ˚C, 5 % $CO_2$ in a RPMI medium containing 5 mM [U-$^{13}$C]glucose and at five distinct conditions: non-stimulated, stimulated and stimulated in addition to FX11 inhibitor (45, 60 or 75 µM). The LDHA activity was then extrapolated by measuring and comparing the [U-$^{13}$C]lactate produced between the different conditions, being the values normalized utilizing the number of cells counted prior to *in vitro* culturing as explained in section **2.3.1**. The NMR measurements were processed using the method described at section **2.3.5**.

### 2.3.9 Statistical analysis

All obtained data was analyzed using GraphPad Prim 7.00 software (GraphPad Software, Inc., San Diego, California, USA). The normal distribution of the values of each group was analyzed by *D'Agostino & Pearson* normality test. If the normality of

distribution was confirmed ($p > 0,05$), *Sidak's* multiple comparisons test (Ordinary one-way ANOVA) was applied, if normality was not confirmed ($p < 0,05$), *Dunn's* multiple comparisons test (non-parametric Kruskal-Wallis test) was applied. In either case, the results were considered statistically different between groups when $p < 0,05$. The charts represent the median with 95 % of confidence interval (95 % CI), being each individual sample value represented by the dots or triangles shown.

# 3 Results and Discussion

## 3.1 $CD4^+$ T cells subsets variability

Analyses previously performed by our group permit us to identify and quantify the different $CD4^+$ T cells subsets presence in peripheral blood samples collected from both CNT and RA group. This distinction was done by FACS and, principally, using antibodies against CD45 RA, CD45 RO and CCR7 that enable the recognition and separation of the distinct subsets.

In **Figure 10** is represented the relative abundance of each type of this $CD4^+$ T cells subsets, namely the Central Memory (CM), Effector Memory (EM), Naïve, Effector (TEMRA), Follicular Helper (Tfh) and Regulatory (Treg) as well as the relative abundance of $CD4^+$ T cells between all cells collected (grey shaded area) in both CNT and RA groups.

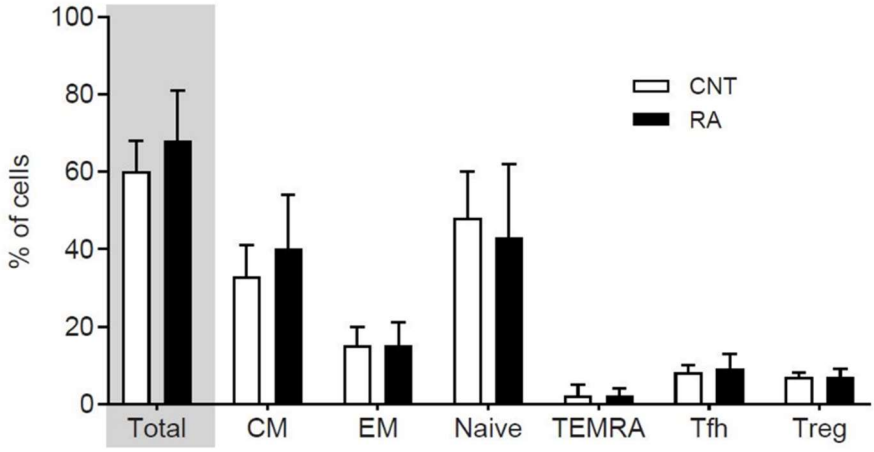


**Figure 10 -** Relative abundance of the different $CD4^+$ T cells subsets isolated from peripheral blood collected from both CNT and RA groups.

This data shows us that the most abundant subsets in $CD4^+$ T cells from both CNT and RA group are the Naïve subset, the Central Memory (CM) subset, and the Effector Memory (EM) subset. As expected, and in accordance to what was explained in the Introduction chapter, in the RA group there is a higher amount of CM than in the CNT group and, on the contrary, the Naïve subset had a higher expression in CNTs than in RAs. All the other $CD4^+$ T cells subsets show little or no variation between the groups.

In this study, the various analyses were done in total of $CD4^+$ T cells collected and not in a specific subset. It is of the utmost importance to retain this information through this Results and Discussion section as well as in the Conclusions, since the

majority of the answers that we will obtain here will be applicable to the whole $CD4^+$ T cells population and not to a specific $CD4^+$ T cells subset. Although, in a latter subsection of this chapter it will be possible to analyze some data related to enzymatic expression where the Naïve and Memory subsets were distinguished.

Looking again to Figure 10, and focusing on the first two columns, one can conclude that in RA patients the relative abundance of $CD4^+$ T cells is higher than in CNT group. However, in terms on absolute numbers, it is important to note that normally the number of $CD4^+$ T cells in RA group is lower when compared with the value obtained from healthy individuals' group as show in **Figure 11**.

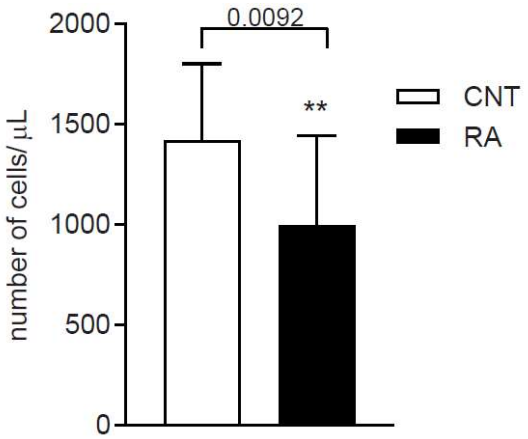


**Figure 11** - Representation of the absolute number of cells per µL isolated from peripheral blood collected from both CNT and RA group.

This evident decrease in the number of $CD4^+$ T cells in peripheral blood from CNT to RA group could be easily explained by the therapies used by the patients, which include immune-suppressive treatments. Although affecting the number of cells in circulation, the referred treatments do not affect the metabolic and cytotoxic function of $CD4^+$ T cells as it was demonstrated previously by our group (data not published).

## 3.2 Preliminary data about $CD4^+$ T cells metabolism

Some data analysis made previously by our group had focused its attention in establishing if there was a clear pattern in terms of metabolic enzymes and structural proteins expression in $CD4^+$ T cells, when comparing healthy individuals (CNT) and disease affected patients (RA), and as well if there existed distinguishable patterns between Central Memory, Effector Memory and Naïve subsets. These patterns could then give us a first idea of the metabolic modulation that $CD4^+$ T cells suffer when in the disease context.

This referred metabolic genes expression analysis were performed using the microarray dataset GSE93776 available in the public Gene Expression Omnibus repository (available at: *www.ncbi.nlm.nih.gov/geo/query/acc.cgi?acc=GSE93776*). The results related to the metabolic gene expression analysis are shown in **Figure 12**.

This data show that for the great majority of metabolic-linked genes, the CNT and RA groups have a different pattern of expression which clearly points towards a metabolic modulation or adaptation in the context of this autoimmune disorder. When looking more specifically to the different subsets analyzed it is also worth to mention that, as expected, Naïve, CM and EM $CD4^+$ T cells present expression variability between them which supports the idea that the metabolic modulation could affect these subsets in a non-homogeneous way.

Although not totally clear, in $CD4^+$ T cells, generally speaking, the enzymes linked to the activation of glycolysis demonstrate a higher expression in the disease context. A quick look to the Lactate Dehydrogenase isoforms, especially the isoform A (LDHA), gives us the clear idea that in $CD4^+$ T cells from RA group this enzyme is being more expressed, which could be indicative of an exacerbated utilization of LDHA probably supporting an increased aerobic glycolysis rate.

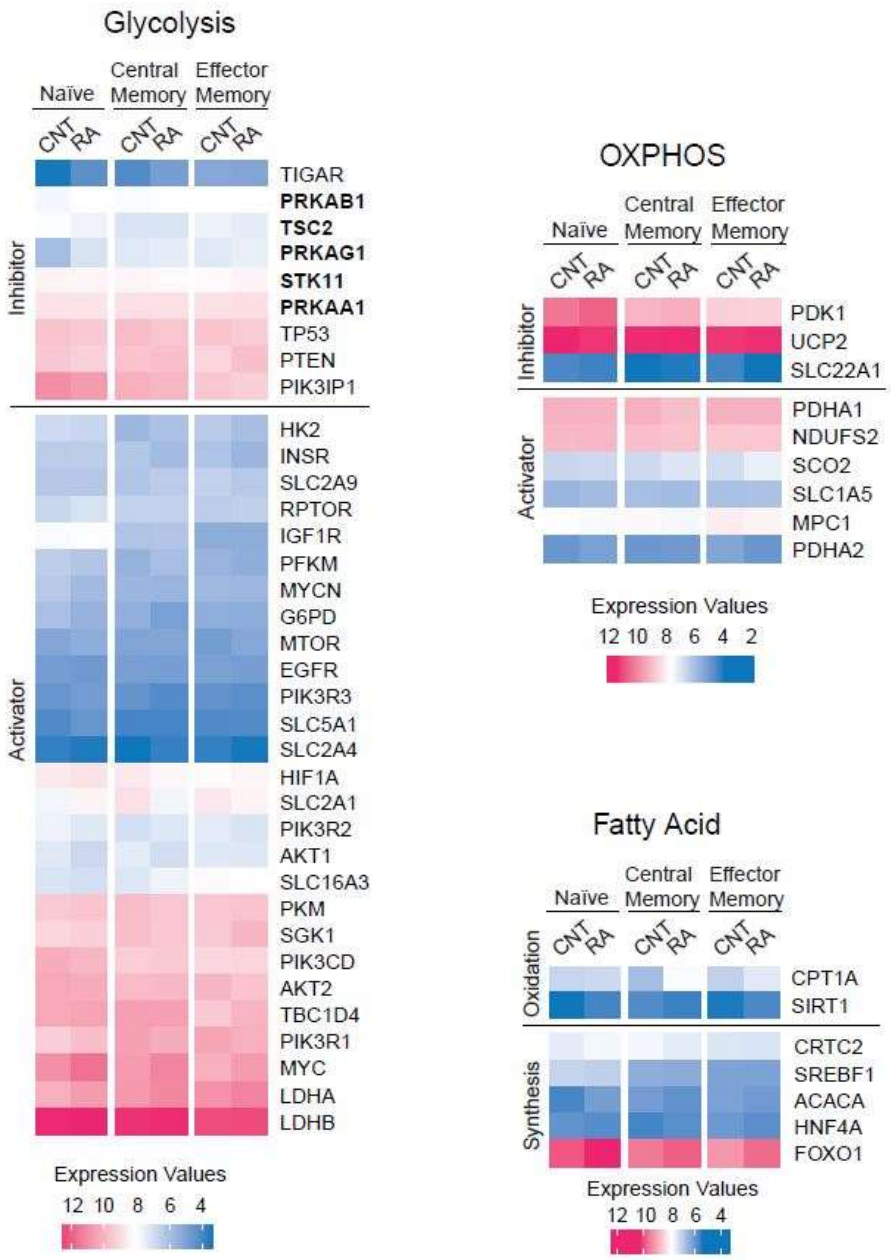


**Figure 12** - Representation, in form of heat-maps, of the metabolic-related genes expression in the different subsets of $CD4^+$ T cells in both CNT and RA group, namely the ones linked to glycolysis, oxidative phosphorylation (OXPHOS) and fatty acid metabolism. Pink represents higher expression, blue lower expression.

Concerning the expression of genes linked to fatty acid metabolism, it is clear that in the RA group, in all subsets, the oxidation-related genes are sub-expressed indicating a lower utilization of this process in the disease context. On the other hand, the genes linked to fatty acid synthesis are, generally speaking, more highly expressed in the RA than in the CNT group. In the OXPHOS-related genes it is difficult to stablish a clear pattern comparison between RA and CNT and even between $CD4^+$ T cells subsets.

Although this preliminary data on $CD4^+$ T cells' metabolic genes is not fully conclusive, it already gives us the idea that the metabolic activity in these cells suffer alterations in the context of RA disease. The objective in the following sections is to determine the metabolic alterations that characterize the RA $CD4^+$ T cells, using the stable isotope implemented methodology.

In addition to the metabolic-related gene expression analysis it is also possible, recurring to the same data base aforementioned, to analyze the variations between CNT and RA group and also between the different $CD4^+$ T cells subsets related to genes connected to immune functions, as well as to the autophagy process. **Figure 13** represents the resulting heat-maps obtained by this analysis.

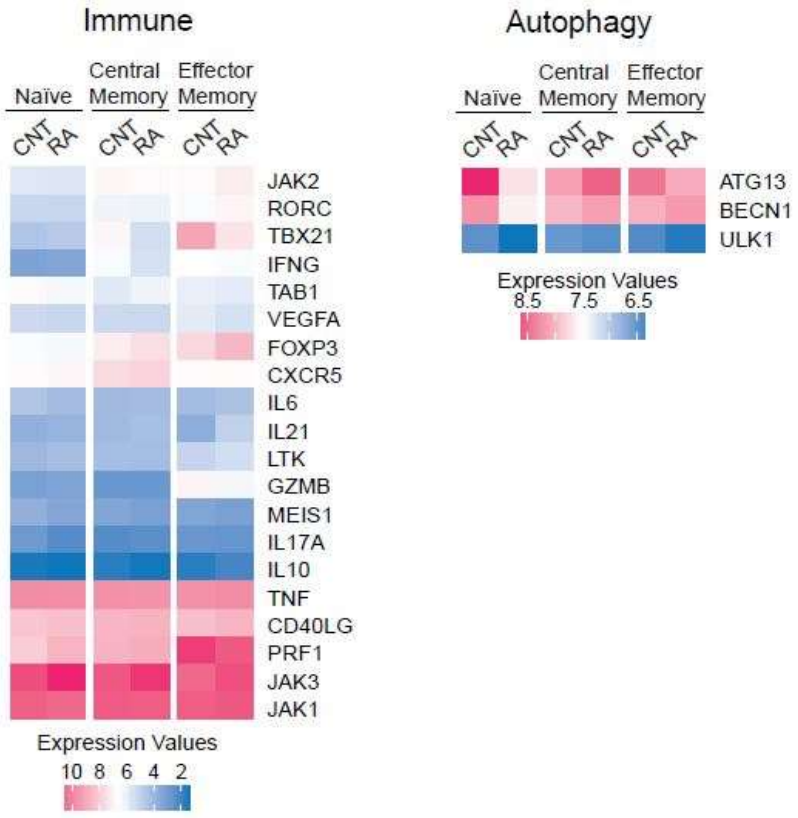


**Figure 13** - Representation, in the form of heat-maps, of the gene expression comparison between CNT and RA group and the distinct of $CD4^+$ T cells subsets immune- and autophagy- related genes. Pink represents higher expression, blue lower expression.

As expected, this data shows us that both between the two groups (CNT and RA) and the distinct $CD4^+$ T cells subsets, there are differences in the expression of both immune-related and autophagy-linked genes. However, these differences are not clear to

the level of defining a pattern that fits each cell subset or conditions. Some cytokines such as IL-21 or IL-10 present a lower expression in RA group than in CNT group, although others (e.g., IL-6 or TNF-α) show little or no variation at all. On the contrary, some enzymes, such as the cytokine receptor associated Janus Kinase 3 (JAK3), present a higher expression in the disease group. Also, when considering autophagy related genes, the pattern is not clearly distinguishable, although we can say that the RA condition induces differences not just between individuals' groups but also between the different cell subsets.

### 3.3 Metabolic modulation approach of $CD4^+$ T cells

In order to get a deeper and clearer understanding of the metabolic adaptation and of the influence that such metabolic modulation has in cells' functions and its importance in disease establishment we developed and employed an experimental approach based in feeding cells with $^{13}C$-enriched substrates and the follow up of $^{13}C$ incorporation in metabolic intermediates to decipher changes in metabolic fluxes. $CD4^+$ T cells were cultured with media containing distinct $^{13}C$-enriched substrates and NMR analysis of cell culture media by NMR allows the monitoring of substrate consumption and production of intermediary metabolites, resulting from the cells' metabolism. Associated with FACS, where the expression of some enzymes and specific proteins like cytokines could be followed, this method gave us the opportunity to evaluate whether and how $CD4^+$ T cells could adapt themselves to distinct substrate availability and, in that way, exert their immunological functions.

As already aforementioned, namely in the Materials and Methods section, $CD4^+$ T cells, after isolation and without separation of the different subsets, were cultured in three different media:

a) Medium Glc: 5 mM [U-$^{13}C$]glucose and 2 mM unlabeled glutamine;

b) Medium GG: 2 mM [1,6-$^{13}C_2$]glucose, 2 mM [U-$^{13}C$]glutamine;

c) Medium Oct: 1.1 mM unlabeled glucose, 2 mM [U-$^{13}C$]glutamine, 1 mM [2,4,6,8-$^{13}C_4$]octanoate.

The composition of these media enabled us to focus our attentions in the main metabolic fluxes of cells, namely the ones involving glucose, glutamine and fatty acids (**Figure 14**). The analysis included two main experimental conditions, the non-stimulated and the stimulated (by plate-bound anti-CD3 and anti-CD28), and the supplementation of

cell culture media with FX11 (LDHA inhibitor) or Rotenone (Mitochondrial Respiratory Chain Complex I inhibitor).

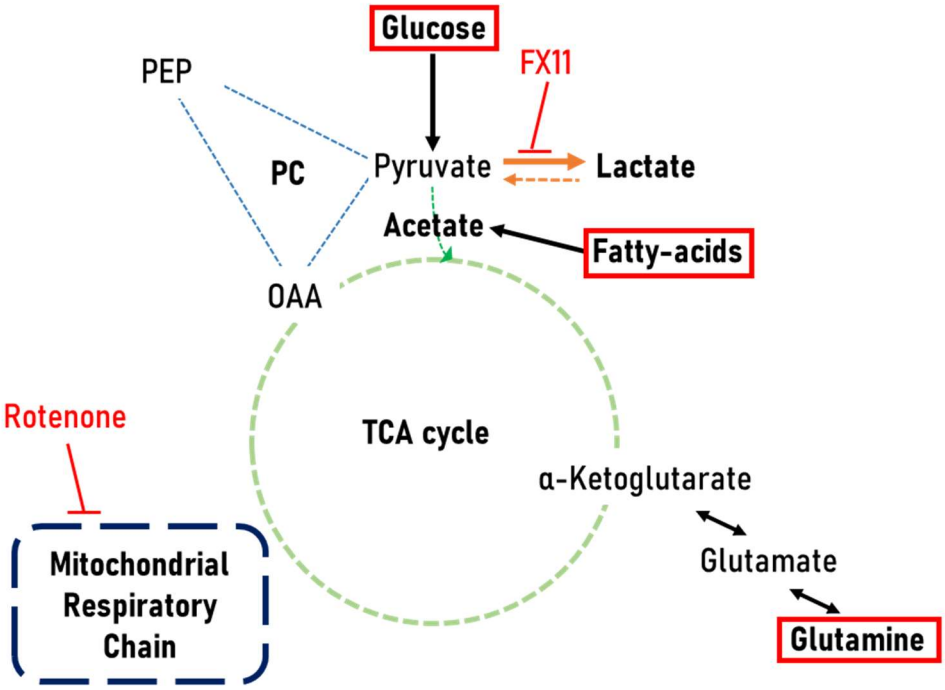


**Figure 14 -** Schematic representation of the main cellular metabolic fluxes with focus in the three main substrates fed to $CD4^+$ T cells in the distinctly $^{13}C$-enriched cell culture media of glucose, glutamine and fatty acids. The inhibitors tested are also represented in the figure in the place of their action. Abbreviations: OAA (Oxaloacetate); PEP (Phosphoenolpyruvate); PC (Pyruvate Cycle); TCA (Tricarboxylic Acid).

As explained in the Introduction section, the evaluation of the metabolic activity of $CD4^+$ T cells was essentially based in the lactate molecule and its $^{13}C$-isotopomers identification and quantification by $^1H$ NMR. The alterations of $^{13}C$-enriched substrates' availability and their consumption by the cells produces distinct $^1H$ NMR multiplets in the resonances of the lactate methyl group, which allows the identification of which substrate is preferably being used at each of the experimental conditions and which metabolic fluxes are involved.

In **Figures 15-17** are represented the metabolic diagrams that resume the cellular metabolic activity that is possible to evaluate by the $^1H$ NMR technique using the distinct $^{13}C$-enriched substrates and measuring the different Lactate isotopomers produced by the consumption of those substrates.

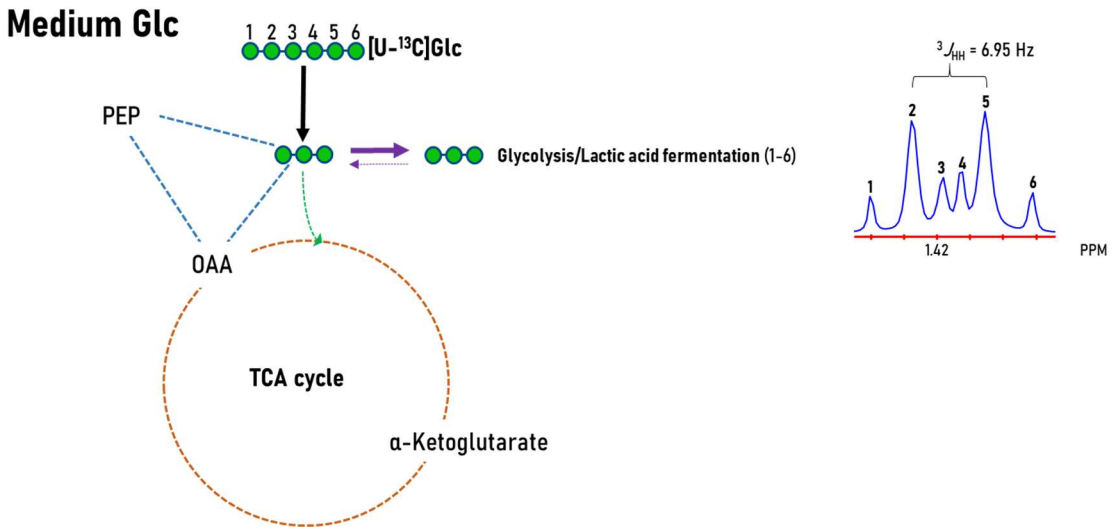


**Figure 15 -** Schematic representation of the Medium Glc where the cells were fed with [U-$^{13}$C]glucose. The utilization of this substrate occurs extensively through the glycolytic pathway, generating [U-$^{13}$C]Lac. The labelling in the third carbon (C3), the methyl one, leads to the appearance of two $^{13}$C satellites ($^{1}J_{CC}$ = 128 Hz), surrounding the central resonances due to the [U-$^{12}$C]Lac. In this case, we have focused our analysis in the 1.41 ppm region, due to one of the $^{13}$C satellites, where it is easily visible a doublet of triplets (resonances 1-6) given by the [U-$^{13}$C]Lac isotopomer, which result from three coupling constants ($^{3}J_{HH}$ = 6.95 Hz, and $^{2}J_{HC} \approx {}^{3}J_{HC} \approx 4.25$ Hz). Abbreviations: Glc (Glucose); OAA (Oxaloacetate); PEP (Phosphoenolpyruvate); TCA (Tricarboxylic Acid).

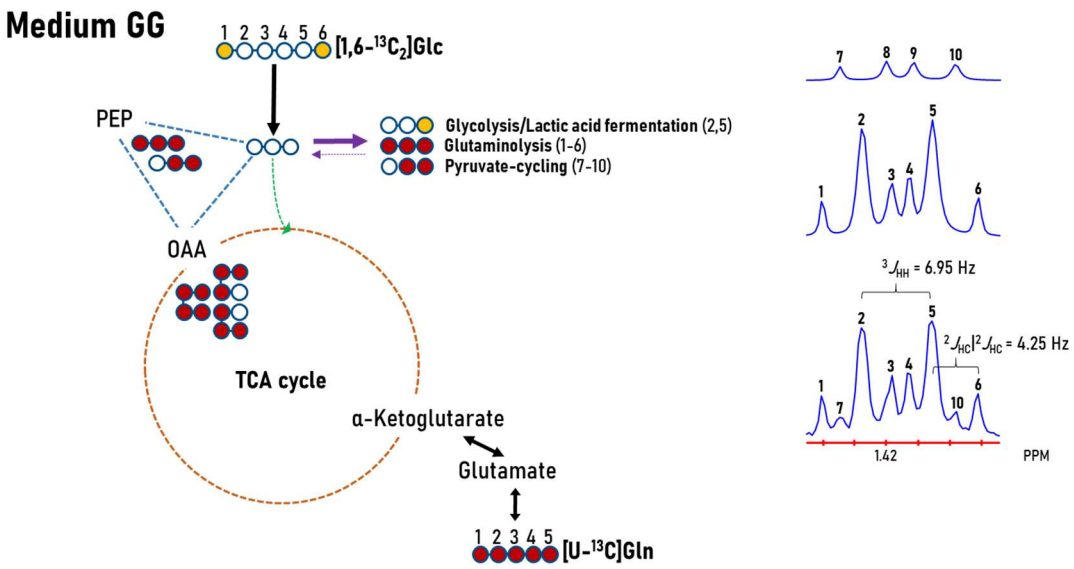


**Figure 16** - Schematic representation of the Medium GG where the cells were fed with both [1,6-$^{13}C_2$]glucose and [U-$^{13}$C]glutamine. The use of [1,6-$^{13}C_2$]glucose occurs almost exclusively by glycolysis, which generates the [3-$^{13}$C]Lac isotopomer. The carbon from the lactate methyl group (C3) is labelled, leading to the appearance of satellites surrounding the resonance of the [U-$^{12}$C]Lac (1.31 ppm). We have focused in the 1.41 ppm region, due to one of the $^{13}$C satellites, where it is easily visible a doublet (**2,5**) due to the coupling between the methyl hydrogens and the vicinal hydrogen, attached to carbon 2 ($^3J_{HH}$ = 6.95 Hz). In the same region it is possible to observe the resonances from [U-$^{13}$C]Lac isotopomer (**1-6**) produced by consumption of [U-$^{13}$C]glutamine by glutaminolysis where glutamine is "directly" oxidized to lactate by passing through the Krebs cycle intermediates until reaching OAA, that is decarboxylated to PEP and subsequently converted to Pyruvate and Lactate. The [2,3-$^{13}C_2$]Lac isotopomer is produced by pyruvate-cycling activity. Due to the "backward scrambling" that occurs with the intermediates of the Krebs cycle (OAA↔Mal↔Fum) in 50% of the situations the cycled [U-$^{13}$C]Lac is converted to [2,3-$^{13}C_2$]Lac, raising at each turn the contribution of this particular lactate isotopomer. In the multiplet expansions are readily visible the different multiplets which are generated by these three isotopomers. A real multiplet that congregates the three isotopomers is presented at the bottom. In the middle spectrum it is visible the doublet of triplets (1-6) given by the [U-$^{13}$C]Lac isotopomer, that is the result of 3 coupling constants (a $^3J_{HH}$ = 6.95 Hz, and a $^2J_{HC} \approx {}^3J_{HC} \approx 4.25$ Hz) as well as the doublet from [3-$^{13}$C]Lac ($^3J_{HH}$ = 6.95 Hz). At the top spectrum is represented the doublet of doublets (pseudo-quartet, resonances **7-10**) due to the [2,3-$^{13}C_2$]Lac isotopomer, the result of the splitting caused by two coupling constants ($^3J_{HH}$ = 6.95 Hz and $^2J_{HC} \approx 4.25$ Hz). Abbreviations: Glc (Glucose); Gln (Glutamine); OAA (Oxaloacetate); PEP (Phosphoenolpyruvate); TCA (Tricarboxylic Acid).

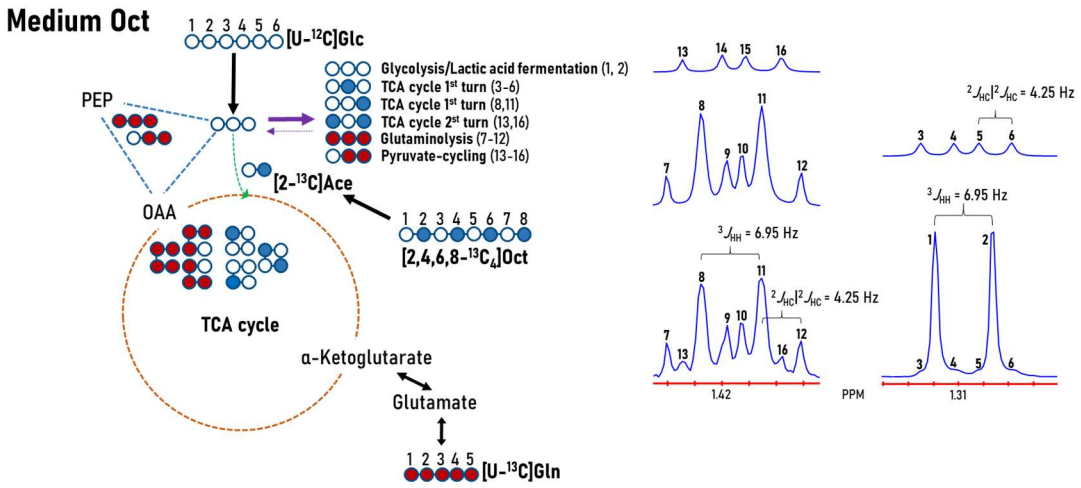


**Figure 17** - Schematic representation of the Medium Oct where the cells were fed with natural-abundance (NA; 1.1% in each carbon) enriched glucose (essentially [U-$^{12}$C]glucose), [U-$^{13}$C]glutamine and [2,4,6,8-$^{13}C_4$]octanoate. The first substrate will produce the [U-$^{12}$C]Lac isotopomer (1.31 ppm, $^3J_{HH}$ = 6.95 Hz) represented by the doublet (1,2) at the right-side bottom spectrum. The use of [U-$^{13}$C]glutamine will produce the [U-$^{13}$C]Lac (7-12) and the [2,3-$^{13}C_2$]Lac (13-16) isotopomers. The use of [2,4,6,8-$^{13}C_4$]octanoate in the TCA cycle (1$^{st}$ turn) will lead to the appearance of the [2-$^{13}$C]Lac (doublet of doublets at 1.31, 3-6) and the [3-$^{13}$C]Lac (doublet at 1.41 ppm, 8,11) isotopomers, represented in the right- and left-side spectra, respectively. In a TCA cycle 2$^{nd}$ turn the [1,3-$^{13}C_2$]lactate isotopomer is produced (doublet of doublets at 1.41 ppm, 13-16), represented in the left side spectrum. Abbreviations: Ace (Acetate); Glc (Glucose); Gln (Glutamine); OAA (Oxaloacetate); Oct (Octanoate); PEP (Phosphoenolpyruvate); TCA (Tricarboxylic Acid).

Based on the information provided, the lactate isotopomers produced will tell us which substrates the cells are preferably using, and with the additional and complementary data provided by enzyme expression and cytokine production analyzes done by FACS it is possible to provide an almost complete analyzes report about CD4$^+$ T cells metabolic modulation in RA.

**Figure 18** summarizes the described experimental approach, aggregating all the $^{13}$C-enriched substrates and their respective $^1$H NMR spectral contributions.

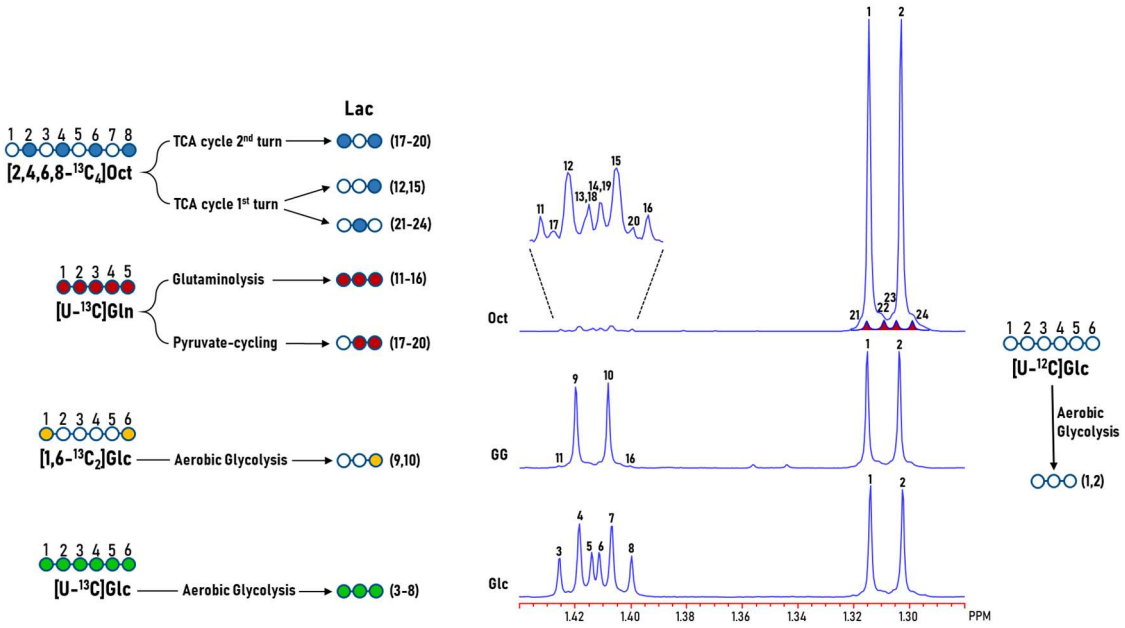


**Figure 18** - Summary of the metabolic approach described. Schematic representation of all $^{13}C$-enriched substrates used in the different media, the lactate isotopomers that could be produced by the utilization of those substrates and the respective $^{1}H$ NMR spectral resonances obtained from the methyl group (C3) of lactate. The composition of each media used: Medium Glc ([U-$^{13}C$]glucose); Medium GG ([1,6-$^{12}C_2$]glucose and [U-$^{13}C$]glutamine); Medium Oct (Natural abundance glucose, [U-$^{13}C$]glutamine and [2,4,6,8-$^{13}C_4$]octanoate). Abbreviations: Glc (Glucose); Gln (Glutamine); Oct (Octanoate); TCA (Tricarboxylic Acid).

Having the fundamentals of the experimental approach used to evaluate the $CD4^+$ T cells metabolism being presented and explained, we will follow with its practical uses in metabolic evaluations. In **Figure 19** could be observed a representative example of the spectra that were obtained in Glc, GG and Oct media for the Stim conditions.

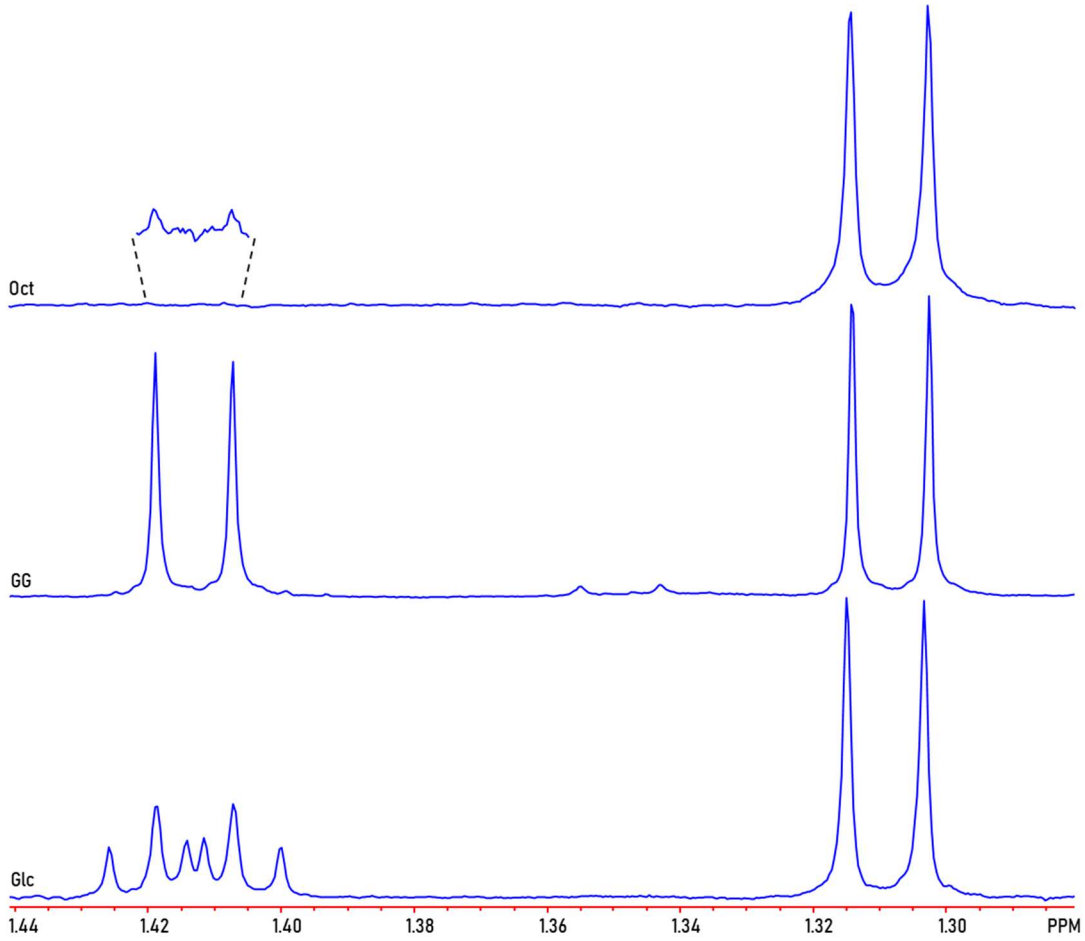


**Figure 19 -** Expansions of the lactate regions obtained from representative $^{1}$H NMR spectra acquired from media when CD4$^{+}$ T cells were cultured in Stim conditions in the three chosen media: Glc, GG and Oct. The different $^{13}$C-labelled substrates, when utilized by the cells, give rise to different combinations of lactate isotopomers, which generate distinct multiplet patterns that are used to quantify each of the isotopomers present in the culture media.

### 3.3.1 Glycolytic and TCA index of CD4$^{+}$ T cells

Two of the most important concepts to evaluate the cellular metabolic activity are glycolytic versus TCA index. As the name indicates, they reflect the extent of usage of glucose by the cells in these two central metabolic fluxes. The generation of lactate under aerobic conditions is frequently used as a measure of glycolytic index and referred as glycolytic character, whilst its full oxidation via TCA cycle is frequently presented as TCA index and frequently referred as being the OXPHOS (oxidative phosphorylation) character. It is of utmost importance to refer that these indexes do not represent the absolute quantity of glucose that is used in each flux (glycolytic or TCA) but instead represent an estimate of the relative preponderance of each metabolic pathway in the utilization of this substrate, independently of initial amount provided to the cells. The

results obtained in both CNT and RA in the three different media in the stimulated (Stim) conditions are presented in **Figure 20**.

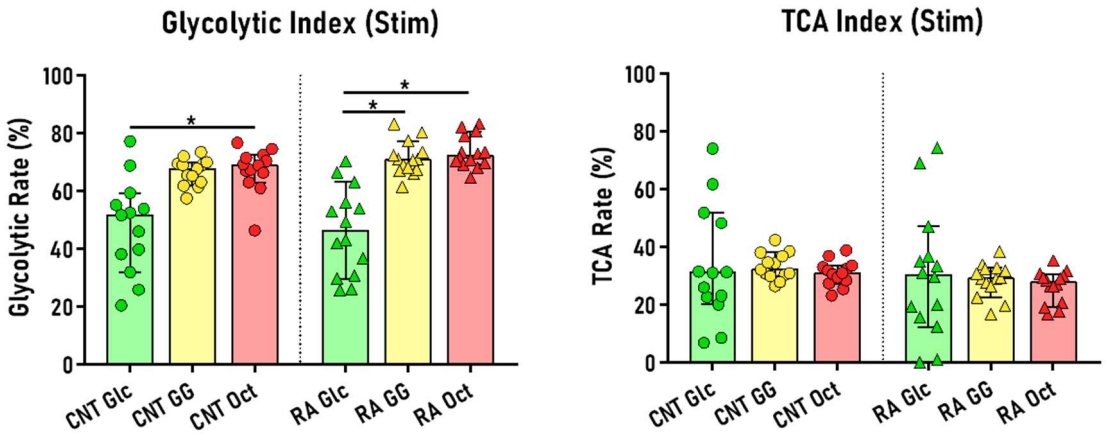


**Figure 20** - Representation of the values of Glycolytic and TCA indexes (in percentage) obtained under Stim conditions. CNT are represented on the left half of the graphs (dots), RA on the right half (triangles). Medium GLC (green), Medium GG (yellow), Medium Oct (red). The bars represent the median value and the confidence interval (CI) at 95%. *: $p<0,05$ with p being calculated using Kruskal-Wallis test with Dunn's multiple comparisons test. Abbreviations: Stim (Stimulated); TCA (Tricarboxylic Acid).

The results suggest that $CD4^+$ T cells, in both CNT and RA group, have a higher glycolytic index in GG and Oct Media when compared to that of Glc Medium. At the first sight this is rather surprising, with the medium where the glucose is more available showing the lower glycolytic index. But it is, in fact, a sustainable result since $CD4^+$ T cells are utilizing all the glucose available in the medium. Being the amount of glucose in the GG (2 mM) and Oct (1.1 mM) media much lower than in the Glc Medium (5 mM), the cells will consume all of the glucose available, being its utilization in the glycolytic flux almost maximal.

When looking to the TCA index, one could assume that the utilization of this metabolic flux for the catabolism of glucose does not change neither between groups or between media. This gives us the indication that the cells, even in more potentially "oxidative" conditions, such as the ones provided by Oct medium, present a still high glycolytic profile, producing large amounts of lactate from glucose. **Figure 21** represents the fold-change between the Stim and non-stimulated (Nstim) conditions.

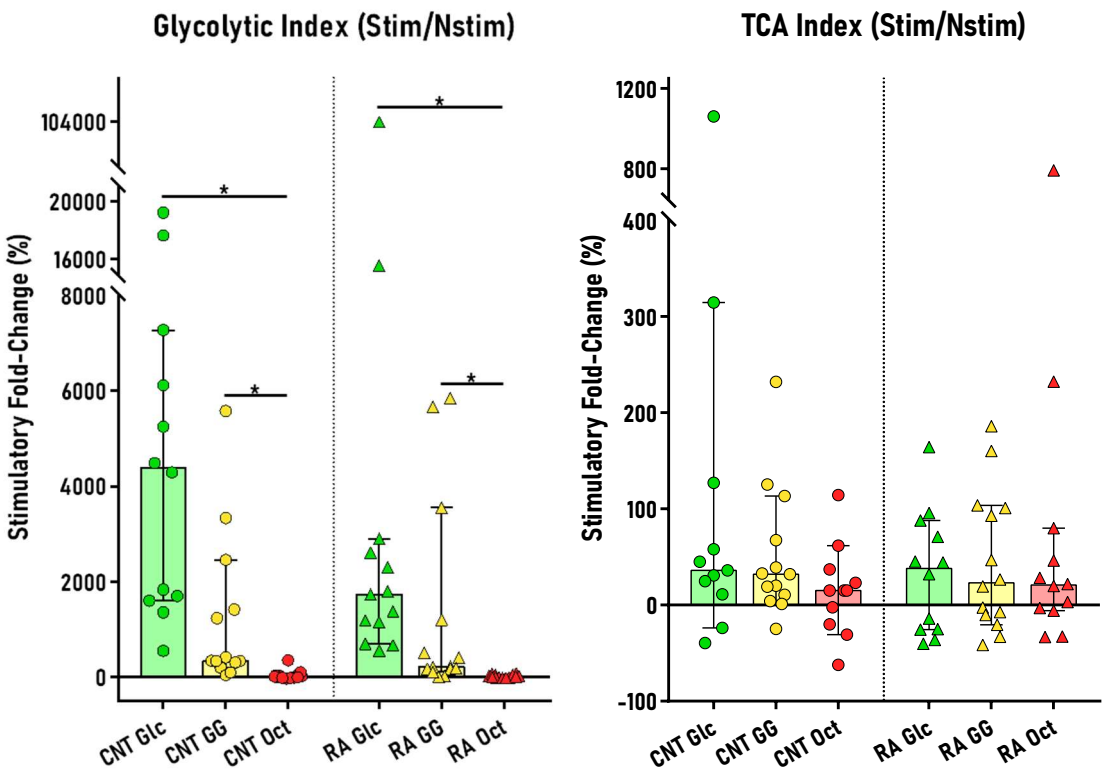


**Figure 21** - Representation of the values of stimulatory fold-change (Stim vs Nstim conditions) of Glycolytic and TCA indexes (in percentage), being the zero (0) value representing no variation. The greater the value, the greater the difference between Stim and Nstim conditions. CNT are represented on the left half of the graphs (dots), RA on the right half (triangles). Medium GLC (green), Medium GG (yellow), Medium Oct (red). The bars represent the median value and the confidence interval (CI) at 95%. *: $p<0,05$ with p being calculated using Kruskal-Wallis test with Dunn's multiple comparisons test. Abbreviations: Nstim (Non-stimulated); Stim (Stimulated); TCA (Tricarboxylic Acid).

The results indicate that the amount of glucose provided to $CD4^+$ T cells in GG and specially in Oct Medium is fully consumed even in a Nstim situation. The larger amount of this substrate provided in Glc Medium allows the cells to expand their consumption of glucose, essentially via glycolysis. There is an astonishing fold-change between Stim and Nstim conditions in both groups, being this degree higher in the CNT group, which could indicate that $CD4^+$ T cells in the RA context already present a stimulated profile, even before being stimulated *in vitro*. On the other hand, the TCA cycle presents a lower fold-change that is transversal to all the media and to both CNT and RA groups.

The effect of FX11, a LDHA inhibitor, and Rotenone, a Mitochondria Respiratory Chain Complex I inhibitor, in both glycolytic and TCA indexes are represented in **Figure 22**.

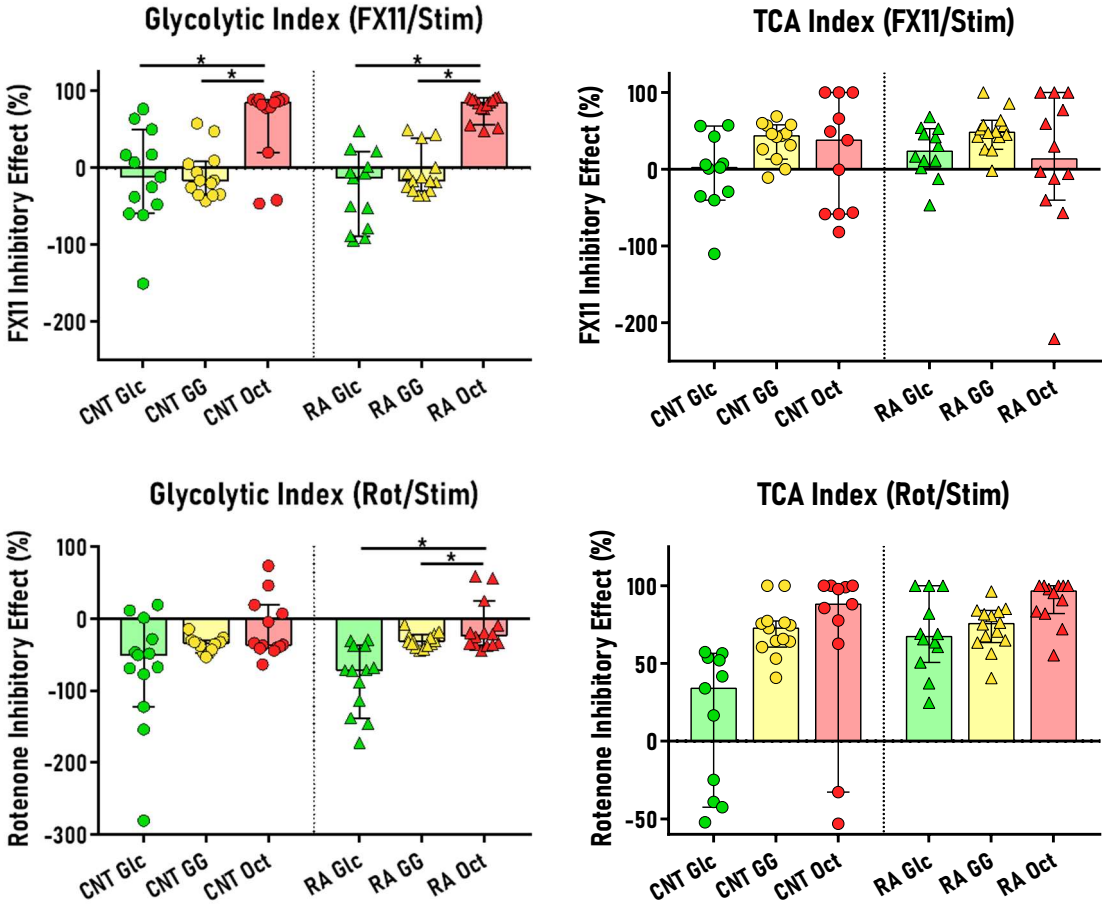


**Figure 22** - Representation of the Inhibitory Effect (in percentage relative to the Stim condition) of FX11 and Rotenone in both Glycolytic and TCA indexes. The zero (0) value represents no change relative to the Stim condition, positive values represent the extend of inhibition, negative values represent the extent of stimulation. CNT are represented on the left half of the graphs (dots), RA on the right half (triangles). Medium Glc (green), Medium GG (yellow), Medium Oct (red). The bars represent the median value and the confidence interval (CI) at 95%. *: $p<0,05$ with p being calculated using Kruskal-Wallis test with Dunn's multiple comparisons test. Abbreviations: Rot (Rotenone); Stim (Stimulated); TCA (Tricarboxylic Acid).

Considering the FX11 effect on $CD4^+$ T cells, in Oct Medium of both CNT and RA groups, we can appreciate a reduction in the global utilization of glucose either in glycolysis or in the TCA cycle, in agreement with expectations, especially considering the predictable influence of this inhibitor in the glycolytic flux. Looking to FX11 effects in Glc and GG media, there is a minimal effect on $CD4^+$ T cells glycolytic flux and, furthermore, FX11 even leads to a slight stimulation of this flux in both CNT and RA groups. Looking for the effects of FX11 in TCA flux of both Glc and GG media, the results insinuate that in both CNT and RA groups the cells from Glc medium show less

sensitivity to this inhibitor, having a lower impact in their OXPHOS activity fed by glucose.

When using Rotenone, we observed an exacerbation of the glycolytic flux in both CNT and RA groups, with an apparent greater effect in Glc Medium, probably due to the higher glucose availability. The impact of this inhibitor is, as expected, much clearer in TCA flux indicators. In all media, but more noticeable in Oct and GG media, Rotenone blocked to a greater extent the TCA flux, which could lead to the exacerbation of the utilization of glucose via glycolysis, as stated before. The suggested greater impact in Oct and GG media may be influenced by the smaller quantity of glucose available in these media and by the potentially preferable oxidative conditions provided, namely in the Oct medium.

In addition to the information provided by the glycolytic and TCA fluxes data regarding the glucose utilization by $CD4^+$ T cells, it should be also analyzed the [U-$^{13}$C]glutamine utilization by these cells in GG and Oct media, which are supplemented with this uniformly $^{13}$C enriched substrate at a concentration of 2 mM. **Figure 23** shows the result of the quantification of lactate (in nmoles per $10^6$ cells) produced by $CD4^+$ T cells by the utilization of [U-$^{13}$C]glutamine in the glutaminolysis flux (producing [U-$^{13}$C]Lac) and in pyruvate cycle followed by glutaminolysis flux (producing [2,3-$^{13}C_2$]Lac), in the referred media.

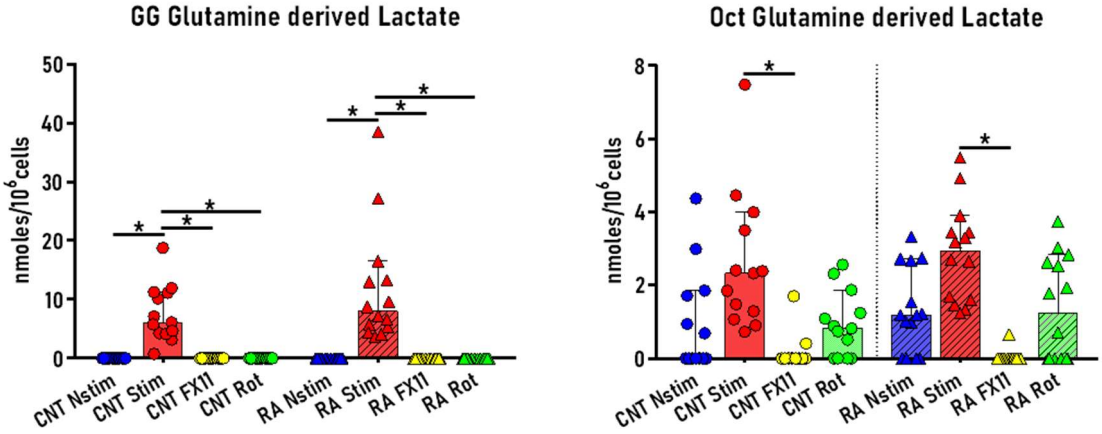


**Figure 23** - Representation of the quantity, in nmoles per $10^6$ cells, of glutamine derived lactate produced by $CD4^+$ T cells by [U-$^{13}$C]glutamine utilization via glutaminolysis ([U-$^{13}$C]Lac) and via pyruvate cycle followed by glutaminolysis ([2,3-$^{13}C_2$]Lac) in both GG medium (left side) and Oct medium (right side). CNT are represented on the left half of the graphs (dots), RA on the right half (triangles). The different conditions in each medium are represented in different colors: Nstim (blue), Stim (red), FX11 (yellow) and Rotenone (green). The bars represent the median value and the confidence interval (CI) at 95%. *: $p<0,05$ with p being calculated using Kruskal-Wallis test with Dunn's multiple comparisons test. Abbreviations: Lac (Lactate).

By observing the results in **Figure 23** we could easily conclude that glutamine is utilized by $CD4^+$ T cells as a last resource substrate, being conceivably metabolized, via glutaminolysis and pyruvate cycle, after all the glucose provided in the media disappears, which frequently occurs in later moments during the 72h incubation period. This hypothesis is supported by the fact that the appearance of glutamine derived lactate is exclusive from the Stim conditions (in both media) and in Rotenone (just in the Oct medium). The availability of glucose in Oct medium is even smaller than in GG medium (1,1 mM vs 2 mM), which may help to explain the distinct impact of Rotenone in both media (lower impact in Oct medium, which has a higher necessity of utilizing glutamine as metabolic substrate).

The results shown here, regarding the glycolytic and TCA fluxes in $CD4^+$ T cells from RA, are not fully compatible to what is published at the moment about these cells metabolism in the RA context. As demonstrated in the Introduction section, the metabolic profile of $CD4^+$ T cells has been associated with a higher utilization of glucose through PPP which has been correlated with the exacerbated biosynthetic needs of these cells and is accompanied by a decrease in the glycolytic flux utilization by $CD4^+$ T cells (Weyand *et al*., 2017; Weyand and Goronzy, 2018). Here it is suggested that, contrary to this information, glucose is being avidly metabolized by these cells via glycolysis and, even in conditions where the oxidative metabolism would be expected to be exacerbated, due to low glucose availability and glutamine/octanoate presence (GG and Oct medium), the glycolytic flux shows its greatest values. On the other hand, TCA flux maintains its levels, regardless of the conditions provided to $CD4^+$ T cells, which contradicts the oxidative profile that is being attributed to these cells (Weyand *et al.*, 2017; Hradilkova *et al.*, 2019). This fact is further reinforced when considering the null utilization of octanoate, a medium-chain fatty acid, by $CD4^+$ T cells in Oct medium, an environment where the glucose availability is particularly low (1.1 mM) and the energetic demands could eventually be satisfied by OXPHOS.

Regarding the glutamine utilization by $CD4^+$ T cells, the results support the idea that these cells just consume this substrate when no more glucose is available in the medium. This possibility is supported by the observation that, when glucose availability is lower, Rotenone shows a lower impact in the glutaminolysis/pyruvate cycle fluxes that lead to the production of glutamine derived lactate. This utilization of glutamine as a substitute of glucose to fulfil the bioenergetic and biosynthetic needs of the cells, especially when the cells are in specific-stimulated states, was already known from

studies performed in other cell types, as mentioned in the Introduction (Vander Heiden *et al.*, 2009; Lunt and Vander Heiden, 2011).

The data provided here, especially that concerning the glycolysis and TCA cycle roles in $CD4^+$ T cells metabolism, urges the need for a reformulation of the current perspective about $CD4^+$ T cells metabolism in the RA context. In this way, it is of utmost importance to complement these metabolic observations with the results provided in the following section involving the analysis of glucose and palmitate incorporation, to understand substrate availability in $CD4^+$ T cells, and the evaluation of the mitochondrial potential to better understand the metabolic remodeling occurring in CD4+ T cells in RA.

### 3.3.2 Glucose and palmitate incorporation and mitochondrial potential in $CD4^+$ T cells

As a complement to these data about $CD4^+$ T cells metabolic indexes it is important to have a more precise look into the capability of these cells to incorporate some important physiological substrates. In this case we tested how the $CD4^+$ T cells from both CNT and RA groups are prone to incorporate glucose and palmitate in the different experimental conditions (Nstim, Stim, FX11 and Rotenone). To measure the incorporation of glucose in $CD4^+$ T cells we used 2-NBDG (2-(N-(7-Nitrobenz-2-oxa-1,3-diazol-4-yl)Amino)-2-Deoxyglucose), a glucose fluorescent analog that allows to follow the cellular glucose uptake. In the case of the fatty acids incorporation, we used a conjugate molecule of the fatty acid palmitate and Bodipy, a fluorescence dye and highly lipophilic small molecule that allows, when conjugated with fatty acid, to follow its transport in to the cells (Byersdorfer *et al.*, 2013). In this way it was possible to follow both glucose and palmitate incorporation in $CD4^+$ T cells.

The selection of $CD4^+$ T cells was performed as depicted in **Figure 24**. This protocol includes several steps that allow the isolation of CD4+ T cells from all other cellular components. This method was used transversely for all the data obtained by FACS, which includes not only the glucose and palmitate incorporation presented in this section, but also the enzymes and PD-1 expression, ROS production, lipid peroxidation, apoptotic activity and cell viability and proliferation presented in further sections. **Figure 25** represents the results concerning the glucose and palmitate incorporation in $CD4^+$ T cells.

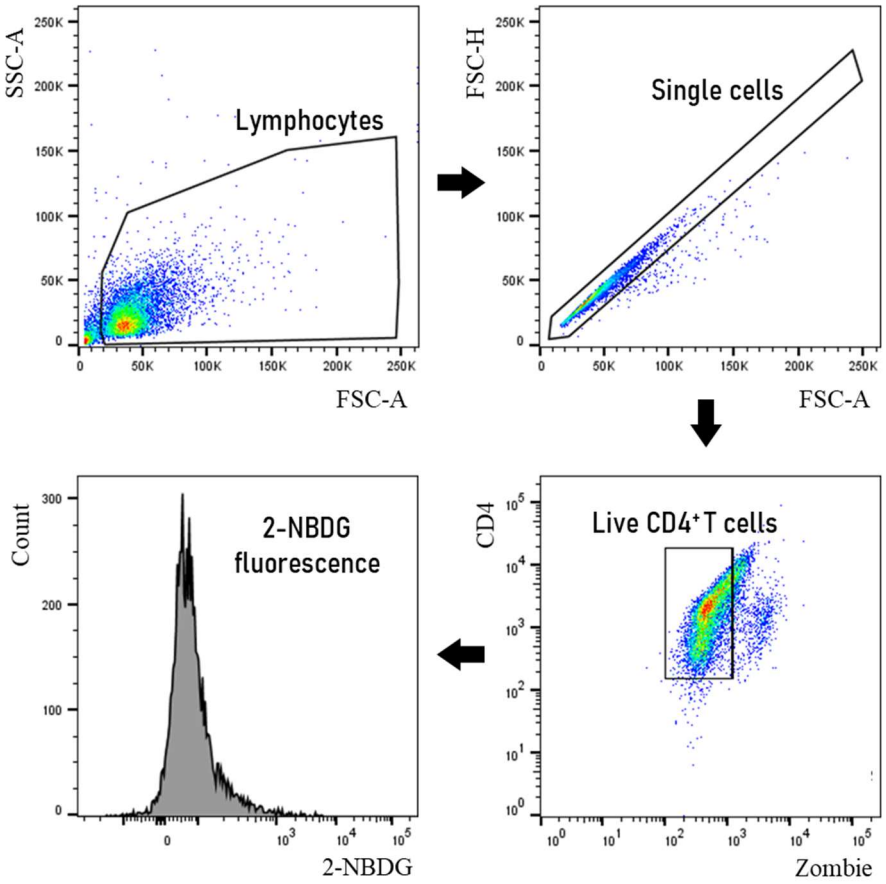


**Figure 24** - Representative example of the experimental procedure adopted for selection $CD4^+$ T cells to be used in FACS analyses and presentation of a result concerning glucose incorporation studies (2-NBDG fluorescence). At the upper left-side of the image, the lymphocytes were first selected in a FSC-A vs SSC-A graph which is followed by a FSC-A vs FSC-H chart that allow to select only the single cells present (excluding possible doublets present in the sample). Before measuring the targeted parameter, we restricted the analyses to the $CD4^+$ T cells that were alive using the combination of CD4 and Zombie antibodies, selecting the ($CD4^+Zombie^-$) population. Abbreviations: 2-NBDG (2-(N-(7-Nitrobenz-2-oxa-1,3-diazol-4-yl)Amino)-2-Deoxyglucose); FSC-A (Forward Scatter Area); FSC-H (Foward Scatter Height); SSC-A (Side Scatter Height).

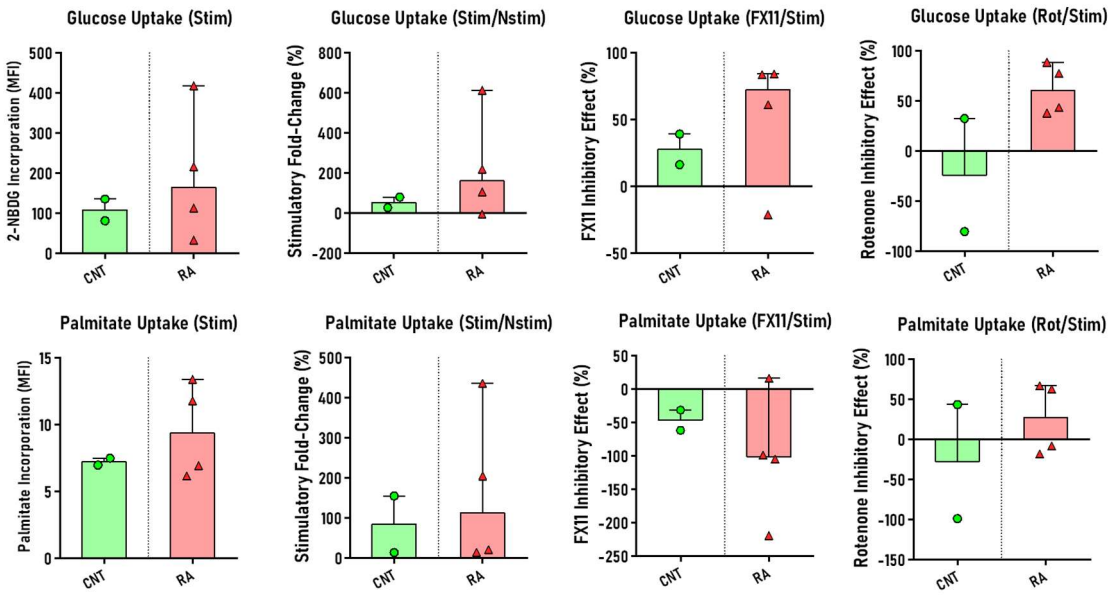


**Figure 25 -** Representation of the results concerning the glucose (top graphs) and palmitate (bottom graphs) incorporation by $CD4^+$ T cells using the tracers 2-NBDG and Bodipy-Palmitate, respectively. From the left to right, for both tracers and CNT and RA groups, are represented the incorporation in the Stim conditions, the stimulatory fold-change (%), and the FX11 and Rotenone inhibitory effects (%) relatively to the Stim condition. CNT are represented on the left half of the graphs (green dots), RA on the right half (red triangles). The bars represent the median value and the confidence interval (CI) at 95%. Number of samples: CNT=2; RA=4. Abbreviations: Nstim (Non-stimulated); Rot (Rotenone); Stim (Stimulated); TCA (Tricarboxylic Acid).

Looking for both 2-NBDG and Bodipy-Palmitate incorporation, the results suggest that $CD4^+$ T cells from the RA group have a larger avidity for these substrates as indicated by the higher incorporation in the Stim conditions. It is also perceptible that there is a higher stimulatory fold-change in RA than in CNT group. This apparent higher incorporation of both glucose and palmitate in RA cells is an indicator that the $CD4^+$ T cells from disease individuals are in exacerbated states of energetic expenditure and biosynthetic demands, leading to higher substrate incorporation and subsequent metabolism. As expected, the FX11 utilization induces the inhibition of the glucose uptake by $CD4^+$ T cells, being perceptible a higher impact in the RA group. On the other hand, the FX11 induces an exacerbation of palmitate incorporation by $CD4^+$ T cells which is in accordance with the result obtained for the impact of the same inhibitor in glucose uptake. It appears that $CD4^+$ T cells could compensate the inhibition of the glycolytic flux with an exacerbation in the palmitate uptake and consequent oxidative metabolism. This $CD4^+$ T cells plasticity is largely known and enable these cells to maintain their bioenergetic and biosynthetic needs even when their metabolism is partial blocked from

the glycolytic or OXPHOS point of view (Renner *et al.*, 2015; Dupage and Bluestone, 2016).

Regarding the results obtained in the Rotenone conditions, it could be suggested that this inhibitor enhances both glucose and palmitate incorporation in the CNT group and, on the contrary, inhibits both substrates uptake in the RA group. Being $CD4^+$ T cells in RA highly glycolytic, an interference in the ETC with Rotenone will have a lesser impact on energetic and biosynthetic fluxes in RA. This result could be explained by the expected higher metabolic activation in RA $CD4^+$ T cells that, although highly glycolytic depend upon OXPHOS to sustain their energetic and biosynthetic needs. Therefore, the inhibition of OXPHOS flux will lead to a general decrease in $CD4^+$ T cells metabolism and, consequently of the glucose and fatty acids uptake by these cells. These results are in accordance to what was observer in the latter section where Rotenone have a higher negative impact in the TCA index in the RA than in the CNT group despite no differences were seen in the glycolytic index.

Another indicator that is very useful for better characterizing $CD4^+$ T cells metabolic activity is the Mitochondrial Membrane Potential. This parameter is measured using the JC-1 molecule, a dye that creates aggregates when in higher concentrations (induced by high mitochondrial activity), which could be distinguished of the JC-1 monomers (formed when the mitochondrial activity is at low levels) by fluorescence techniques such as FACS. The ratio between the quantity of JC-1 aggregates and monomers formed by $CD4^+$ T cells is a good indicator of mitochondrial activity and the results obtained in $CD4^+$ T cells are presented in **Figure 26**.

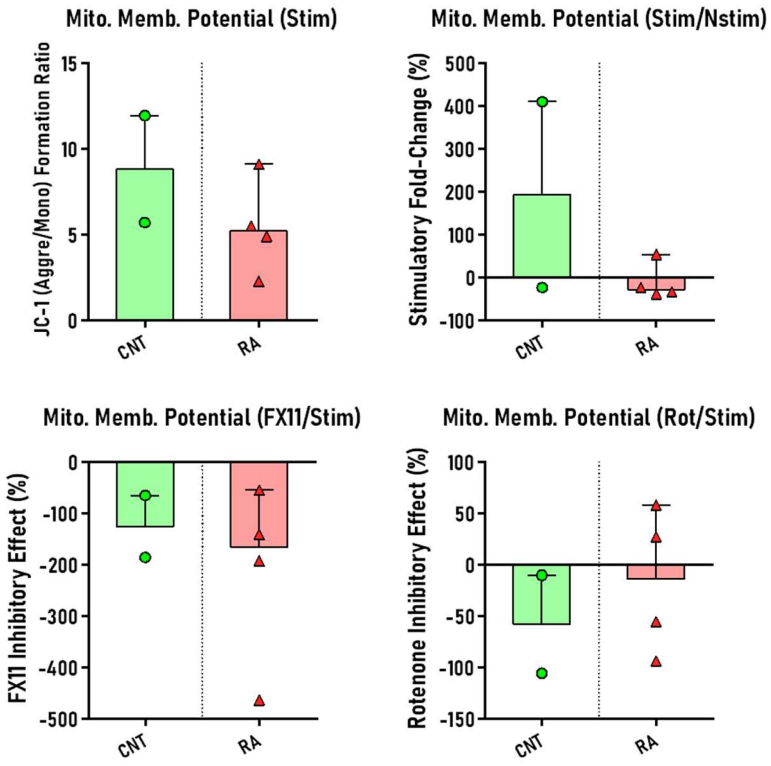


**Figure 26** - Representation of the results concerning the $CD4^+$ T cells Mitochondrial Membrane Potential in both CNT and RA groups by the utilization of the JC-1 cationic dye. In the top line, left side, is represented the ratio of JC-1 aggregates/monomers production in $CD4^+$ T cells in the Stim conditions. In the same line, but in the right side, is present the stimulatory fold-change (%). At the bottom line are represented the inhibitory effects (%) of both FX11 and Rotenone (left and right side, respectively), with the value zero representing no effect and negative values meaning promotion of the parameter by FX11/Rotenone. CNT are represented on the left half of the graphs at (green dots), RA on the right half (red triangles). The bars represent the median value and the confidence interval (CI) at 95%. Number of samples: CNT=2; RA=4. Abbreviations: Nstim (Non-stimulated); Rot (Rotenone); Stim (Stimulated).

Regarding the results obtained in the Stim conditions it could be alleged that $CD4^+$ T cells from the RA group present a lower mitochondrial membrane potential than CNT cells. Observing the stimulatory fold-change it could be seen that in RA the difference between the Nstim and Stim conditions is minimal, but in CNT $CD4^+$ T cells it could be suggested that the stimulation induces a higher potential probably due to the much greater utilization of the mitochondrial machinery. These results may indicate that the

mitochondrial machinery in RA $CD4^+$ T cells is already working at a high pace even in a non-stimulatory condition, being that for the CNT cells the stimulation induces the mitochondrial activity. Looking to the impact of FX11 in the formation of JC-1 aggregates we could conclude that the utilization of this inhibitor, as shown before, leads to an increase in the utilization of the mitochondrial machinery and, therefore, to the exacerbation of the mitochondrial membrane potential which seems to be slightly higher in RA than in CNT. Rotenone, contrary to what was expected, shows a stimulatory effect in the mitochondrial membrane potential in CNT and almost no-effect in RA $CD4^+$ T cells, which could be correlated with the higher glucose uptake (observed in CNT group) and, consequently, with an increase in the glycolytic flux and the production of ATP by phosphorylation at the substrate level, reducing the need to use oxidative phosphorylation and preserving mitochondrial membrane potential.

These results obtained about $CD4^+$ T cells substrates incorporation and mitochondrial membrane potential suggest that, in general, $CD4^+$ T cells from RA patients could be in a higher metabolic activity state than the $CD4^+$ T cells from healthy individuals even in non-stimulatory conditions. In addition to what was discussed above about the glycolytic index, these results corroborate the current knowledge about high-proliferative cells that was presented in the Introduction, which attributes to these type of cells an higher metabolic activity (Lunt and Vander Heiden, 2011). On the other hand, the glucose incorporation data insinuates that $CD4^+$ T cells in RA are still utilizing this substrate to sustain their metabolism, which is in line with what was shown before about the maintenance of a high glycolytic index and a low TCA flux in RA cells, contradicting, in this way, the current established paradigm about $CD4^+$ T cells metabolism in RA and other chronic autoimmune arthritic diseases (Weyand *et al.*, 2017; Hradilkova *et al.*, 2019).

In order to further characterize and understand the metabolic pattern in $CD4^+$ T cells in RA, the following subsection presents data about the expression of specific enzymes, central in the cellular metabolic activity.

### 3.3.3 Enzyme expression on $CD4^+$ T cells

To achieve an enzymatic characterization of $CD4^+$ T cells we focused our attentions in 4 main metabolic enzymes: LDHA (Lactate Dehydrogenase A), PDH (Pyruvate Dehydrogenase), GDH (Glutamate Dehydrogenase) and SDHA (Succinate Dehydrogenase A). The expressions of these enzymes were accessed in both CNT and

RA groups, in the 3 different mediums and in the 4 distinct conditions: Nstim, Stim, FX11 and Rotenone. The results in the Stim conditions and the comparation between Stim/Nstim for the 4 enzymes referred above are shown in the **Figure 27**.

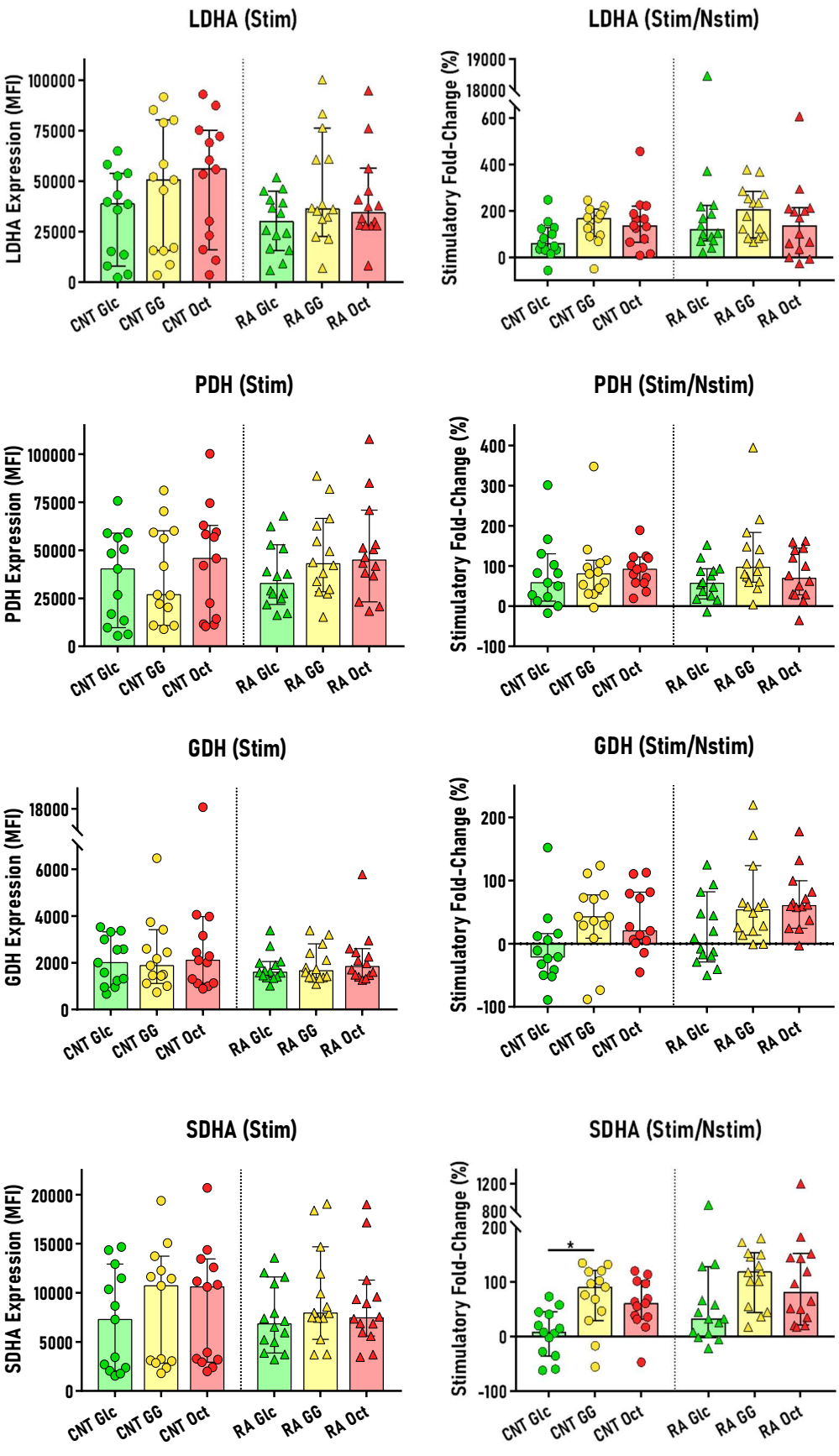
LDHA (Stim)
LDHA Expression (MFI)
100000
75000
50000
25000
0
CNT Glc
CNT GG
CNT Oct
RA Glc
RA GG
RA Oct
LDHA (Stim/Nstim)
Stimulatory Fold-Change (%)
19000
18000
600
400
200
0
PDH (Stim)
PDH Expression (MFI)
PDH (Stim/Nstim)
Stimulatory Fold-Change (%)
400
300
200
100
0
-100
GDH (Stim)
GDH Expression (MFI)
18000
6000
4000
2000
0
GDH (Stim/Nstim)
Stimulatory Fold-Change (%)
SDHA (Stim)
SDHA Expression (MFI)
20000
15000
10000
5000
0
SDHA (Stim/Nstim)
Stimulatory Fold-Change (%)
1200
800
200
*

**Figure 27** - Representation of the expression of the enzymes LDHA, PDH, GDH and SDHA in $CD4^+$ T cells. The left side graphics represent the expression, in MFI (Mean Fluorescence Intensity), on Stim conditions. The right side graphics represent the stimulatory fold-change in percentage (Stim vs Nstim), being that the zero value represents no variation. In all graphs the CNT are represented on the left half of the graphs (dots), RA on the right half (triangles). Medium GLC (green), Medium GG (yellow), Medium Oct (red). The bars represent the median value and the confidence interval (CI) at 95%. *: $p<0,05$ with p being calculated using Kruskal-Wallis test with Dunn's multiple comparisons test. Number of samples: CNT=13; RA=14. Abbreviations: Nstim (Non-stimulated); Stim (Stimulated).

LDHA is the enzyme that catalyzes the conversion of pyruvate to lactate, being one of the major players in stimulation of glycolysis by regenerating $NAD^+$. Regarding the LDHA expression on Stim conditions, the relative levels of expression in the different mediums in both groups, CNT and RA, are quite similar to the values of glycolytic index shown above, that is, the results suggest that the level of LDHA expression is lower in the Glc medium than in GG or Oct Media, something that is also observed when talking about the glycolytic flux. As stated above about glycolytic index, this apparent higher expression in the media where the glucose availability is lower could be explained by a sense of starvation by the cells, that consume all the glucose available via glycolysis increasing, in that way, the glycolytic flux and, consequently, the expression of LDHA. Something that also attracted our attention was the fact that LDHA, in all media, seems to be consistently more expressed in CNT than in the RA group, although the glycolytic fluxes between the groups are very similar in all media. This could mean that the LDHA may be more active in RA $CD4^+$ T cells than in $CD4^+$ T cells from healthy individuals. The stimulatory fold-change appears to be higher in RA for Glc and GG media when comparing with CNT group, but no variations between both groups are visible in Oct Medium. Nevertheless, a general observation is that the stimulation enhances the expression of the LDHA enzyme in all media, being transversal to both CNT and RA groups.

PDH is the enzyme complex responsible for the oxidative decarboxylation of pyruvate, converting pyruvate and $NAD^+$ into Acetyl-CoA, $CO_2$ and $NADH/H^+$. This reaction is therefore intimately linked to the TCA cycle and, consequently, to OXPHOS, being the Acetil-CoA essential to sustain this inner-mitochondrial flux. The expression of this enzyme, in the RA group, is apparently higher in GG and Oct Media what can be explained by a higher utilization of OXPHOS, fomented by the lower concentration of glucose and the presence of octanoate. In the CNT group the pattern is similar, however the GG medium presents an apparent lower expression of PDH, suggestive of a lower prevalence of OXPHOS in the CNT group in this medium due to possibility of resorting to the glycolytic flux for its less demanding bioenergetic and biosynthetic needs. The stimulatory fold-change is similar between the CNT and RA groups, being that the stimulation of $CD4^+$ T cells enhanced the expression of PDH.

GDH is the enzyme responsible to convert glutamate, $NAD^+$ and $H_2O$ in α-ketoglutarate and $NADH/H^+$ and $NH_4^+$. This enzyme is intimately linked to OXPHOS metabolism, by providing TCA cycle intermediates, and nitrogen equilibria in the

organism. As it could be observed, the expression of this enzyme is very similar between groups and media, suggesting just a small increase in Oct medium in both groups. As stated above, this could be linked to the higher oxidative metabolism induced in this medium, which should increase the expression of both TCA cycle enzymes and enzymes feeding the TCA cycle. The stimulatory fold-change in GG and Oct media, in both groups, appears to have an expected increase in the expression of GDH in Stim conditions when compared to the Nstim ones. Regarding the Glc medium, the expression of GDH shows no variation between Stim and Nstim conditions (RA group) or even an apparent lower expression in the Stim relatively to the Nstim condition (CNT group). This last result could be explained by the lack of necessity of $CD4^+$ T cells, in presence of sufficient glucose availability, to use the oxidative pathways to fulfill their biosynthetic and energetic needs, using glycolysis for such processes.

SDHA is a subunit of the complex II of the Mitochondrial Respiratory Chain and is responsible for catalyzing the conversion of succinate and FAD to fumarate and $FADH_2$. As suggested by the graphics, the expression of this enzyme in $CD4^+$ T cells seems to be higher in GG and Oct media than in Glc medium, something that is more perceptible in CNT group. This apparent higher amount of SDHA in GG and Oct media, in the same way of what was observed and explained for PDH, is grounded by the higher oxidative profile of the cells in these media due to lower concentrations of glucose in both media and the addition of the fatty acid octanoate in the Oct medium. Regarding the stimulatory fold-change, the stimulation of $CD4^+$ T cells exacerbated the expression of SDHA in GG medium, especially, but also on Oct medium in a lower extent. For Glc medium, the stimulatory fold-change is minimal for both groups being this explained by the lower utilization of the OXPHOS metabolic flux due to the higher availability of glucose. In this way, the extent of utilization of OXPHOS and consequent expression of SDHA is clearly influenced by substrate availability.

Subsequently, we also analyzed the impact of the inhibitors FX11 and Rotenone in the expression of these four enzymes. The results are presented in **Figure 28**.

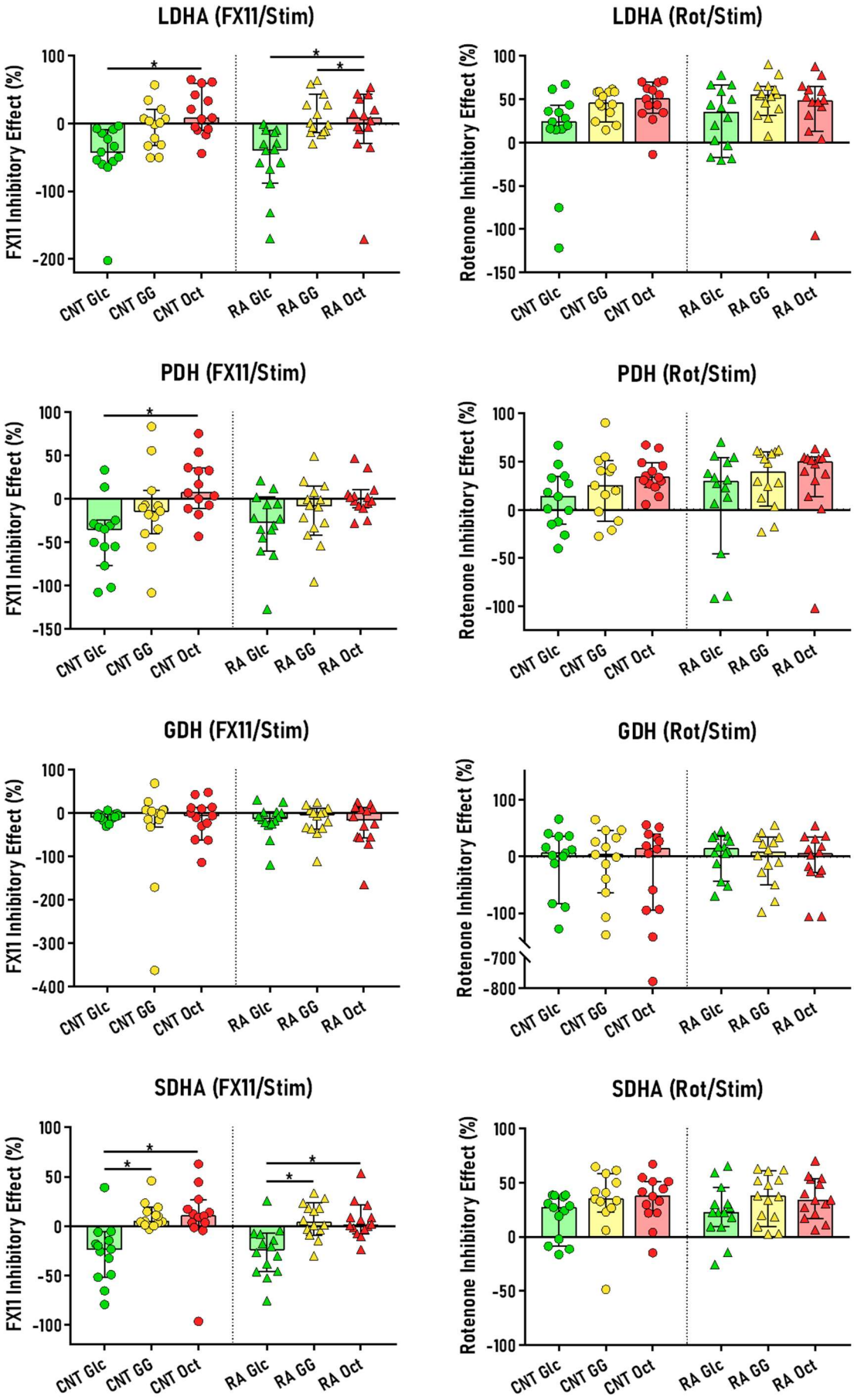
LDHA (FX11/Stim)
FX11 Inhibitory Effect (%)
LDHA (Rot/Stim)
Rotenone Inhibitory Effect (%)
PDH (FX11/Stim)
FX11 Inhibitory Effect (%)
PDH (Rot/Stim)
Rotenone Inhibitory Effect (%)
GDH (FX11/Stim)
FX11 Inhibitory Effect (%)
GDH (Rot/Stim)
Rotenone Inhibitory Effect (%)
SDHA (FX11/Stim)
FX11 Inhibitory Effect (%)
SDHA (Rot/Stim)
Rotenone Inhibitory Effect (%)
CNT Glc
CNT GG
CNT Oct
RA Glc
RA GG
RA Oct

**Figure 28** - Representation of the inhibitory effect (in percentage) of FX11 (left side) and Rotenone (right side) in the expression of the enzymes LDHA, PDH, GDH and SDHA in $CD4^+$ T cells when compared to the Stim condition. The value of zero means no effect in the expression. Negative values mean an increase of expression. In all graphs the CNT are represented on the left half of the graphs (dots), RA on the right half (triangles). Medium GLC (green), Medium GG (yellow), Medium Oct (red). The bars represent the median value and the confidence interval (CI) at 95%. *: $p<0,05$ with p being calculated using Kruskal-Wallis test with Dunn's multiple comparisons test. Number of samples: CNT=13; RA=14. Abbreviations: Rot (Rotenone); Stim (Stimulated).

Regarding the results obtained by FX11 inhibition it could be observed that, in all enzymes analyzed here, this compound has a stimulatory effect in the enzymatic expressions on $CD4^+$ T cells when they are exposed to a normal-concentration glucose medium (Glc medium). This increased expression of the whole set of enzymes suggests that the metabolic inhibition caused by FX11 elicits a cellular response to counteract such metabolic inhibitory action. An increased expression of LDHA can sustain or even increase lactate production even in the continuous presence of FX11. The increases in the expressions of the other three enzymes can be explained by the higher availability of pyruvate throughout the whole incubation period due to the FX11 inhibitory effect on LDHA. When looking into the other two media, in the GG medium FX11 has no effect in the different enzymes' expressions and in the Oct medium FX11 shows also no effect or even a mild inhibitory impact in the expression of some enzymes. The concentration of glucose in the media seems to be the most determinant factor in the action of FX11 in enzymatic expressions. In additional experiments, using a medium containing 5 mM of [U-$^{13}$C]glucose, we have seen that the positive impact of FX11 in LDHA expression is accompanied by an apparent increase in the lactate secretion by $CD4^+$ T cells even when these cells were exposed to higher FX11 concentrations (60 µM and 75 µM) than the ones used in the studies of LDHA expression (45 µM). These complementary results are shown in **Figure 29**.

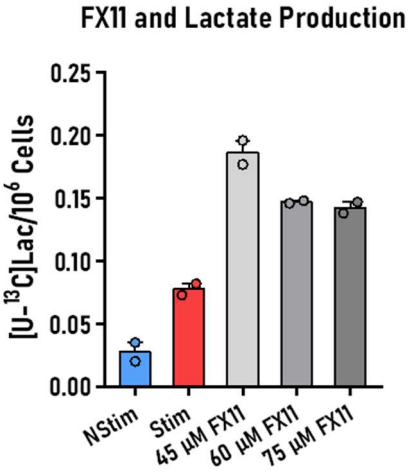


**Figure 29 -** Impact of FX11 in [U-$^{13}$C]Lac production when $CD4^+$ T cells were cultured in 5 mM of [U-$^{13}$C]glucose in different conditions: Nstim (blue), Stim (red), 45 µM FX11 (light grey), 60 µM FX11 (grey) or 75 µM FX11 (dark grey). The bars represent the median value and the confidence interval (CI) at 95%. Number of samples: CNT=2. Abbreviations: Lac (Lactate); Nstim (Non-stimulated); Stim (Stimulated).

Concerning the effects of Rotenone, we could see a different pattern of expression in all four enzymes. The expressions of LDHA in all media in both CNT and RA groups were to a high extent impaired by Rotenone, being that, apparently, the higher impacts are visible in GG and Oct media. Although LDHA is intrinsically linked to the glycolytic pathway and Rotenone inhibits, at least partially the OXPHOS flux, this result clearly shows that this inhibitor interferes in the cellular metabolic machinery as a whole. When looking to what happened to the glycolytic index under the same conditions, it seems contradictory that LDHA expression is lower but the glycolytic activity is exacerbated by the usage of Rotenone. This could simply mean that the expression of LDHA is being negatively affected by Rotenone but the level of utilization of the enzyme (enzymatic activity) is actually higher when compared to the Stim condition.

PDH expression in $CD4^+$ T cells is also downregulated in Rotenone presence when compared to the Stim condition. This inhibition is apparently higher in GG and Oct media, being that the lower glucose availability and the presence of potentially oxidative substrates such as octanoate in the latter case could explain this fact considering the contribution of PDH to the TCA cycle initiation. In Glc medium, on the other hand, the inhibition of OXPHOS by Rotenone had a minor impact in PDH expression specially in the CNT group. The apparent higher impact in the RA group could be related to the higher energetic and biosynthetic needs of $CD4^+$ T cells in the disease context. The SDHA expressions in this Rotenone condition, even for the Glc medium, are more similar between CNT and RA groups. When analyzing the results obtained for GDH, the impact of Rotenone in this enzyme seems minor which may reflect the fact that this enzyme is only indirectly associated with the TCA cycle but is pivotal in amino acid metabolism, being not as affected by Rotenone.

The results acquired regarding the enzyme expression in $CD4^+$ T cells and the effect of both inhibitors are in line to what was said before about these cells metabolic activity, which is corroborated by the current knowledge about the metabolism of highly activated cells (Lunt and Vander Heiden, 2011). It is, one more time, suggested that the glucose is the main utilized substrate in these cells, which is principally reflected in the apparent exacerbation of the expression of LDHA in cells cultured in media where this substrate is at lower availability (GG and Oct) and by the counteraction of $CD4^+$ T cells when they suffer the action of FX11, increasing the expression of LDHA as a way to overtake the glycolytic blockage imposed by the inhibitor. In addition, the already referred counterintuitive FX11 impact in LDHA activity and, consequently, in cellular

metabolism is not totally unknown. It was previously demonstrated, in tumor cells from pancreatic cancer, that the effect of FX11 is negatively correlated with the presence of the protein p53, a tumor suppressor protein (Rajeshkumar *et al.*, 2014), being the glycolytic activity of the cells not affected when p53 was present. Moreover, it was demonstrated that p53 is overexpressed in RA (Salvador *et al.*, 2005) and, in this way, although the mechanism by which this protein could act to prevent the blockage of the metabolic activity of the cells by FX11 is unknown, it could be inferred that the results obtained in our FX11 conditions are not totally out of scope and be explanation may be the higher expression of p53. In future projects this protein should be one of the major targets of analysis by the therapeutic importance that could assume in RA and other chronic inflammatory diseases.

As discussed in earlier subsections, the results obtained could lead to a reformulation of the current metabolic profile attributed to $CD4^+$ T cells in RA, having these being presented as highly oxidative and possibly sustainable only by fatty acids utilization (Weyand *et al.*, 2017; Hradilkova *et al.*, 2019).

### 3.3.4 Lipids peroxidation, ROS production and PD-1 expression in $CD4^+$ T cells

Beside the enzymatic activity, there are other cellular indicators that could open our understanding about the $CD4^+$ T cells metabolism modulation and response in RA. In this subsection we will present and discuss the results obtained for some indicators linked to reactive oxygen species (ROS) production, an apoptosis inductor expression (PD-1) and to lipid peroxidation levels. These 3 distinct indicators could be intrinsically interlinked as one will see.

As stated in the Introduction, ROS are really crucial species in the cellular machinery and, consequently, for their metabolism. ROS are mostly produced during OXPHOS and a narrow control of the levels of ROS is essential to control both cellular apoptotic mechanisms and proliferation induction, namely in $CD4^+$ T cells (Weyand and Goronzy, 2017; Weyand, Shen and Goronzy, 2018). We measured the quantity of ROS production by $CD4^+$ T cells by using the cellular membrane permeable CellRox reagent which exhibits a strong fluorescence upon oxidation by ROS.

An important indicator, in $CD4^+$ T cells, of the apoptotic events referred above is the so-called PD-1, the programed cell death protein 1 (also known as CD279). This protein upon interaction with specific ligands such as PD ligand 1 (PD-L1) or PD ligand 2 (PD-L2) leads to a decrease in the lymphocytes proliferation and cytokine production,

ultimately leading to an immunological inactivity by these cells (Konkel *et al.*, 2010; Droeser *et al.*, 2013). The expression of PD-1 in $CD4^+$ T cells was indirectly measured by FACS, using a fluorescent anti-body specific for this protein.

Lipid peroxidation is a process in which lipids, especially the ones that form the cellular membranes, are "attacked" by free radicals or non-radical species, leading to the removal of hydrogen and the insertion of oxygen, more frequently in the carbon-carbon double bonds of unsaturated fatty acids. Although the most affected lipids are the poly-unsaturated fatty acids, glycolipids, phospholipids and cholesterol could also be targets of this peroxidation process (Ayala *et al,*, 2014; Dingjan *et al.*, 2016). This process occurs at a low rate in normal conditions, being the cells capable of producing sufficient anti-oxidants to manage with the peroxidation threat. However, an excessive rate of lipid peroxidation is one of the most known triggers of the autophagy-related machinery and, more importantly, to the apoptotic processes (Negre-Salvayre *et al.*, 2010; Ayala *et al.*, 2014). In this case we followed the lipid peroxidation levels in $CD4^+$ T cells by using a Bodipy fluorescence dye which is systemically used as a lipid peroxidation sensor.

The results obtained for these three parameters and their correlations are of extreme relevance to understand the metabolic modulation that $CD4^+$ T cells from CNT and RA suffer in the different media. **Figure 30** represents the results obtained in the Stim conditions and the comparison between Stim and Nstim conditions for ROS production, PD-1 expression and lipid peroxidation level.

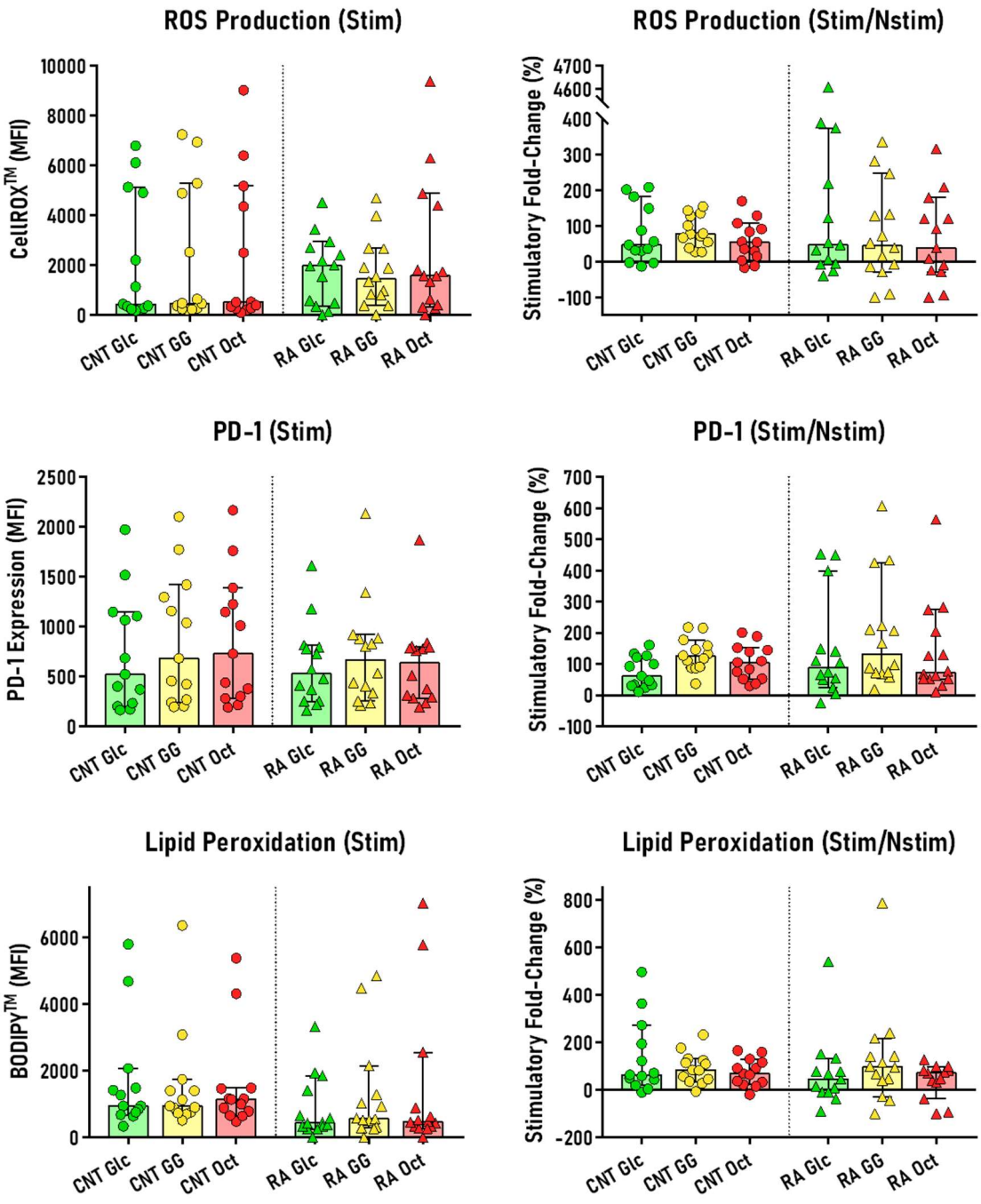


**Figure 30** - Representation of the results obtained for the ROS production, PD-1 expression and lipid peroxidation level in $CD4^+$ T cells in the Stim conditions and the comparison between Stim and Nstim conditions. The ROS production was accessed by the utilization of CellRox reagent. PD-1 expression was measured by using antibodies against this protein. Lipid peroxidation level was measured by Bodipy fluorescence dye. All the results were obtained by FACS. In all graphs the CNT are represented on the left half of the graphs (dots), RA on the right half (triangles). Medium Glc (green), Medium GG (yellow), Medium Oct (red). The bars represent the median value and the confidence interval (CI) at 95%. Number of samples: CNT=13; RA=14. Abbreviations: Nstim (Non-stimulated); Stim (Stimulated).

Considering the ROS data obtained, it is suggested that the RA group shows a higher production of ROS when compared to the CNT group. Such result is transversal to all the media, being that Glc medium in RA shows, apparently, the largest amount of ROS in comparison with the other media in the same group. This could be explained by the extensive usage of glucose that it was provided to $CD4^+$ T cells, leading to the accumulation of high levels of glycolytically derived $NADH/H^+$, which oxidation in the ETC represents a major source of ROS. Regarding the stimulatory fold-change, the stimulation enhances the production of ROS when comparing with the Nstim conditions, being this increase accomplished in the same scale in both CNT and RA groups and in all media.

The apparent higher amount of ROS production in the RA group may lead us to the assumption that this will lead to the increase of the activity in the apoptotic machinery and an exacerbation of lipid peroxidation levels. Neither of these theories is correct. As could be observed in the PD-1 graphs, the expression of this apoptotic inductor protein has no variation between CNT and RA groups in the Stim conditions, showing a consistent level of expression in all media between the groups. Although the apoptotic machinery activity was not directly measured, the PD-1 expression levels should give us an idea of this activity and, therefore, we could conclude that apoptosis was not exacerbated by the increased ROS production in the RA group. Looking to the stimulatory fold-change there is essentially no variation in each media between both CNT and RA groups and minimal variations between media within experimental group. The results suggest that the GG medium is the one that shows the highest variation when comparing Stim and Nstim conditions. Regarding the results obtained for the lipid peroxidation, the RA group shows an apparent lower peroxidation than the CNT group in all media, although having, seemingly, the higher ROS production, as explained above. The stimulatory fold-change in lipid peroxidation is also similar between groups and media and increase upon stimulation of $CD4^+$ T cells.

Taking together, these results suggest that even though $CD4^+$ T cells from RA group, contradicting some published data (Weyand *et al.*, 2017; Weyand *et al.*, 2018), present an apparent higher production of ROS, eventually associated with enhanced metabolic and, therefore, cytotoxic functions, these disease-derived cells do not show variations in the apoptotic machinery activity and even present a lower level of lipid peroxidation in their membranes. In the following sections it will be presented results that could help explain this phenomenon, namely the results concerning $CD4^+$ T cells

proliferation. The impacts of FX11 and Rotenone in ROS production, PD-1 expression and lipid peroxidation levels were also evaluated and the results presented in **Figure 31**.

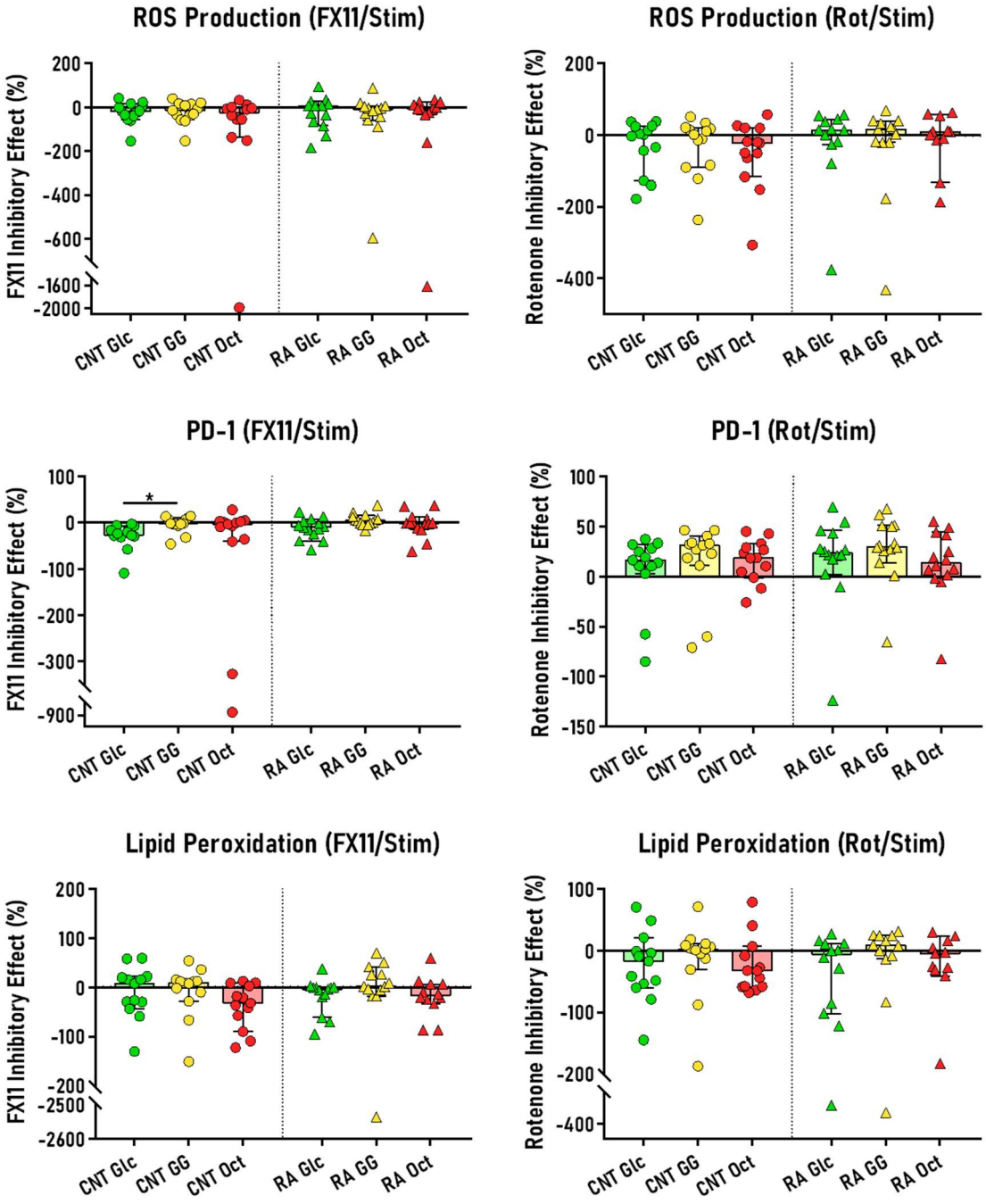

**Figure 31** - Impact of FX11 and Rotenone (when compared to the Stim condition) in ROS production, PD-1 expression and lipid peroxidation level in $CD4^+$ T cells. The ROS production was accessed using the CellRox reagent. PD-1 expression was measured by using antibodies against this protein. Lipid peroxidation level was measured using the Bodipy fluorescence dye. All results were obtained by FACS. In all graphs the CNT are represented on the left half of the graphs (dots), RA on the right half (triangles). Medium GLC (green), Medium GG (yellow), Medium Oct (red). The bars represent the median value and the confidence interval (CI) at 95%. *: $p<0,05$ with p being calculated using Kruskal-Wallis test with Dunn's multiple comparisons test. Number of samples: CNT=13; RA=14. Abbreviations: Rot (Rotenone); Stim (Stimulated).

Concerning the ROS production, we could conclude that neither FX11 nor Rotenone had any significant impact. Surprisingly, even Rotenone, in the Oct media of both CNT and RA groups, presents minimal or no-effect at all in ROS levels. For the PD-1 expression the impact of FX11 was also minimal. Only in the Glc medium, in both CNT and RA groups, FX11 shows a mild stimulatory effect in the expression of this pro-apoptotic protein. On the contrary, Rotenone had an inhibitory effect that was transversal to all media in both CNT and RA groups, which could be correlated with the general decrease in enzymatic expression abovementioned. Thus, it could be inferred that the lower cellular metabolic activity induced by Rotenone lead to the reduction of the apoptotic machinery of $CD4^+$ T cells.

Regarding the lipid peroxidation results we observed an apparent stimulatory effect of FX11 in Oct medium of both CNT and RA groups but no effect in other media. The same result is observed for Rotenone, suggesting that the Oct medium in the CNT group shows the higher (positive) impact. This vulnerability of $CD4^+$ T cells in Oct medium demonstrates how important it is for cells to have present substrates like glucose that can feed glycolysis and sustain major cellular functions.

Experiments performed in a smaller number of cases (2 CNTs, 3 RAs) without FX11 or Rotenone, allowed an additional measure of apoptotic activity of $CD4^+$ T cells. Using a fluorescent conjugate of annexin V detectable by FACS, it was possible to indirectly quantify the amount of phosphatidylserine (PS), which is normally localized in inner-side (cytoplasm) of the cell membrane but, due to the structural changes that occur in the cellular membrane during the apoptosis process, migrates to the outer-side, allowing the detection of apoptotic cells. The results obtained concerning this procedure are shown in **Figure 32**.

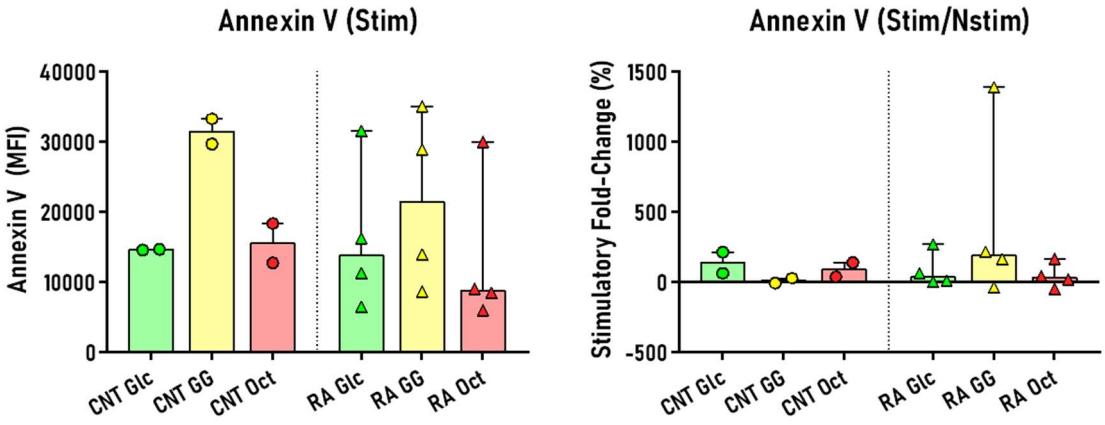


**Figure 32** - Use of a fluorescent conjugate of annexin V to measure the apoptotic activity of $CD4^+$ T cells. At the left are represented the fluorescence values obtained in the Stim conditions (in MFI). At the right are represented the comparisons between Stim and Nstim conditions (stimulatory fold-change, in percentage). In all graphs the CNT are represented on the left half of the graphs (dots), RA on the right half (triangles). Medium Glc (green), Medium GG (yellow), Medium Oct (red). The bars represent the median value and the confidence interval (CI) at 95%. Number of samples: CNT=2; RA=3. Abbreviations: Nstim (Non-stimulated); Stim (Stimulated).

In the Glc medium there is no variation in the cellular apoptotic activity between CNT and RA groups. On the contrary, in GG and Oct media it is suggested that there is a clear decrease in the apoptotic activity in $CD4^+$ T cells in the RA compared to the CNT group. The stimulation enhances the amount of PS in the outer membrane and, therefore, the number of apoptotic events in $CD4^+$ T cells. Together with the results shown and discussed above related to PD-1, we can conclude that in RA, $CD4^+$ T cells show no variation or even a lower apoptotic activity even though being metabolically more active and presenting higher ROS production. This correlation is contradicted by the hypothesis, presented in the Introduction, that lower levels of ROS are linked to T cells' higher proliferation and that high ROS levels should induce the apoptotic machinery in these cells, imposing restrictions in the clonal expansion potential of $CD4^+$ T cells (Yang *et al.*, 2016; Weyand *et al.*, 2018). The further analysis of cytokines production by $CD4^+$ T cells in the different conditions provided, presented in a later section, could permit to infer what is the real impact of ROS production in the cytotoxic functions of these cells.

### 3.3.5 $CD4^+$ T cells viability and proliferation

Two parameters of extreme relevance when analyzing the adaptability of any type of cells to different environments are cellular viability and proliferation. Thus, the analysis of $CD4^+$ T cells from healthy individuals and RA patients in the different media chosen and conditions adopted cannot dodge the observance of these referred parameters.

The concept of viability lays on the relative quantity of cells that stay alive in the given conditions in the final of the culturing period and, therefore, could be described as the percentage of $CD4^+$ T cells that keep alive from the total number of cells present (alive or death). Here we achieved this parameter by using a viability essay by Flow Cytometry, staining $CD4^+$ T cells, before FACS, with Zombie Aqua$^{TM}$ dye (Biolegend) which, being an amine-reactive fluorescence dye, will penetrate in the compromised membranes of death cells. In this way it could be known the number of death cells (the ones stained with the dye) in the sample and, consequently, the cellular viability.

Before presentation of the viability results obtained using the staining method mentioned above, it is important to show simple representative examples of scatter-plots (FSC-A vs SSC-A) obtained in FACS analysis of all cells from each medium and respective conditions (Nstim, Stim, FX11 and Rotenone) which could already give us the idea of how the cells, in general, are responding to the different environment provided in the cultures. These examples are presented in **Figure 33**.

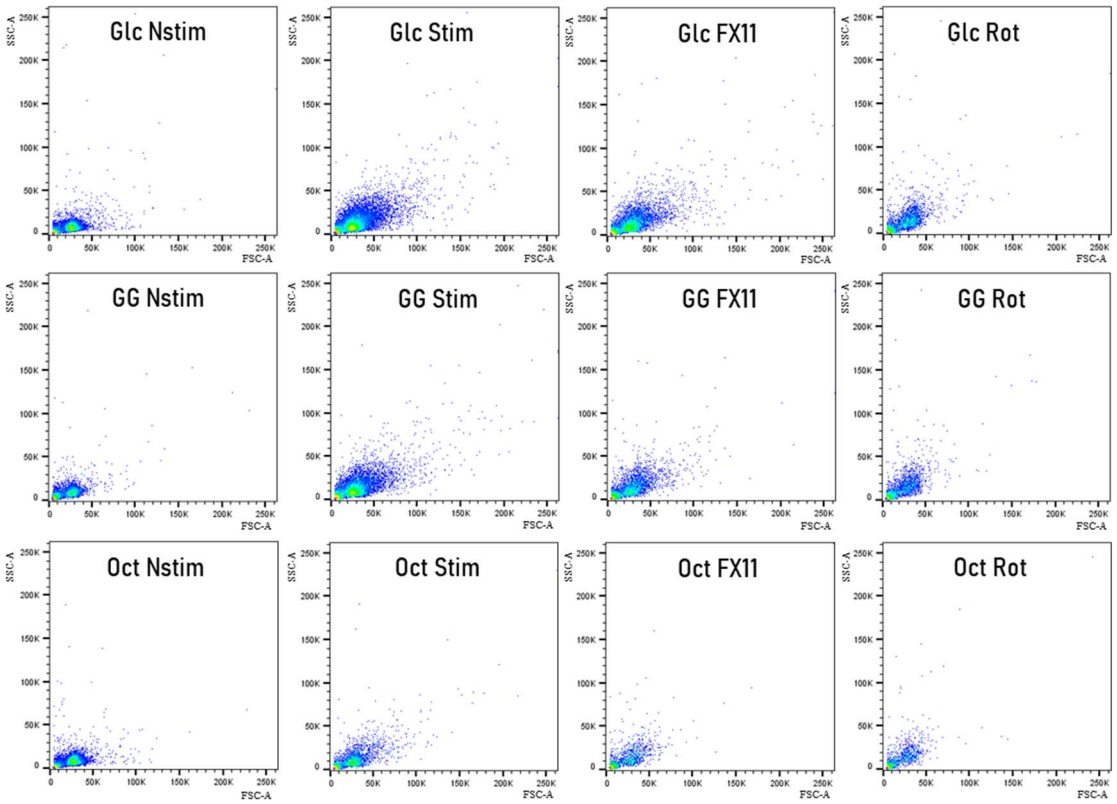


**Figure 33** - Representative examples of scatter-plots (FCS-A vs SSC-A) obtained for each medium and their respective conditions for one sample. It could be observed the impact that the different environments provided to the cells, which are composed by distinct substrates and/or inhibitors, affect their viability. Abbreviations: FSC-A (Forward Scatter Area); SSC-A (Side Scatter Height).

These representative examples suggest that the total number of cells in the Oct medium is lower than in the Glc or GG media, which insinuate that the scarce glucose available, even in the presence of fatty acids, induces a reduction in cell survival. Similarly, it is also perceptible the slight negative effect of both inhibitors, FX11 and Rotenone, in the total cellular content as well as the difference between Nstim and Stim conditions, where the number of cells after 72h of culturing seems to be relatively greater when the cells were stimulated.

In **Figure 34** are represented the results obtained for $CD4^+$ T cells viability in the different media chosen and adopted experimental conditions, including the impact of FX11 and Rotenone.

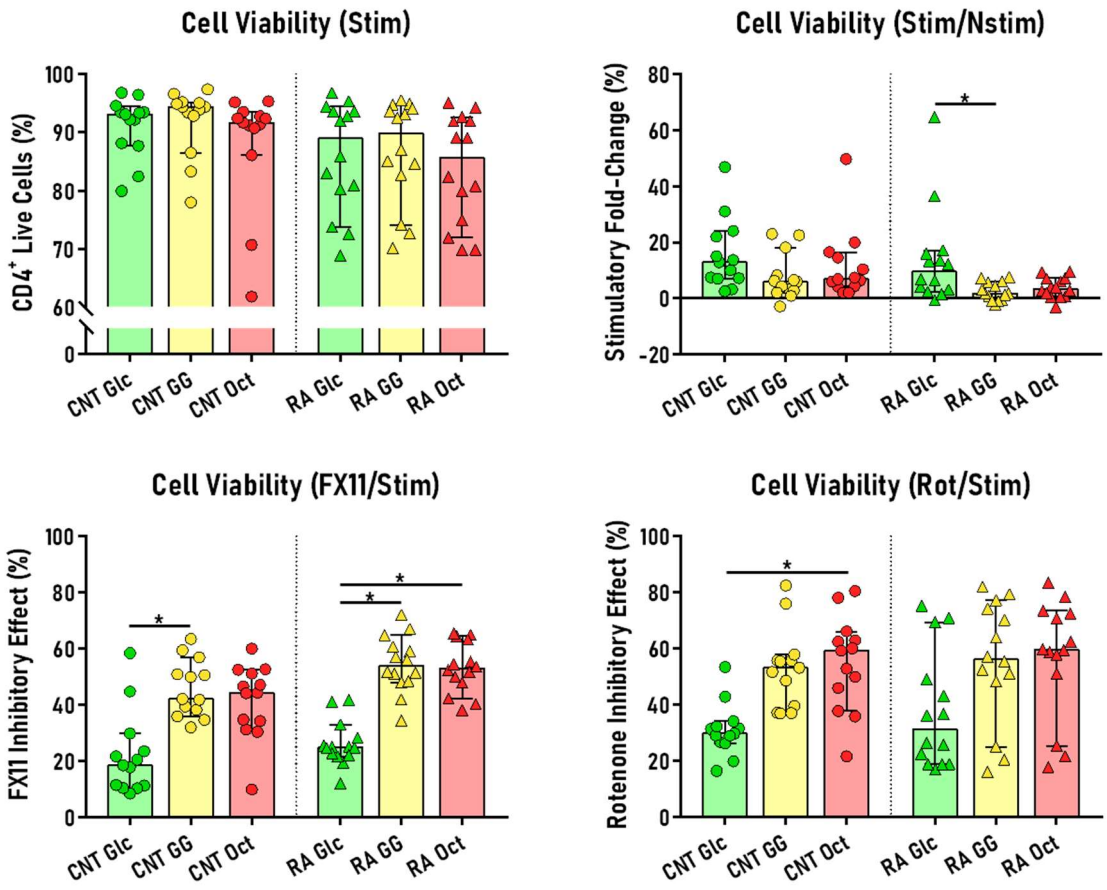


**Figure 34** - Viability of $CD4^+$ T cells from CNT and RA groups in the different media provided. At the top left corner, it could be observed the viability of $CD4^+$ T cells in the Stim conditions. The stimulatory fold-change (%), that is, the comparation between Stim and Nstim conditions, is represented at the top right corner. At the bottom there is the representation of the impact (inhibitory effect, %) of FX11 and Rotenone (left and right, respectively) in the $CD4^+$ T cells viability when comparing to the results obtained for the Stim condition. In all graphs the CNT are represented on the left half of the graphs (dots), RA on the right half (triangles). Medium Glc (green), Medium GG (yellow), Medium Oct (red). The bars represent the median value and the confidence interval (CI) at 95%. *: $p<0,05$ with p being calculated using Kruskal-Wallis test with Dunn's multiple comparisons test. Number of samples: CNT=13; RA=14. Abbreviations: Nstim (Non-stimulated); Rot (Rotenone); Stim (Stimulated).

Considering these results it could be suggested that $CD4^+$ T cells viability in the Stim conditions is slightly lower in the RA that in the CNT group, observation that is transversal to all media. This apparent decrease in cells viability in the RA condition could be related to the stress induced by a higher state of cellular activation in metabolic and biosynthetic terms. It could be also proposed that, in both CNT and RA groups, the viability in the Oct medium is lower when comparing to the viability in the Glc and GG media, indicating that the lower levels of glucose could induce cell death in $CD4^+$ T cells

specially derived from RA. In addition, the above mentioned lower total number of cells present in Oct Medium after the 72 hours of culturing clearly suggests that this medium is not favorable for the survival of $CD4^+$ T cells. Looking to the stimulatory fold-change obtained for this parameter, it is observed a minimal stimulatory impact in $CD4^+$ T cells viability and, even considering that it happens at a low extent, the medium that seems to have the higher stimulatory fold-change in viability is the Glc medium. One more time this indicates that the greater availability of glucose supports $CD4^+$ T cells viability.

Looking to FX11 and Rotenone impact in $CD4^+$ T cells viability we could conclude that the two inhibitors have very similar impacts in both CNT and RA groups. It is clear that the impact of both inhibitors in cell viability is much higher in the GG and Oct media, being the Glc medium the least affect by far. These results just corroborate the hypothesis that the medium Glc, with its higher availability of glucose (5 mM), promotes a higher viability for $CD4^+$ T cells even in the presence of metabolic inhibitors that could block partially the glycolytic pathway (FX11) and OXPHOS flux (Rotenone). The impact in cell viability observed for the low glucose GG and Oct media, although stronger, is very similar for both FX11 and Rotenone.

The concept of proliferation means the capability of the cells to divide and multiply themselves in the given conditions, that is, to proliferate. For accessing the proliferation of $CD4^+$ T cells of both healthy individuals and RA patients in the media provided we have used the capabilities of Carboxyfluorescein succinimidyl ester (CFSE) to follow the lymphocyte division. The lower levels of toxicity of this reagent and practical and easy way of appliance to the cells makes CFSE an uncontestable choice to measure $CD4^+$ T cells proliferation. When added to the cells this compound will label the $CD4^+$ T cells intracellular molecules with his fluorescence dye and, when the cells divide and give rise to 2 daughter cells the intensity of the fluorescence provided will be decreased. By FACS it is possible to follow the proliferation of $CD4^+$ T cells labeled with CFSE by observing the decrease in fluorescence intensity, being that lower intensity of CFSE fluorescence means a higher level of cell proliferation (higher dispersion of the fluorescence through the new cells.

**Figure 35** shows a representative example of the way by which $CD4^+$ T cells were selected from the acquired FACS data and an example of the result obtained for CFSE fluorescence in one of our samples. The results obtained for the proliferation assays are shown in **Figure 36**.

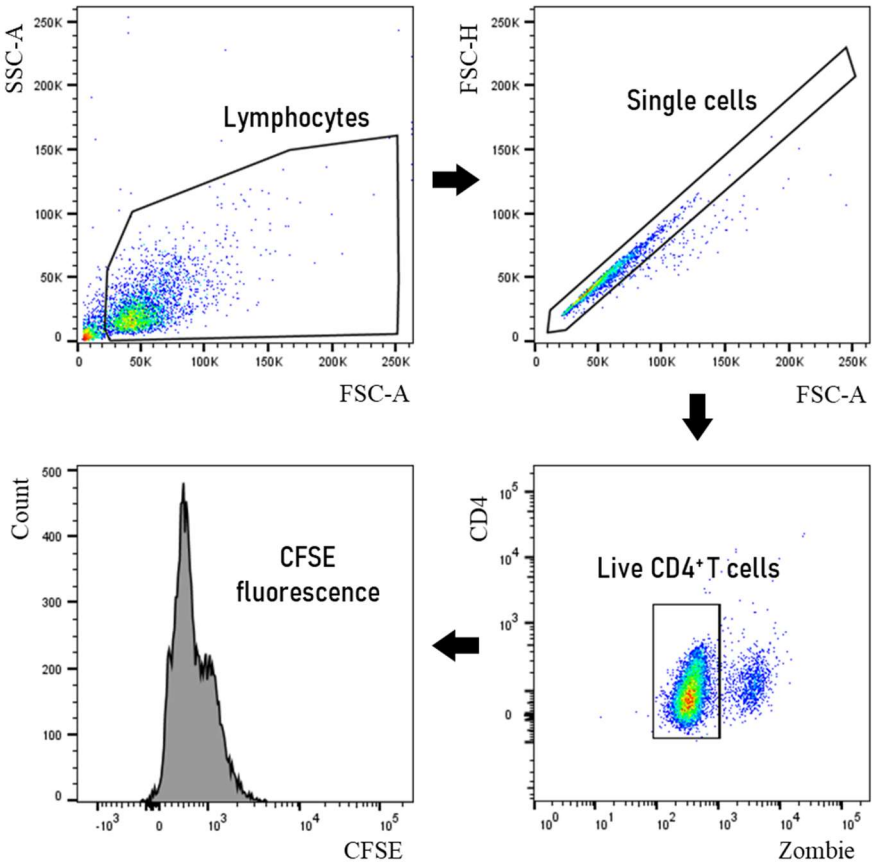


**Figure 35 -** Representative example of the way by which $CD4^+$ T cells were selected in the data obtained by FACS and presentation of one result concerning the cellular proliferation (CFSE fluorescence). At the upper left-side of the image, the lymphocytes were first selected in a FSC-A vs SSC-A graph which is followed by a FSC-A vs FSC-H chart that allow to select only the single cells present (excluding possible doublets present in the sample). Before measuring the CFSE fluorescence, we restricted the analyses to the $CD4^+$ T cells that were alive using the combination of CD4 and Zombie antibodies, selecting the ($CD4^+Zombie^-$) population. Abbreviations: CFSE (Carboxyfluorescein succinimidyl ester); FSC-A (Forward Scatter Area); FSC-H (Foward Scatter Height); SSC-A (Side Scatter Height).

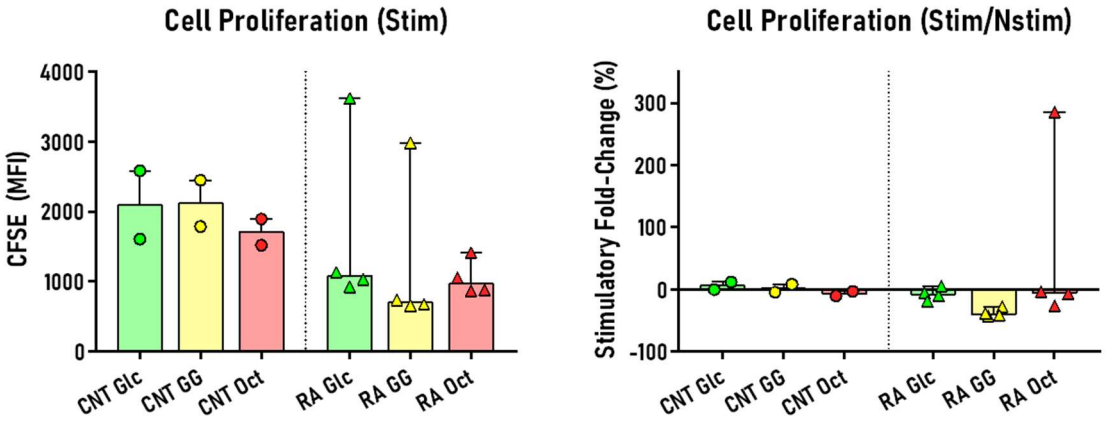


**Figure 36 -** Proliferation assay results for $CD4^+$ T cells from both CNT and RA groups in the three media provided to the cells. At the left the results show the $CD4^+$ T cells proliferation in the Stim conditions, at the right is represented the stimulatory fold-change (%) on the cells proliferation. In all graphs the CNT are represented on the left half of the graphs (dots), RA on the right half (triangles). Medium Glc (green), Medium GG (yellow), Medium Oct (red). The bars represent the median value and the confidence interval (CI) at 95%. *: $p<0,05$ with p being calculated using Kruskal-Wallis test with Dunn's multiple comparisons test. Number of samples: CNT=2; RA=3. Abbreviations: Nstim (Non-stimulated); Stim (Stimulated).

It could be suggested that $CD4^+$ T cells from the RA group have a higher proliferation rate when compared to the ones coming from healthy individuals, observation that is transversal to all media and is in accordance with the known hyper-activated state that these cells present in RA context (Chemin *et al.*, 2019). Even though the differences are minimal, in the CNT group the Oct medium seems to have a higher proliferation rate than the Glc and GG media, which are similar between them. On the other hand, in the RA group, the GG medium presents, apparently, the highest proliferation, being that the cells from Glc and Oct media present a similar proliferation extent. Regarding the results obtained for the comparation between Stim and Nstim conditions, there is a minimal impact of the stimulation in the $CD4^+$ T cells proliferation. This result suggests that, although $CD4^+$ T cells could change their metabolism in order to fulfill their biosynthetic needs in a Stim situation, these referred needs do not mean that the cells divide more than in a basal Nstim situation. Further analysis will be important to clarify if, despite the almost null effect in the proliferation of $CD4^+$ T cells, the stimulation alters the effector activity of these cells, namely in what concerns the cytokines production.

Taken together, the observations on $CD4^+$ T cells viability and proliferation suggest that in RA the $CD4^+$ T cells may be in a higher proliferative and biosynthetic stress, which could reduce their survival in the disease context.

### 3.3.6 Cytotoxic functions modulation in RA $CD4^+$ T cells

In addition to their important role in $CD4^+$ T cells fate after the antigen recognition, helping to define the subset that the original naïve cell will generate, cytokines are also major players in the subsequent immune response (Zhu and Paul, 2009; Luckheeram *et al.*, 2012). These small proteins could be considered the most important resources of $CD4^+$ T cells to help and regulate the reaction of the organism to the new or repeated pathogen, inclusively by potentially controlling the action of both $CD4^+$ and $CD8^+$ T cells (Zhu and Paul, 2009). Considering their different functions and mechanism of action, the cytokines produced by $CD4^+$ T cells could be divided in two major groups: pro-inflammatory cytokines and anti-inflammatory cytokines (Zhang and An, 2007; Zhu and Paul, 2009). Depending on their targets, cytokines action could be considered autocrine (when acting on the same cells that produce and secrete them), paracrine (when acting on other cells) or endocrine (when acting on distant cells, e.g. in different tissues).

Considering the high impact of the cytokines in the process of immune response, it could be inferred the utmost importance that these molecules have in autoimmune diseases triggering and sustenance, namely in the RA pathology. As referred in the Introduction section, the advance of clinical status of RA, namely the joint region destruction and consequent patient's pain is accompanied by the accumulation of $CD4^+$ and $CD8^+$ T cells in the synovial membrane, conducing to the increase in cytokines concentration in this region (Carvalheiro, 2014; Klocke *et al.*, 2017). Given this, it is of utmost importance to measure the cytokine secretion pattern in RA and CNT $CD4^+$ T cells when they are subjected to the different substrate's availability and to the metabolic inhibitors already referred in earlier subsections. This will help to understand the immunological modulation that $CD4^+$ T cells suffer in the distinct conditions provided and, correlating these results with the metabolic information analyzed in past subsections, it will be possible to get a wide spectrum of the immunometabolic modulation of $CD4^+$ T cells in RA.

Before presenting the results obtained it is important to briefly mention the cytokines that were the target of our analysis. Included in the group of pro-inflammatory cytokines are Interleukin-2 (IL-2), IL-4, IL-5, IL-6, IL-9, IL-13, IL-17A, IL-17F, IL-21,

IL-22, Interferon-γ (IFN-γ) and Tumor Necrosis Factor-α (TNF-α) (Luckheeram *et al.*, 2012). IFN- γ is the main cytokine produce by T helper 1 (Th1) cells subset, which leads to the activation of macrophages and, therefore, enhances the phagocytic activity of the immune response (Luckheeram *et al.*, 2012; Rodeghero *et al.*, 2013). Waiting for deeper understanding and confirmation is the suspicion that IFN- γ produced by Th1 cells could block Th17 cells responses in the specific context of RA disease, which give this cytokine a regulatory role, reducing the inflammation in the synovial region (Chemin *et al.*, 2019). Th1 cells, involved in organ-specific autoimmunity, also secrete IL-2 which increases the proliferation of $CD8^+$ T cells, inducing a higher cytolytic phenotype in these cells (Luckheeram *et al.*, 2012). IL-17A, IL-17F, IL-21 and IL-22 are the main cytokines secreted by Th17 cells, being this subset of $CD4^+$ T cells highly involved in the generation and sustenance of autoimmune diseases, namely RA. Due to the wide expression of the IL-17 receptor in skin, lung, intestine and joints, IL-17A and IL-17F are crucial mediators of the inflammatory response, being capable of induce the secretion of additional pro-inflammatory cytokines such as IL-6 or TNF- α (Luckheeram *et al.*, 2012). IL-21 is linked to the amplification of Th17 cells development. to the activation of B and T cells and NK cells (Luckheeram *et al.*, 2012). IL-22 is being associated with the induction of cell proliferation and antimicrobial peptides production (Luckheeram *et al.*, 2012; Rodeghero *et al.*, 2013). Th2 cells secrete some important pro-inflammatory effector cytokines such as IL-4, IL-5, IL-9 and IL-13. IL-4 is mainly connected to the activation of B cells, specially to the switching and secretion of IgE by these cells, being in this way linked to the allergic inflammation (Luckheeram *et al.*, 2012). IL-4 is also linked to the induction of IL-6 secretion, being that IL-5 plays an important role in the activation of eosinophils and its precursors (Luckheeram *et al.*, 2012). IL-9 has a wide spectrum of targets that include mast cells, B cells, eosinophils and neutrophils, being linked to several immunopathogenesis including asthma (Reader *et al.*, 2003; Luckheeram *et al.*, 2012). IL-13 is being associated with the stimulation of tissue fibrosis localized in the inflammation local (Wynn, 2003; Luckheeram *et al.*, 2012). IL-6 has been regarded as a pro-inflammatory cytokine by its role in promoting the secretion of IL-4 and Il-17 cytokines from both Th2 and Th17 cells, therefore acting as a $CD4^+$ T cells modulator (Dienz and Rincon, 2009; Luckheeram *et al.*, 2012). Finally, TNF-α is an important regulator of T cells interaction and differentiation, being also promotor of their pro-inflammatory effector functions by directly inducing IL-4 and IFN-γ secretion (Croft, 2009).

In the group of anti-inflammatory/regulatory cytokines it was analyzed IL-10 (Luckheeram *et al.*, 2012). This cytokine has been defined as a regulator of both innate and adaptive immune responses, helping the organism to achieve the homeostasis after the pathogen clearance by inhibiting, for example, Th1 cells (Couper, Blount and Riley, 2008; Ouyang *et al.*, 2011). IL-10 is mainly secreted by Treg cells (Dupage and Bluestone, 2016) but could also be both secrete by Th1 and Th2 cells (Ouyang *et al.*, 2011; Luckheeram *et al.*, 2012). Considering its suppressive actions, it is of the utmost importance to analyze the state of secretion of IL-10 in the context of RA.

Cytokines secretion levels by $CD4^+$ T cells in both healthy individuals and RA patients, in the different media chosen and adopted experimental conditions, are presented in **Figure 37.** This data includes the pro-inflammatory cytokines and regulatory/suppressive cytokine IL-10.

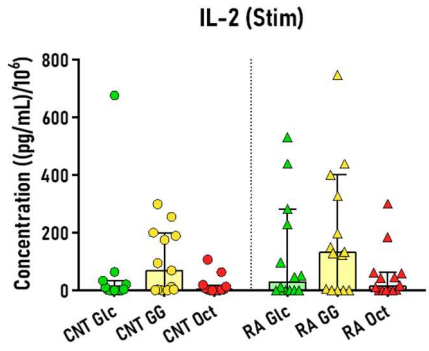
IL-2 (Stim)
Concentration ((pg/mL)/10^6)
800
600
400
200
0
CNT Glc
CNT GG
CNT Oct
RA Glc
RA GG
RA Oct

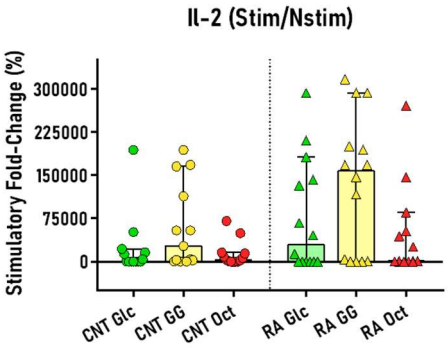
Il-2 (Stim/Nstim)
Stimulatory Fold-Change (%)
300000
225000
150000
75000
0
CNT Glc
CNT GG
CNT Oct
RA Glc
RA GG
RA Oct

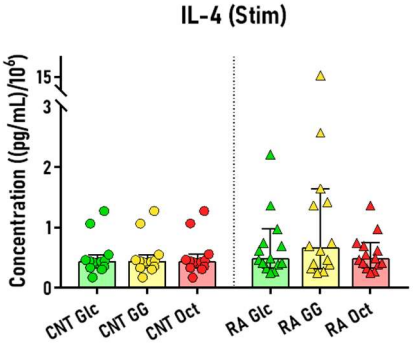
IL-4 (Stim)
Concentration ((pg/mL)/10^6)
15
3
2
1
0
CNT Glc
CNT GG
CNT Oct
RA Glc
RA GG
RA Oct

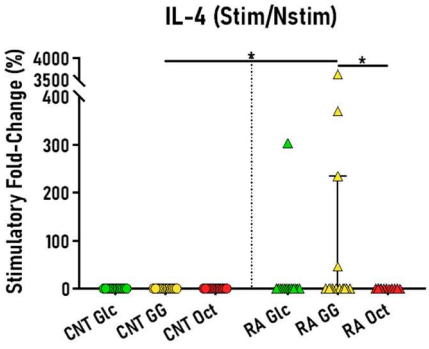
IL-4 (Stim/Nstim)
Stimulatory Fold-Change (%)
4000
3500
400
300
200
100
0
*
*
CNT Glc
CNT GG
CNT Oct
RA Glc
RA GG
RA Oct

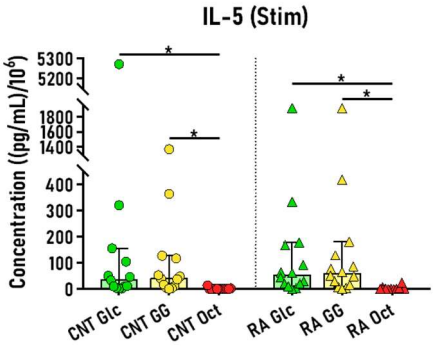
IL-5 (Stim)
Concentration ((pg/mL)/10^6)
5300
5200
1800
1600
1400
400
300
200
100
0
*
*
*
CNT Glc
CNT GG
CNT Oct
RA Glc
RA GG
RA Oct

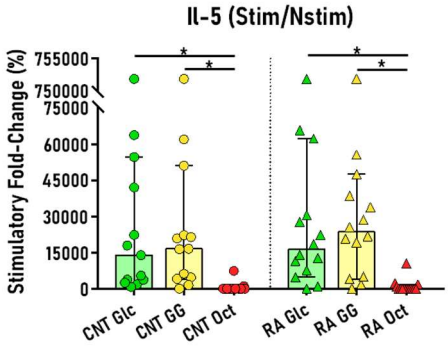
Il-5 (Stim/Nstim)
Stimulatory Fold-Change (%)
755000
750000
75000
60000
45000
30000
15000
0
*
*
*
*
CNT Glc
CNT GG
CNT Oct
RA Glc
RA GG
RA Oct

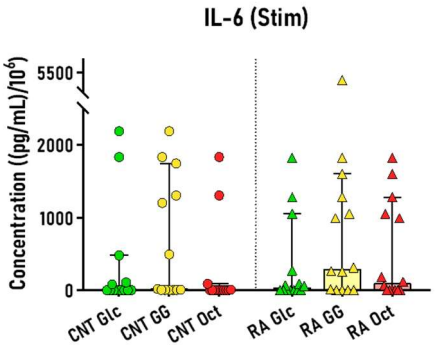
IL-6 (Stim)
Concentration ((pg/mL)/10^6)
5500
2000
1000
0
CNT Glc
CNT GG
CNT Oct
RA Glc
RA GG
RA Oct

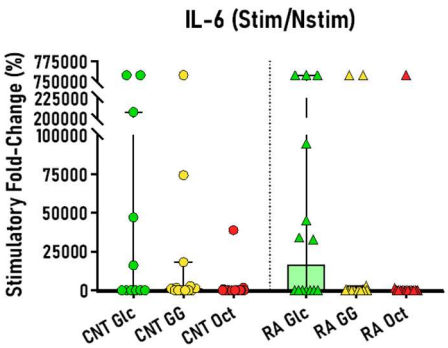
IL-6 (Stim/Nstim)
Stimulatory Fold-Change (%)
775000
750000
225000
200000
100000
75000
50000
25000
0
CNT Glc
CNT GG
CNT Oct
RA Glc
RA GG
RA Oct

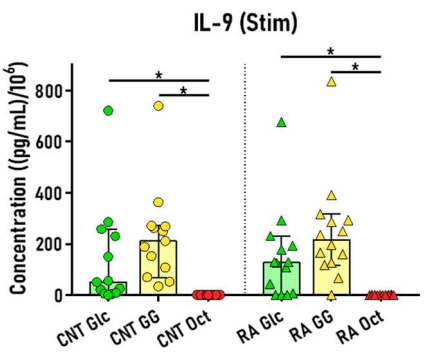
IL-9 (Stim)
Concentration ((pg/mL)/10^6)
800
600
400
200
0
*
*
*
*
CNT Glc
CNT GG
CNT Oct
RA Glc
RA GG
RA Oct

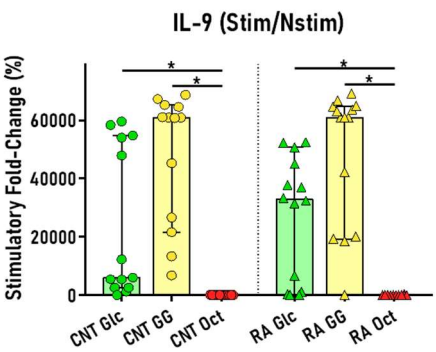
IL-9 (Stim/Nstim)
Stimulatory Fold-Change (%)
60000
40000
20000
0
*
*
*
*
CNT Glc
CNT GG
CNT Oct
RA Glc
RA GG
RA Oct

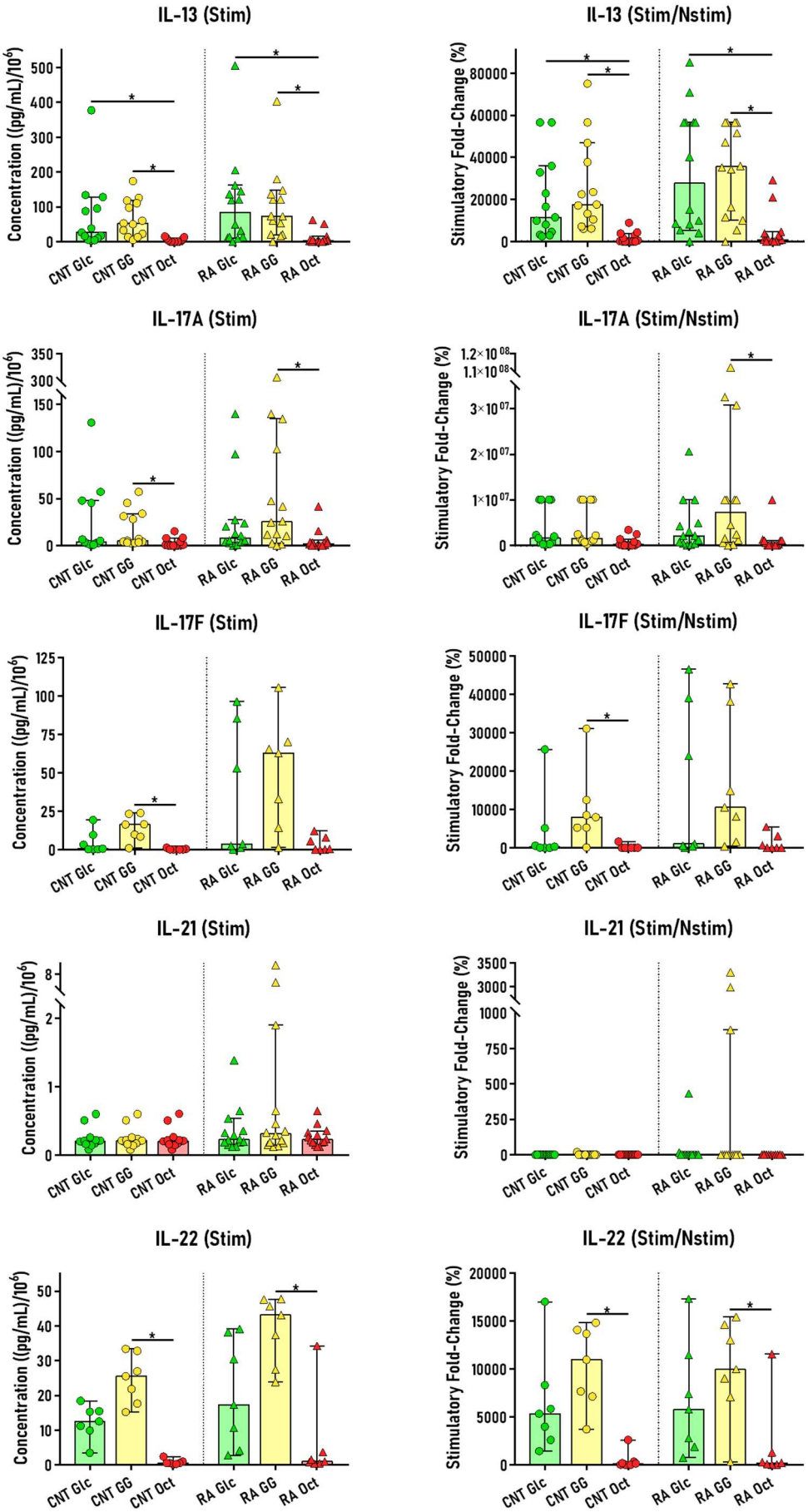
IL-13 (Stim)
Concentration ((pg/mL)/10^6)
IL-13 (Stim/Nstim)
Stimulatory Fold-Change (%)
IL-17A (Stim)
Concentration ((pg/mL)/10^6)
IL-17A (Stim/Nstim)
Stimulatory Fold-Change (%)
IL-17F (Stim)
Concentration ((pg/mL)/10^6)
IL-17F (Stim/Nstim)
Stimulatory Fold-Change (%)
IL-21 (Stim)
Concentration ((pg/mL)/10^6)
IL-21 (Stim/Nstim)
Stimulatory Fold-Change (%)
IL-22 (Stim)
Concentration ((pg/mL)/10^6)
IL-22 (Stim/Nstim)
Stimulatory Fold-Change (%)
CNT Glc
CNT GG
CNT Oct
RA Glc
RA GG
RA Oct

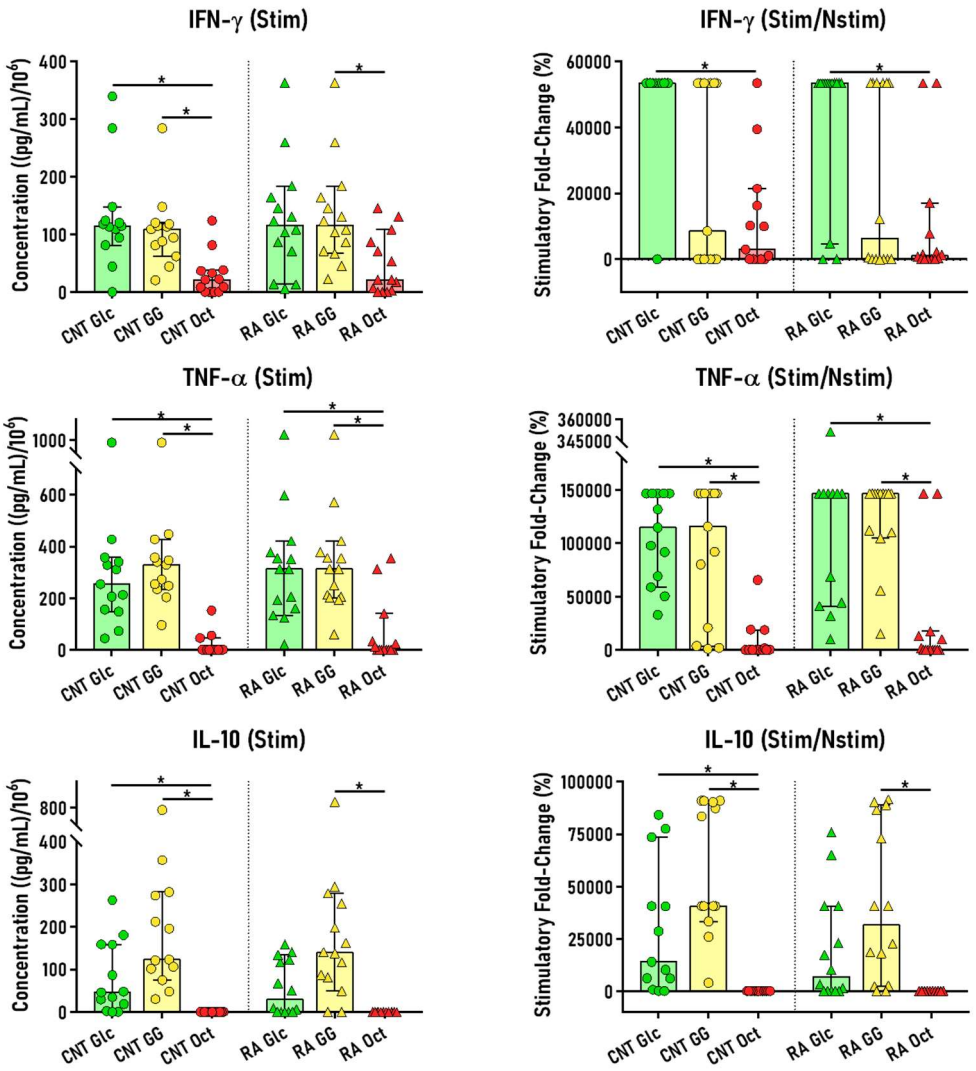


**Figure 37** - Cytokine secretion in $CD4^+$ T cells in the Stim conditions (presented in concentration, pg/ml, per $10^6$ cells) and the comparison between Stim and Nstim conditions (stimulatory fold-change in %). From top to bottom, the cytokines presented are the pro-inflammatory cytokines IL-2, IL-4, IL-5, IL-9, IL-6, IL-13, IL-17A, IL-17F, IL-21. IL-22, IFN-γ and TNF-α and the regulatory/suppressive cytokine IL-10. All the results were obtained by FACS. In all graphs the CNT are represented on the left half of the graphs (dots), RA on the right half (triangles). Medium Glc (green), Medium GG (yellow), Medium Oct (red). The bars represent the median value and the confidence interval (CI) at 95%. *: $p<0,05$ with p being calculated using Kruskal-Wallis test with Dunn's multiple comparisons test. Number of samples: CNT=13; RA=14. Abbreviations: Nstim (Non-stimulated); Stim (Stimulated).

As it could be observed in the graphics presented above, there is a clear pattern of cytokine's production in $CD4^+$ T cells from both CNT and RA group and in all 3 media provided to the cells when looking for the concentration (pg/mL per $10^6$ cells) obtained in the Stim conditions.

In general, the secretion of cytokines by $CD4^+$ T cells is apparently higher in RA group than in CNT group, particularly for the Glc and GG media. It could also be suggested that the medium where the production and subsequent secretion of cytokine shows higher values is the GG medium. The apparent higher concentrations of cytokines in this medium than in Glc or Oct media is transversal to almost all cytokines, as it is the minimal or essentially null secretion of cytokines in the Oct medium, with some exceptions observed (IL-4 and IL-21). Even when looking for the secretion levels of a regulatory/inflammatory suppressive cytokine such as IL-10 it is clear that the pattern described above is also applicable to this cytokine.

Regarding the results obtained in the stimulatory fold-change (Stim vs Nstim conditions) it is clear that Glc and, principally, GG media present, in a transversal way to all cytokines studied, a higher stimulation impact than Oct medium.

These results suggest that the ideal combination of substrates, from the ones provided, to feed cytokines production and secretion by $CD4^+$ T cells is glucose in addiction to glutamine in fair concentrations (5 mM or 2 mM in the case of glucose, 2 mM in the case of glutamine), being this is in line with the known increased consumption of these substrates observed after $CD4^+$ T cells activation (Renner *et al.*, 2015). This conclusion is supported by the scarce glucose levels in the Oct medium (where 1.1 mM glucose, 2 mM glutamine, 1 mM octanoate were present) which could indicate that the $CD4^+$ T cells are not prone to compensate a huge lack of glucose availability with the usage of fatty acids when talking about their cytokine production. This absence of cytotoxic activity from $CD4^+$ T cells in Oct medium could be also related with the aforementioned lower levels of cells survival in this medium due to the scarce glucose availability. In addition, the lack of this substrate and its influence in the effector functions of $CD4^+$ T cells finds some support in the literature, where it has been already described that aerobic glycolysis activity could positively control the production of some cytokines, namely IFN-γ, being suggested that the enzyme GADPH (which takes part in the glycolytic flux)

may interfere in the transcriptional activity involved in the cytotoxic machinery (Dennis *et al.*, 2012).

The fact that some cytokines, namely IL-2, IL-4, IL-6, IL-9, IL-17A, IL-17F, IL-22 and IL-10, were more produced in the medium GG that in the medium Glc is somehow surprising giving the fact the only difference between these two media is the glucose concentration, which is actually higher in the Glc medium (5 mM vs 2 mM). Although this difference could not be totally explained by the data that we have at our disposal, there is available published data, from other research groups, that indicates that a reduction in the glucose may have an impact in $CD4^+$ T cells proliferation but does not interfere with their cytotoxic functions (Tripmacher *et al.*, 2008; Renner *et al.*, 2015). Actually, it was already observed that glucose deprivation could lead to the increase in IL-4 production in $CD4^+$ T cells from peripheral blood, which were attributed to a higher presence of Th2 cells and to the dysfunction of Th1 cells, being this associated with tumor microenvironments (Ota *et al.*, 2016). One of the studies previously mentioned studied the effects of glucose deprivation and mitochondrial restriction, separately, and of the simultaneous blockade of both glycolysis and respiration, using 2-deoxyglucose (2-DG) (Renner *et al.*, 2015), concluding that the cells presented great functional plasticity when only one of the two fluxes was inhibited but were unable to sustain their cytotoxic capability when both pathways were targeted. In addition to what was referred above, this could help to explain the shy cytokine production in the Oct medium, which had the lower glucose availability from all the media and, being the cells not prone to use octanoate as substrate, as demonstrated in earlier sections, their general metabolic activity will be overly affected, having a negative impact in their cytokine production.

Considering the results of viability and proliferation presented previously, it could be suggested that all substrate combinations provided to $CD4^+$ T cells are capable of supporting their metabolic activity in order to survive and even proliferate, being that in Oct medium they already show a decrease in their survival. When looking for the capacity of $CD4^+$ T cells to exert their immunological functions, and specifically their cytokine production and secretion task, it is clear that these cells require specific conditions, namely a minimal availability of glucose. We therefore conclude that $CD4^+$ T cells, although surviving and proliferating, cannot perform their effector and regulatory functions without

sufficient glucose availability. The results obtained concerning the effect of both FX11 and Rotenone in the $CD4^+$ T cells cytokine production levels are represented in **Figure 38**.

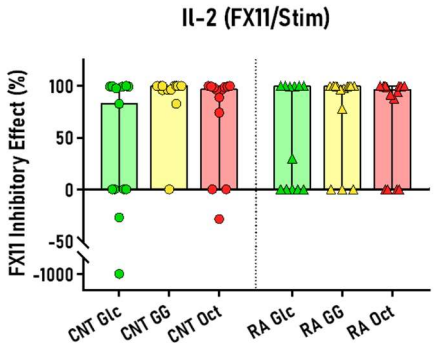
Il-2 (FX11/Stim)
FX11 Inhibitory Effect (%)
100
50
0
-50
-1000
CNT Glc
CNT GG
CNT Oct
RA Glc
RA GG
RA Oct

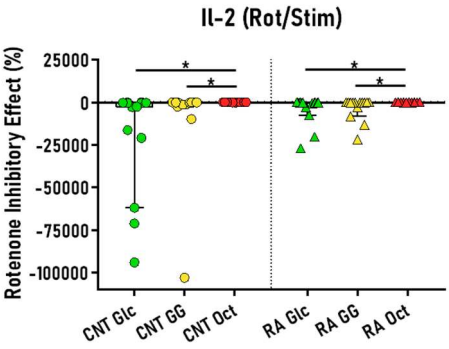
Il-2 (Rot/Stim)
Rotenone Inhibitory Effect (%)
25000
0
-25000
-50000
-75000
-100000
CNT Glc
CNT GG
CNT Oct
RA Glc
RA GG
RA Oct

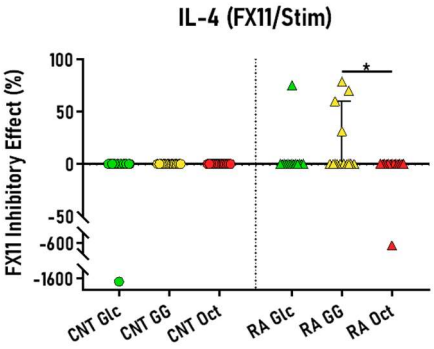
IL-4 (FX11/Stim)
FX11 Inhibitory Effect (%)
100
50
0
-50
-600
-1600
CNT Glc
CNT GG
CNT Oct
RA Glc
RA GG
RA Oct

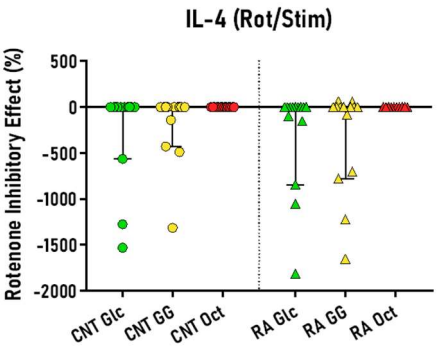
IL-4 (Rot/Stim)
Rotenone Inhibitory Effect (%)
500
0
-500
-1000
-1500
-2000
CNT Glc
CNT GG
CNT Oct
RA Glc
RA GG
RA Oct

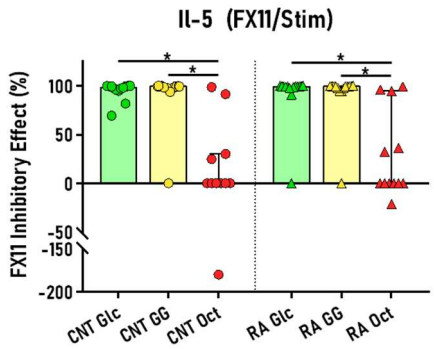
Il-5 (FX11/Stim)
FX11 Inhibitory Effect (%)
100
50
0
-50
-150
-200
CNT Glc
CNT GG
CNT Oct
RA Glc
RA GG
RA Oct

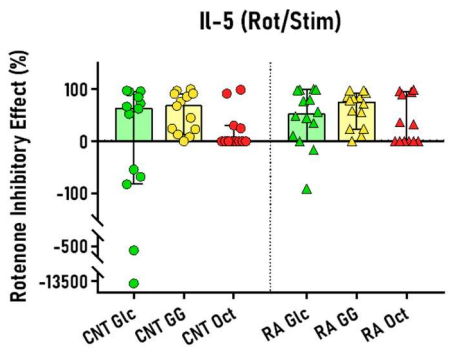
Il-5 (Rot/Stim)
Rotenone Inhibitory Effect (%)
100
0
-100
-500
-13500
CNT Glc
CNT GG
CNT Oct
RA Glc
RA GG
RA Oct

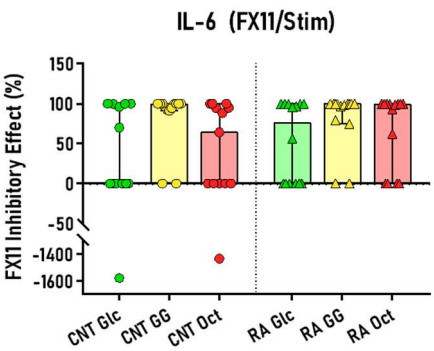
IL-6 (FX11/Stim)
FX11 Inhibitory Effect (%)
150
100
50
0
-50
-1400
-1600
CNT Glc
CNT GG
CNT Oct
RA Glc
RA GG
RA Oct

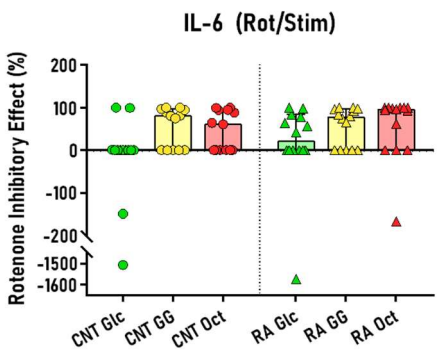
IL-6 (Rot/Stim)
Rotenone Inhibitory Effect (%)
200
100
0
-100
-200
-1500
-1600
CNT Glc
CNT GG
CNT Oct
RA Glc
RA GG
RA Oct

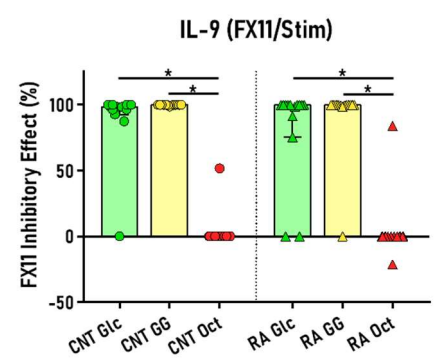
IL-9 (FX11/Stim)
FX11 Inhibitory Effect (%)
100
50
0
-50
CNT Glc
CNT GG
CNT Oct
RA Glc
RA GG
RA Oct

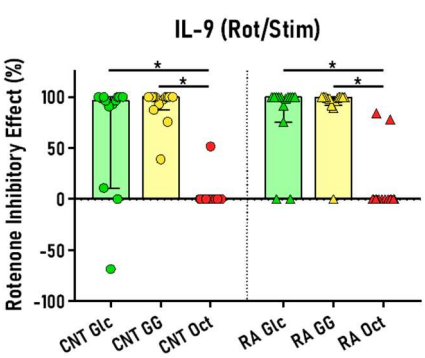
IL-9 (Rot/Stim)
Rotenone Inhibitory Effect (%)
100
50
0
-50
-100
CNT Glc
CNT GG
CNT Oct
RA Glc
RA GG
RA Oct

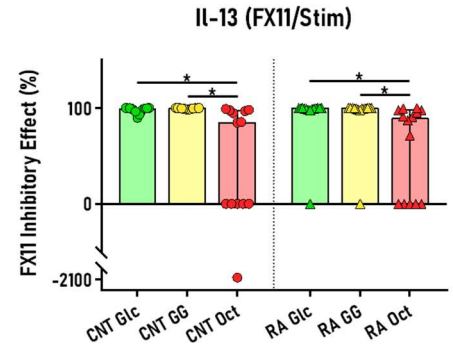
IL-13 (FX11/Stim)
FX11 Inhibitory Effect (%)
100
0
-2100
CNT Glc
CNT GG
CNT Oct
RA Glc
RA GG
RA Oct

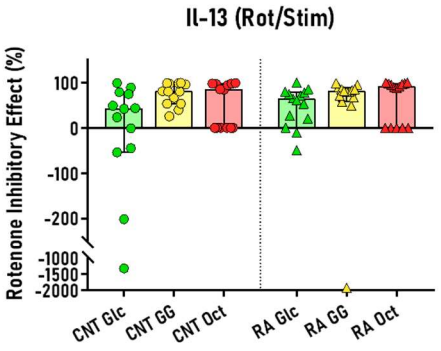
IL-13 (Rot/Stim)
Rotenone Inhibitory Effect (%)
100
0
-100
-200
-1000
-1500
-2000
CNT Glc
CNT GG
CNT Oct
RA Glc
RA GG
RA Oct

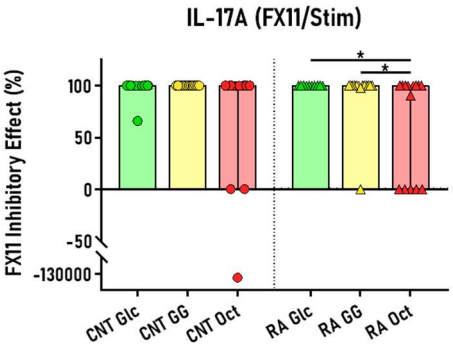
IL-17A (FX11/Stim)
FX11 Inhibitory Effect (%)
100
50
0
-50
-130000
CNT Glc
CNT GG
CNT Oct
RA Glc
RA GG
RA Oct

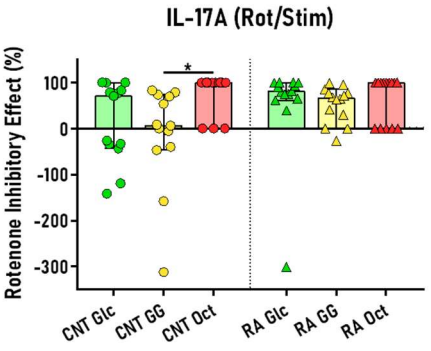
IL-17A (Rot/Stim)
Rotenone Inhibitory Effect (%)
100
0
-100
-200
-300
CNT Glc
CNT GG
CNT Oct
RA Glc
RA GG
RA Oct

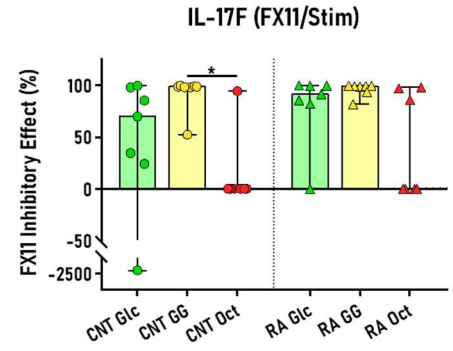
IL-17F (FX11/Stim)
FX11 Inhibitory Effect (%)
100
50
0
-50
-2500
CNT Glc
CNT GG
CNT Oct
RA Glc
RA GG
RA Oct

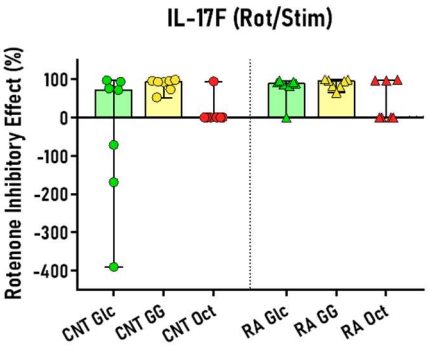
IL-17F (Rot/Stim)
Rotenone Inhibitory Effect (%)
100
0
-100
-200
-300
-400
CNT Glc
CNT GG
CNT Oct
RA Glc
RA GG
RA Oct

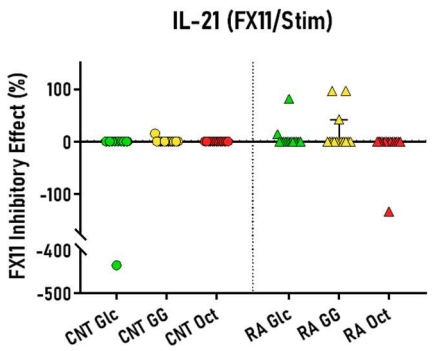
IL-21 (FX11/Stim)
FX11 Inhibitory Effect (%)
100
0
-100
-400
-500
CNT Glc
CNT GG
CNT Oct
RA Glc
RA GG
RA Oct

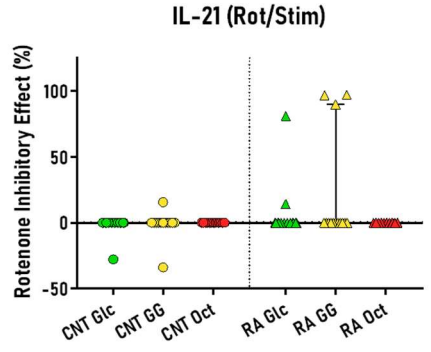
IL-21 (Rot/Stim)
Rotenone Inhibitory Effect (%)
100
50
0
-50
CNT Glc
CNT GG
CNT Oct
RA Glc
RA GG
RA Oct

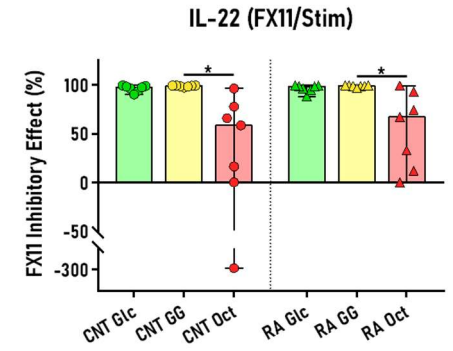
IL-22 (FX11/Stim)
FX11 Inhibitory Effect (%)
100
50
0
-50
-300
CNT Glc
CNT GG
CNT Oct
RA Glc
RA GG
RA Oct

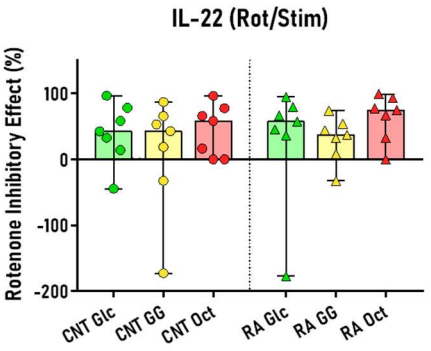
IL-22 (Rot/Stim)
Rotenone Inhibitory Effect (%)
100
0
-100
-200
CNT Glc
CNT GG
CNT Oct
RA Glc
RA GG
RA Oct

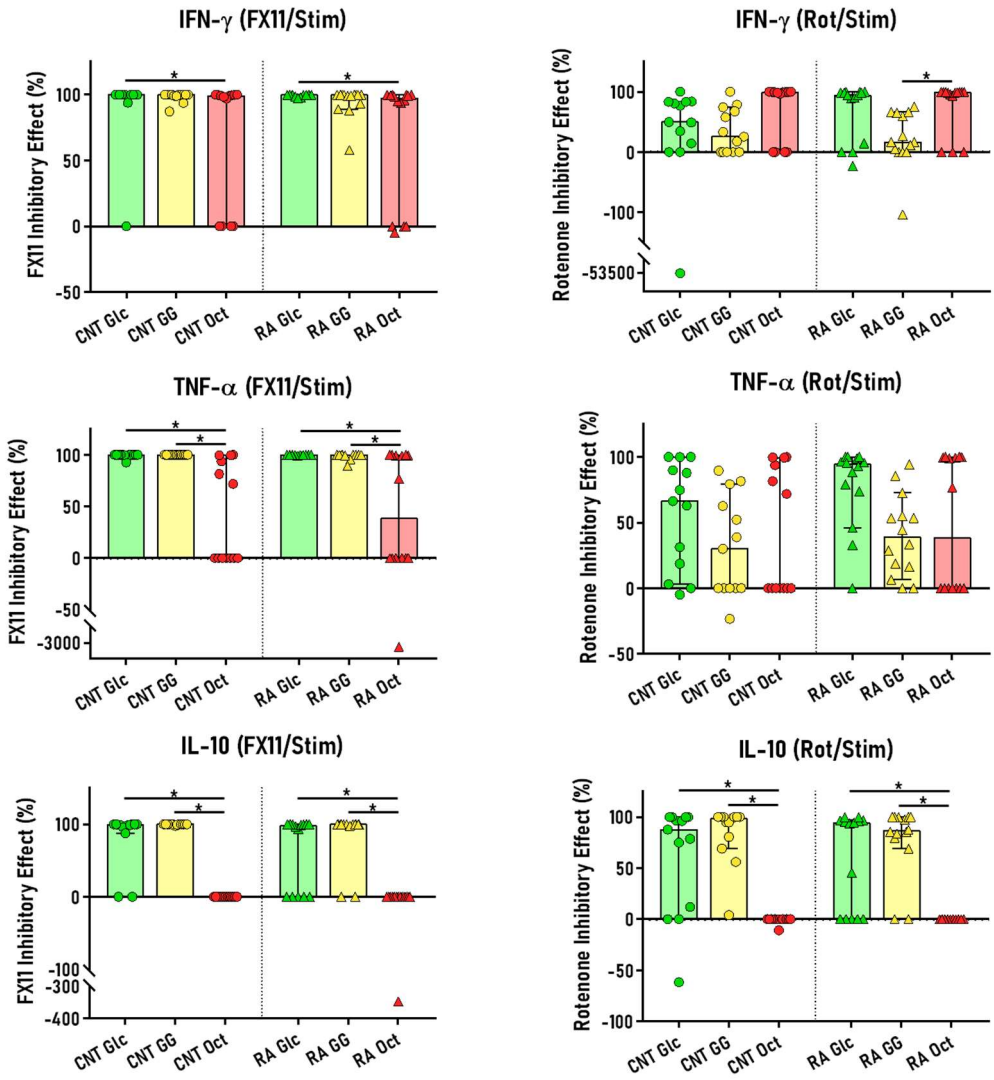


**Figure 38** - Impact of FX11 and Rotenone in cytokine secretion in $CD4^+$ T cells (compared to the Stim condition, in %). From top to bottom, the cytokines presented are the pro-inflammatory cytokines IL-2, IL-4, IL-5, IL-9, IL-6, IL-13, IL-17A, IL-17F, IL-21. IL-22, IFN-γ and TNF-α and the regulatory/suppressive cytokine IL-10. All the results were obtained by FACS. In all graphs the CNT are represented on the left half of the graphs (dots), RA on the right half (triangles). Medium GLC (green), Medium GG (yellow), Medium Oct (red). The bars represent the median value and the confidence interval (CI) at 95%. *: $p<0,05$ with p being calculated using Kruskal-Wallis test with Dunn's multiple comparisons test. Number of samples: CNT=13; RA=14. Abbreviations: Rot (Rotenone); Stim (Stimulated).

As it could be observed by the data provided, in general, the inhibitors used (FX11 and Rotenone) have a negative impact in what concerns the production and secretion of cytokines by $CD4^+$ T cells in both CNT and RA groups. The inhibitory effect of FX11 and Rotenone, when compared with the Stim condition, did not impact uniformly in all media or has a clear pattern, with the exception of both IL-4 and IL-21 that show no variation with any inhibitor (FX11 or Rotenone), which could be explained by the lower concentrations of these cytokines secreted even in the Stim condition (approximately 0.5 and 0.2 pg/ml per $10^6$ cells for IL-4 and IL-21, respectively). There are some other cytokines where there is no impact of FX11 or Rotenone in Oct medium, not necessarily because these inhibitors did not exert any effects in the cells but, much probably, due to their already minimal levels or even absence of cytokine production in the Stim condition, supposedly the condition that elicits more cytokine production (this could be observed for IL-4, IL-5, IL-9, IL-10, IL-17F, IL-21 and TNF-α).

The inhibitory effect of FX11 in the cytokine secretion from $CD4^+$ T cells in GG medium is clear and transversal to almost all cytokines evaluated. The same could be said for the Glc medium, with the exceptions of IL-4, IL-6 and IL-21, which had considerably lower secretion levels. In the Oct medium the impact of this inhibitor is clearly negative in IL-2, IL-6, IL-13, IL-17A, IL-22 and IFN-γ, cytokines that show some level of secretion in the Stim condition. It could be therefore concluded that FX11 has a negative impact in the immunological functions of $CD4^+$ T cells, decreasing in a high or total extent (inhibitory effect near 100%) the cytokine production and secretion in all media provided to the cells. These results are not totally corroborated by the metabolic data presented before, where it was shown that FX11 had a minor or even stimulatory role in $CD4^+$ T cells metabolism, namely by increasing LDHA expression and lactate production. Although no literature is currently available about this subject, it could be suggested by our data that FX11 may have a direct impact in the cytokine production mechanisms, explaining its high impact in the cytokine production in $CD4^+$ T cells despite the minor metabolic impact observed before.

The evaluation of the impact of Rotenone in the cytokine secretion of $CD4^+$ T cells might be done in the same line of thought followed for FX11. In general, this inhibitor shows also a negative impact in the production and secretion of cytokines, with the exceptions for the cytokines that had their levels already low in the Stim conditions. It could not be stablished a clear and specific pattern for the impact of Rotenone in $CD4^+$ T cells in the media provided but, together with the results obtained for FX11 it may be

concluded that, independently of the metabolic impact of these inhibitors (presented above), the immunological functions of $CD4^+$ T cells concerning the production and secretion of pro-inflammatory and regulatory cytokines are at risk. As stated above, there is evidence that low glucose levels, to a certain limit, and OXPHOS blockage, when applied separately, do not exert a significant impact in $CD4^+$ T cells cytokine production (Tripmacher *et al.*, 2008). Thus, considering the previously exposed and discussed metabolic impact of FX11 and Rotenone and, moreover, the fact that these two inhibitors were applied separately to the cells, we are prone to suggest that the negative impact that they had in the cytokine production levels in $CD4^+$ T cells could be instigated by a direct action of these molecules in the cytotoxic machinery of these cells being that, in the case of Rotenone, and as shown before, the metabolic machinery was also negatively affected, which do not occur with FX11, and could be correlated with this lower cytotoxic activity. In future projects it will be of outstanding interest to clarify the specific role of FX11 and Rotenone in T cells effector functions, namely their cytokine production.

Considering the presented results, it could be suggested that $CD4^+$ T cells could not accomplish their cytotoxic action in conditions of low glucose availability such as the ones provided by the Oct medium, where the presence of fatty acids (octanoate) do not compensate for the lack of glucose, being this substrate pivotal for fulfilling $CD4^+$ T cells bioenergetic and biosynthetic needs. The current perspective of $CD4^+$ T cells exclusively relying on fatty acids utilization to proliferate and exert their immune functions (Hradilkova *et al.*, 2019) is, once more, contradicted by the results presented here.

### 3.3.7 Naïve vs memory $CD4^+$ T cells

In the final subsection of this Results and Discussion section it will be shown some data concerning the potential differences between two subsets of $CD4^+$ T cells when concerning their metabolic activity. This analysis was possible by the FACS separation of these $CD4^+$ T cells' subsets, naïve and memory, using antibodies against CD45 RO and CD45 RA, two $CD4^+$ T cells transmembrane located proteins that, due to their extracellular domain, could be used to distinguish these 2 $CD4^+$ T cells subsets. The naïve $CD4^+$ T cells are characterized by a higher expression of CD45RA ($CD4^+CD45RA^+CD45RO^-$), being the higher expression of CD45RO characteristic of the memory $CD4^+$ T cells ($CD4^+CD45RO^+CD45RA^-$). Using this separation technique, which is represented in **Figure 39**, it was possible to measure the expressions of some enzymes and proteins involved in the metabolic processes of $CD4^+$ T cells (LDHA, PDH,

GDH and SDHA) but also in apoptosis (such as PD-1), when these cells were subjected to the distinct media aforementioned (Glc, GG and Oct).

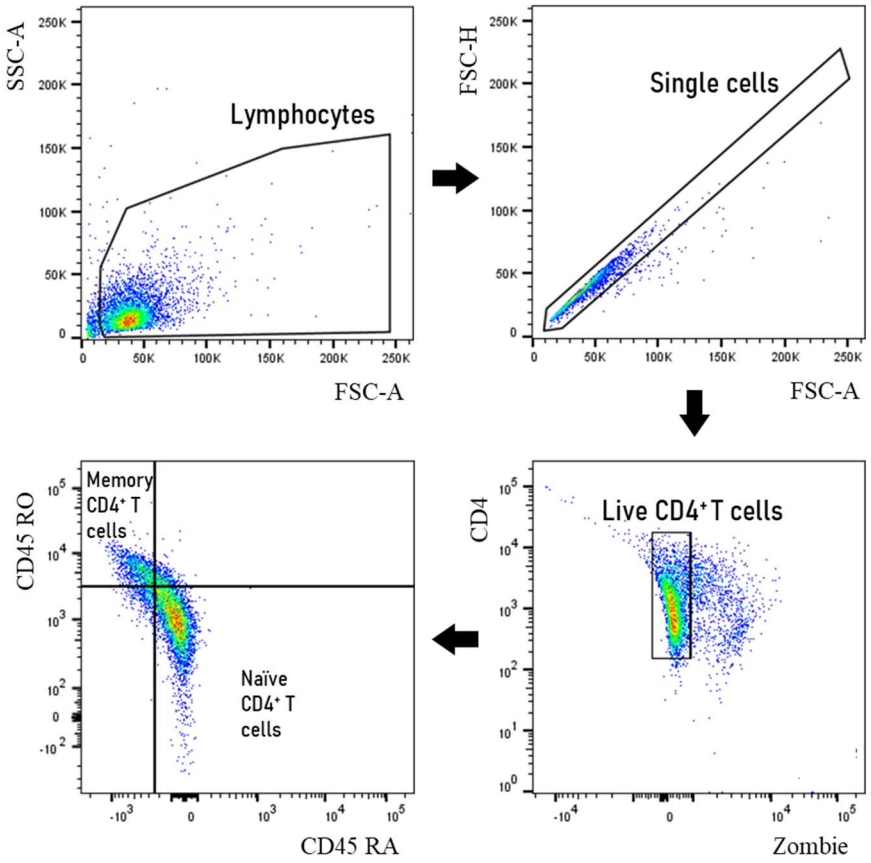


**Figure 39** - Representative example of the way by which naïve and memory $CD4^+$ T cells were selected in the data acquired by FACS. At the left-side of the image, the lymphocytes were first selected in a FSC-A vs SSC-A graph which is followed by a FSC-A vs FSC-H chart that allow to select only the single cells present (excluding possible doublets present in the sample). After restricting the analyses to the $CD4^+$ T cells that were alive using the combination of CD4 and Zombie antibodies, selecting the ($CD4^+Zombie^-$) population, we were able to separate the naïve ($CD45RA^+CD45RO^-$) from the memory ($CD4^+CD45RO^+CD45RA^-$) population before measuring the targeted parameters. Abbreviations: FSC-A (Forward Scatter Area); FSC-H (Foward Scatter Height); SSC-A (Side Scatter Height).

As stated at the Introduction, the naïve subset is the "untouched" type of $CD4^+$ T cells. This subset did not interact with any antigen presenting cell activated by any antigen. Upon contact there is activation and clonal expansion of these naïve cells to, for example, effector or memory subsets. Cells from this subset are thus expected to have a basal metabolic level to support their relatively low energetic and biosynthetic needs. On

the contrary, the memory CD4$^+$ T cells, which are produced in the remission process of the immune response, are part of a more active immune response when an antigen re-enters the organism. It is expected that these memory cells, although being in a more passive state that their effector counter-parts, are metabolically more active that the naïve subset, especially in the RA context where a constant immune activation is observed. Thus, memory CD4$^+$ T cells are expected to have a higher utilization of their metabolic machinery in order to fulfill their energetic and biosynthetic requirements.

The expressions of the metabolic enzymes aforementioned in naïve and memory CD4$^+$ T cells in the three different media are presented in **Figure 40**.

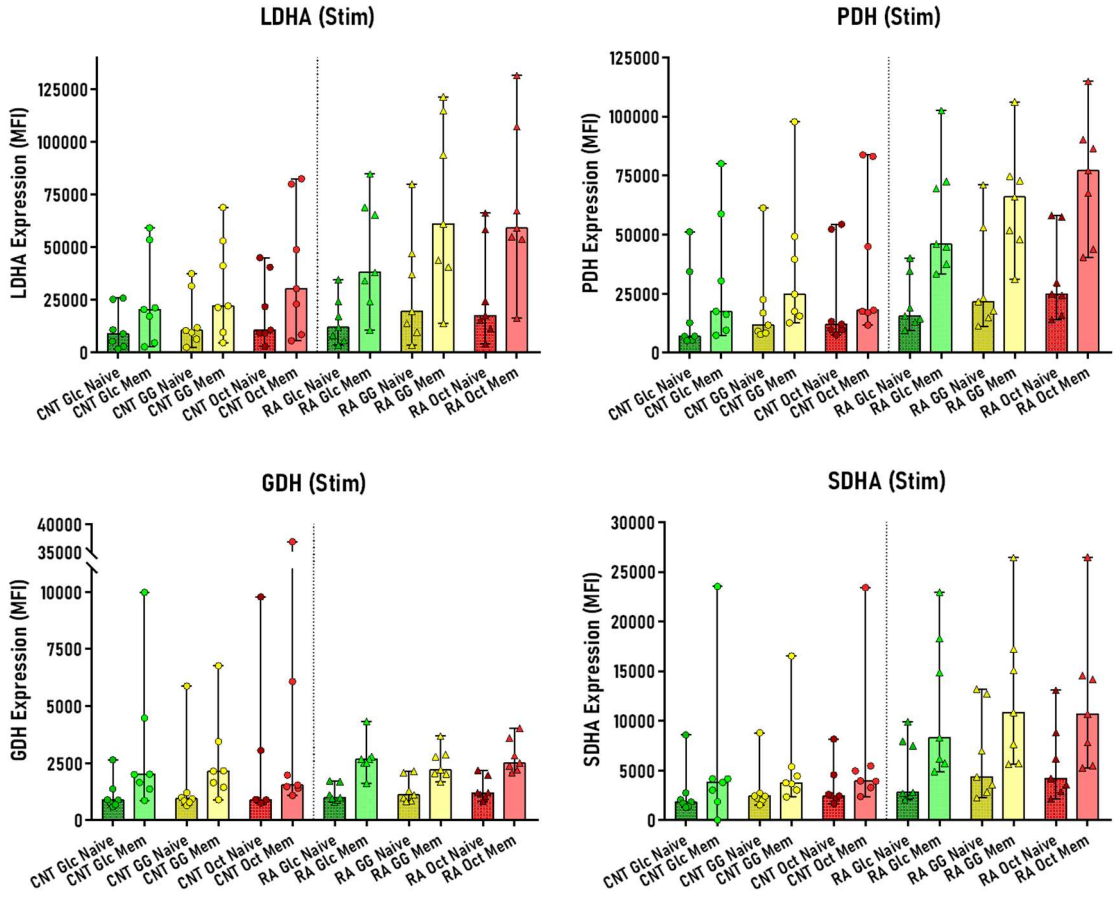


**Figure 40** - Expressions of LDHA, PDH, GDH and SDHA in the stimulated conditions (Stim) for both naïve and memory CD4$^+$ T cells in CNT and RA group. In all graphs the CNT are represented on the left half of the graphs (dots), RA on the right half (triangles). Medium GLC (green), Medium GG (yellow), Medium Oct (red). For each media the naïve subset is represented at the left and the memory subset at the right side. The bars represent the median value and the confidence interval (CI) at 95%. Number of samples: CNT=7; RA=7. Abbreviations: Stim (Stimulated).

Looking to the results presented in the figure above, and corroborating what was expected, it could be suggested that the expressions of all enzymes presented are higher in memory $CD4^+$ T cells than in naïve $CD4^+$ T cells, being the apparent differences transversal to all media and more pronounced in the RA group. This supports the idea of a higher metabolic activation in memory than in naïve $CD4^+$ T cells which is true in both glycolytic pathway (LDHA) or TCA cycle/OXPHOS flux (PDH, GDH and SDHA). In addition to these enzymatic expression analyses, and in a similar way to what was presented in earlier results subsections, we also looked to the ROS production, PD-1 expression and lipid peroxidation levels in naïve and memory $CD4^+$ T cells in the CNT and RA groups (**Figure 41**).

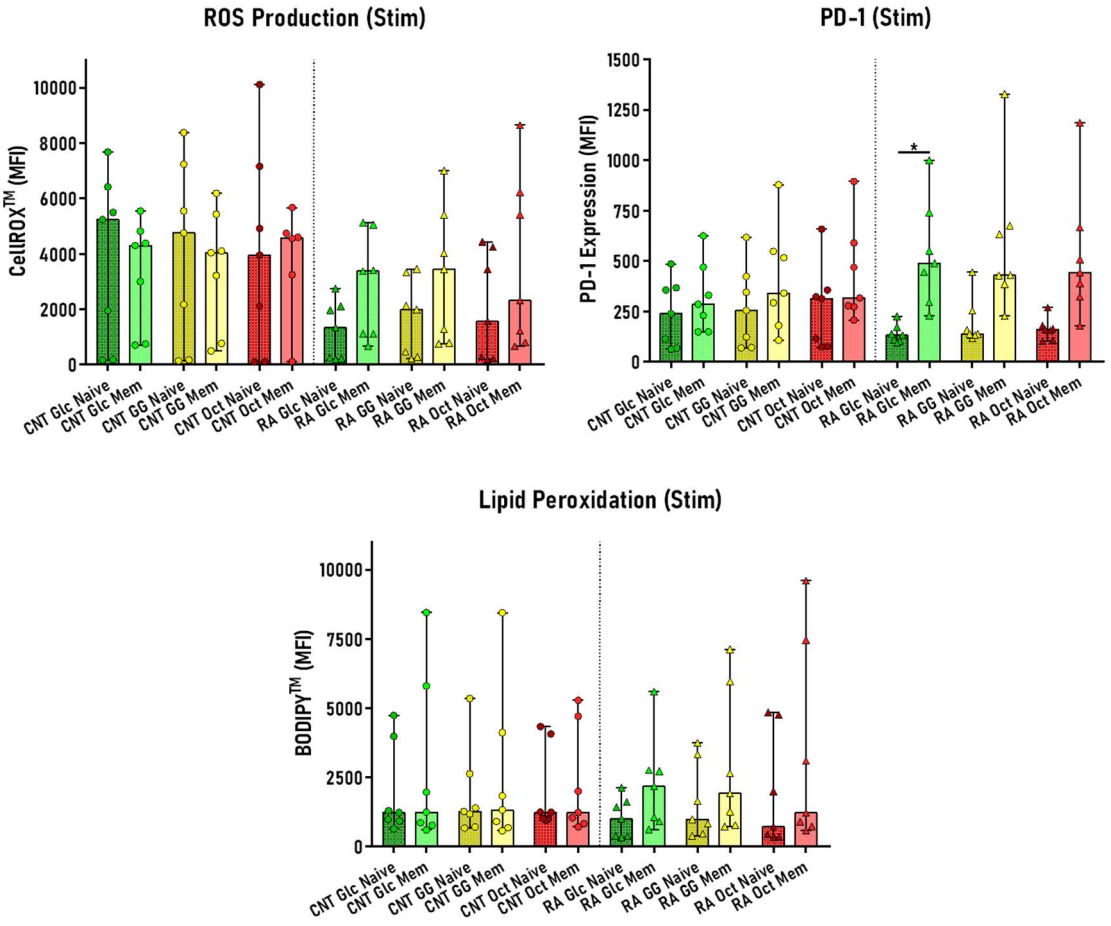


**Figure 41** - ROS production, PD-1 expression and lipid peroxidation in the stimulated conditions (Stim) for both naïve and memory $CD4^+$ T cells in CNT and RA group. In all graphs the CNT are represented on the left half of the graphs (dots), RA o the right half (triangles). Medium GLC (green), Medium GG (yellow), Medium Oct (red). For each media the naïve subset is represented at the left and the memory subset at the right side. The bars represent the median value and the confidence interval (CI) at 95%. *: $p<0,05$ with p being calculated using Kruskal-Wallis test with Dunn's multiple comparisons test. Number of samples: CNT=7; RA=7. Abbreviations: Stim (Stimulated).

ROS productions in the CNT group are similar in both subsets being just slightly higher in naïve $CD4^+$ T cells than in memory $CD4^+$ T cells in the Glc and GG media, being the contrary true for the Oct medium. In the RA group, in general, the levels of ROS production are apparently lower when compared with the CNTs but, on the other hand, it could be suggested that the differences between naïve and memory $CD4^+$ T cells regarding this parameter are much more clear, with the memory subset exhibiting higher levels of ROS production. These apparent differences between the 2 subsets could indicate that, in the RA context, the bioenergetic and biosynthetic needs of naïve and memory $CD4^+$ T cells are more dissimilar than in healthy individuals, being the memory subset subject to a higher activation state supported by the disease than their naïve counterparts.

Regarding the results obtained in PD-1 expression, they suggest a higher level of expression in memory $CD4^+$ T cells from both groups, being the differences more pronounced in the RA group and transversal to all three media. In addition, the data from lipid peroxidation levels show, again, that the differences between the $CD4^+$ T cells subsets are apparently higher in RA group, being the memory $CD4^+$ T cells the ones that have higher levels of lipid peroxidation. Together these results suggest that both the apoptosis and autophagy machinery are more activated in the memory subset of $CD4^+$ T cells, being the difference between the two subsets much higher, in all media, in the RA group, probably linked to the specificity of the disease context and its metabolic and biosynthetic consequences in $CD4^+$ T cells.

Overall, it could be said that memory $CD4^+$ T cells were in a higher activation state than the naïve ones. This observation was expected due to the co-stimulation that was given to the cells in the *in vitro* culture which, as stated in the Introduction, will have a higher and faster impact in the memory subset, being this related with the ultimate goal of memory T cell, the counter-attack of a repeated antigen (Delves *et al.*, 2017). This higher activation state is reflected in the exacerbated expression of all metabolic enzymes, but also in the stress indicators analyzed here, which were in accordance to the known upregulation of glycolysis, as well as OXPHOS, in memory $CD4^+$ T cells upon activation (Yanes and Goronzy, 2016).

Although some important insights are given by the data presented here, the differences between naïve and memory $CD4^+$ T cells are, undoubtedly, a source of new questions regarding the immunometabolism modulation of $CD4^+$ T cells in the context of the autoimmune disorders, namely RA. Further developments regarding this matter will

be of utmost importance to advance in this field of research, being the results shown here a significant motivation to future exploration.

# 4 Conclusions

Our initial research objective was the understanding of how the metabolism of $CD4^+$ T cells could be modulated by different environment's provided to the cells and, in that way, alter the mode they exert their effector functions in the context of RA.

In this study we were able to see that $CD4^+$ T cells, both from RA and CNT, maintain their avidity of glucose even when this substrate is presented at scarce levels. The results suggest an increment in the glycolytic index in media where glucose was scarce, which was accompanied by an apparent increase of the expression of the enzyme LDHA, which is key for sustaining the glycolytic flux. We could presume that this represents an adaptation of the $CD4^+$ T cells to respond the stress imposed by the environment of low glucose. In the medium where initial glucose provided was lower (1.1 mM), $CD4^+$ T cells showed no capacity to utilize octanoate as an alternative substrate which is suggested by the lower survival and viability, but also in the almost null effector capacity, as demonstrated by the inability to produce most cytokines.

Together, our results demonstrate that the metabolic adaptation of $CD4^+$ T cells to the distinct substrates' combination is highly dependent of glucose availability to fulfil their bioenergetic and biosynthetic needs and that glutamine plays an important role in overall $CD4^+$ T cells metabolism. Contradicting the current purely oxidative and fatty acids sustainable portrait suggested for $CD4^+$ T cells in RA, we could reiterate the glycolytic preponderance for these cells maintenance and the incapacity of these cells to exert their effector function in an environment where glucose availability is low and fatty acids are present, reflecting the inability of $CD4^+$ T cells to use these latter substrates to effectively compensate the lack of glucose in what concerns to their own survival and, consequently, cytokine production. With the objective of simplifying the interpretation of our results and corroborating the conclusions offered here, **Tables 4** and **5**, present the multiple comparison between CNT and RA groups, between media inside the same group and, additionally, between inhibitory conditions in the same medium and group.

In general, the major conclusion originated from this work could only foment the interest and motivation to further characterize $CD4^+$ T cells in the specific context of RA. From our side, we hope that this research project could contribute to get a clearer vision of $CD4^+$ T cells adaptation in different substrate availability contexts and, ultimately, to help reaching the ultimate aim of being capable to control the negative impact that some immune cells' functions have in certain pathologies as is the case of $CD4^+$ T cells in RA.

**Table 4 -** Resume of the results obtained in the different parameters analyzed in $CD4^+$ T cells, including the comparation between CNT and RA group in the different media provided to the cells and, in the Stim conditions for each group, the comparation between the different media.

| Parameter | CNT vs RA (Stim) | | | CNT | RA |
|---|---|---|---|---|---|
| | | | | Media (Stim) | Media (Stim) |
| | Glc | GG | Oct | Glc vs GG vs Oct | Glc vs GG vs Oct |
| Glycolytic Index | = | = | = | Glc << GG = Oct | Glc << GG = Oct |
| TCA Index | = | = | = | Glc = GG = Oct | Glc = GG = Oct |
| Glucose Uptake | RA | | | | |
| Palmitate Uptake | RA | | | | |
| Mitochondrial Potential | CNT | | | | |
| LDHA | CNT | CNT | CNT | Glc < GG < Oct | Glc < GG = Oct |
| PDH | CNT | RA | = | Glc > GG < Oct | Glc < GG = Oct |
| GDH | = | = | = | Glc = GG = Oct | Glc = GG = Oct |
| SDHA | = | CNT | CNT | Glc < GG = Oct | Glc < GG = Oct |
| ROS Production | RA | RA | RA | Glc = GG = Oct | Glc > GG = Oct |
| PD-1 | = | = | = | Glc < GG = Oct | Glc < GG = Oct |
| Lipid Peroxidation | CNT | CNT | CNT | Glc = GG = Oct | Glc = GG = Oct |
| Annexin V (apoptosis) | = | CNT | CNT | Glc << GG >> Oct | Glc << GG >> Oct |
| Cell Viability | CNT | CNT | CNT | Glc = GG > Oct | Glc = GG > Oct |
| Cell Proliferation | CNT | CNT | CNT | Glc = GG > Oct | Glc > GG < Oct |
| IL-2 | RA | RA | = | Glc << GG >> Oct | Glc << GG >> Oct |
| IL-4 | = | RA | = | Glc = GG = Oct | Glc < GG > Oct |
| IL-5 | = | = | = | Glc = GG > Oct | Glc = GG > Oct |
| IL-6 | = | RA | RA | Glc = GG = Oct | Glc << GG >> Oct |
| IL-9 | RA | RA | = | Glc << GG >> Oct | Glc < GG >> Oct |
| IL-13 | RA | RA | = | Glc << GG >> Oct | Glc = GG >> Oct |
| IL-17A | RA | RA | = | Glc = GG = Oct | Glc << GG >> Oct |
| IL-17F | = | RA | = | Glc << GG >> Oct | Glc << GG >> Oct |
| IL-21 | = | = | = | Glc = GG = Oct | Glc = GG = Oct |
| IL-22 | = | RA | = | Glc < GG >> Oct | Glc < GG >> Oct |
| IFN-y | = | = | = | Glc = GG >> Oct | Glc = GG >> Oct |
| TNF-a | RA | = | = | Glc = GG >> Oct | Glc = GG >> Oct |
| IL-10 | = | = | = | Glc << GG >> Oct | Glc << GG >> Oct |

**Table 5 -** Resume of the results obtained in the different parameters analyzed in $CD4^+$ T cells, including the comparation, inside each group (CNT and RA), of the variation between: Stim and Nstim; FX11 and Stim; Rot and Stim.

| Parameter | CNT | | | | | | | | | RA | | | | | | | | |
|---|---|---|---|---|---|---|---|---|---|---|---|---|---|---|---|---|---|---|
| | Stim vs Nstim | | | FX11 vs Stim | | | Rot vs Stim | | | Stim vs Nstim | | | FX11 vs Stim | | | Rot vs Stim | | |
| | Glc | GG | Oct | Glc | GG | Oct | Glc | GG | Oct | Glc | GG | Oct | Glc | GG | Oct | Glc | GG | Oct |
| Glycolytic Index | ↑↑ | ↑ | - | ↑ | ↑ | ↓↓ | ↑ | ↑ | ↑ | ↑↑ | ↑ | - | ↑ | ↑ | ↓↓ | ↑ | ↑ | ↑ |
| TCA Index | ↑ | ↑ | ↑ | - | ↓ | ↓ | ↓ | ↓↓ | ↓↓ | ↑ | ↑ | ↑ | ↓ | ↓ | ↓ | ↓ | ↓↓ | ↓↓ |
| Glucose Uptake | | | | | | | | | | ↑ | | | ↓↓ | | | ↓ | | |
| Palmitate Uptake | | | | | | | | | | ↑ | | | ↑↑ | | | ↓ | | |
| Mitochondrial Potential | | | | | | | | | | ↓ | | | ↑↑ | | | ↑ | | |
| LDHA | ↑ | ↑ | ↑ | ↑ | = | ↓ | ↓ | ↓ | ↓ | ↑ | ↑ | ↑ | ↑ | = | = | ↓ | ↓ | ↓ |
| PDH | ↑ | ↑ | ↑ | ↑ | ↑ | ↓ | ↓ | ↓ | ↓ | ↑ | ↑ | ↑ | ↑ | ↑ | = | ↓ | ↓ | ↓ |
| GDH | ↓ | ↑ | ↑ | = | = | = | = | = | ↓ | = | ↑ | ↑ | = | = | = | = | = | = |
| SDHA | = | ↑ | ↑ | ↑ | = | ↓ | ↓ | ↓ | ↓ | ↑ | ↑ | ↑ | ↑ | = | = | ↓ | ↓ | ↓ |
| ROS Production | ↑ | ↑ | ↑ | = | = | = | = | = | ↑ | ↑ | ↑ | ↑ | = | = | = | = | = | = |
| PD-1 | ↑ | ↑ | ↑ | ↑ | = | = | ↓ | ↓ | ↓ | ↑ | ↑ | ↑ | = | = | = | ↓ | ↓ | ↓ |
| Lipid Peroxidation | ↑ | ↑ | ↑ | = | = | ↑ | ↑ | = | ↑ | ↑ | ↑ | ↑ | = | = | ↑ | = | = | = |
| Annexin V (apoptosis) | ↑ | = | ↑ | | | | | | | = | ↑ | = | | | | | | |
| Cell Viability | ↑ | ↑ | ↑ | ↓ | ↓↓ | ↓↓ | ↓ | ↓↓ | ↓↓ | ↑ | = | = | ↓ | ↓↓ | ↓↓ | ↓ | ↓↓ | ↓↓ |
| Cell Proliferation | = | = | = | | | | | | | = | ↓ | = | | | | | | |
| IL-2 | = | ↑ | = | ↓↓ | ↓↓ | ↓↓ | = | = | = | ↑ | ↑↑ | = | ↓↓ | ↓↓ | ↓↓ | = | = | = |
| IL-4 | = | = | = | = | = | = | = | = | = | = | = | = | = | = | = | = | = | = |
| IL-5 | ↑ | ↑ | = | ↓↓ | ↓↓ | = | ↓↓ | ↓↓ | = | ↑ | ↑ | = | ↓↓ | ↓↓ | = | ↓↓ | ↓↓ | = |
| IL-6 | = | = | = | = | ↓↓ | ↓↓ | = | ↓↓ | ↓↓ | ↑ | = | = | ↓↓ | ↓↓ | ↓↓ | ↓ | ↓↓ | ↓↓ |
| IL-9 | ↑ | ↑↑ | = | ↓↓ | ↓↓ | = | ↓↓ | ↓↓ | = | ↑↑ | ↑↑ | = | ↓↓ | ↓↓ | = | ↓↓ | ↓↓ | = |
| IL-13 | ↑ | ↑ | = | ↓↓ | ↓↓ | ↓↓ | ↓ | ↓↓ | ↓↓ | ↑↑ | ↑↑ | = | ↓↓ | ↓↓ | ↓↓ | ↓↓ | ↓↓ | ↓↓ |
| IL-17A | ↑ | ↑ | = | ↓↓ | ↓↓ | ↓↓ | ↓↓ | = | ↓↓ | ↑ | ↑ | = | ↓↓ | ↓↓ | ↓↓ | ↓↓ | ↓↓ | ↓↓ |
| IL-17F | = | ↑ | = | ↓ | ↓↓ | = | ↓↓ | ↓↓ | = | = | ↑ | = | ↓↓ | ↓↓ | = | ↓↓ | ↓↓ | = |
| IL-21 | = | = | = | = | = | = | = | = | = | = | = | = | = | = | = | = | = | = |
| IL-22 | ↑ | ↑↑ | = | ↓↓ | ↓↓ | ↓ | ↓ | ↓ | ↓ | ↑↑ | ↑↑ | = | ↓↓ | ↓↓ | ↓↓ | ↓↓ | ↓↓ | ↓↓ |
| IFN-y | ↑↑ | ↑ | = | ↓↓ | ↓↓ | ↓↓ | ↓ | ↓ | ↓↓ | ↑↑ | ↑ | = | ↓↓ | ↓↓ | ↓↓ | ↓↓ | = | ↓↓ |
| TNF-a | ↑↑ | ↑↑ | = | ↓↓ | ↓↓ | = | ↓↓ | ↓ | = | ↑↑ | ↑↑ | = | ↓↓ | ↓↓ | ↓ | ↓↓ | ↓ | ↓ |
| IL-10 | ↑ | ↑↑ | = | ↓↓ | ↓↓ | = | ↓↓ | ↓↓ | = | ↑ | ↑↑ | = | ↓↓ | ↓↓ | ↓ | ↓↓ | ↓↓ | ↓ |

# 5 References


Andersen, M. H. *et al.* (2006) 'Cytotoxic T cells', *Journal of Investigative Dermatology*. Elsevier Masson SAS, 126(1), pp. 32–41. doi: 10.1038/sj.jid.5700001.

Annunziato, F. and Romagnani, S. (2009) 'Heterogeneity of human effector CD4+ +T cells', *Arthritis Research and Therapy*, 11(6), pp. 1–8. doi: 10.1186/ar2843.

Ayala, A., Muñoz, M. F. and Argüelles, S. (2014) 'Lipid Peroxidation: Production, Metabolism, and Signaling Mechanisms of Malondialdehyde and 4-Hydroxy-2-Nonenal', *Hindawi Publishing Corporation Oxidative Medicine and Cellular Longevity*, p. 31. doi: 10.1155/2014/360438.

Byersdorfer, C. A. *et al.* (2013) 'Effector T cells require fatty acid metabolism during murine graft-versus-host disease', *Blood*, 122(18), pp. 3230–3237. doi: 10.1182/blood-2013-04-495515.

Campbell, A. *et al.* (2018) *Law of conservation of energy*. Available at: https://energyeducation.ca/encyclopedia/Law_of_conservation_of_energy (Accessed: 29 February 2020).

Carvalheiro, H. *et al.* (2015) 'CD8+ T cell profiles in patients with rheumatoid arthritis and their relationship to disease activity', *Arthritis and Rheumatology*, 67(2), pp. 363–371. doi: 10.1002/art.38941.

Carvalheiro, H. M. (2014) 'The role of CD8 T cells in the pathogenesis of rheumatoid arthritis', *Estudo Geral UC*. Available at: http://hdl.handle.net/10316/26119.

Chemin, K., Gerstner, C. and Malmström, V. (2019) 'Effector functions of CD4+ T cells at the site of local autoimmune inflammation-lessons from rheumatoid arthritis', *Frontiers in Immunology*, 10(March), pp. 1–15. doi: 10.3389/fimmu.2019.00353.

Cooper, G. S., Bynum, M. L. K. and Somers, E. C. (2009) 'Recent Insights in the Epidemiology of Autoimmune Diseases: Improved Prevalence Estimates and Understanding of Clustering of Diseases', *Journal of Autoimmunity*, 33(3–4), pp. 197–207. doi: 10.1016/j.jaut.2009.09.008.Recent.

Couper, K. N., Blount, D. G. and Riley, E. M. (2008) 'IL-10: The Master Regulator of Immunity to Infection', *The Journal of Immunology*, 180(9), pp. 5771–5777. doi: 10.4049/jimmunol.180.9.5771.

Croft, M. (2009) 'The role of TNF superfamily members in T-cell function and diseases', *Nat Rev Immunology*, 9(4), pp. 271–285. doi: 10.1038/nri2526.

Delves, P. J. *et al.* (2017) *Roitt's Essential Immunology*. 13th Editi. Wiley Blackwell.

Dennis, M. K. *et al.* (2012) 'Postranscriptional control of T cell effector function by aerobic glycolysis', *Cell*, 127(6), pp. 358–366. doi: 10.1016/j.jsbmb.2011.07.002.Identification.

Dienz, O. and Rincon, M. (2009) 'The effects of IL-6 on CD4 T cell responses', *Clinical Immunology*, 130(1), pp. 27–33. doi: 10.1016/j.clim.2008.08.018.

Dingjan, I. *et al.* (2016) 'Lipid peroxidation causes endosomal antigen release for cross-presentation', *Scientific Reports*. Nature Publishing Group, 6(July 2015), pp. 1–12. doi: 10.1038/srep22064.

Droeser, R. A. *et al.* (2013) 'Clinical impact of programmed cell death ligand 1 expression in colorectal cancer', *European Journal of Cancer*. Elsevier Ltd, 49(9), pp. 2233–2242. doi: 10.1016/j.ejca.2013.02.015.

Dupage, M. and Bluestone, J. A. (2016) 'Harnessing the plasticity of CD4+ T cells to treat immune-mediated disease', *Nature Reviews Immunology*. Nature Publishing Group, 16(3), pp. 149–163. doi: 10.1038/nri.2015.18.

Elkon, K. and Casali, P. (2008) 'Nature and functions of autoantibodies', *Nature Clinical Practice Rheumatology*, 4(9), pp. 491–498. doi: 10.1038/ncprheum0895.

Geginat, J. *et al.* (2016) 'Reverse plasticity: TGF-β and IL-6 induce Th1-to-Th17-cell transdifferentiation in the gut', *European Journal of Immunology*, 46(10), pp. 2306–2310. doi: 10.1002/eji.201646618.

Glick, D., Barth, S. and Macleod, K. F. (2010) 'Autophagy : cellular and molecular mechanisms', *Journal of Pathology*, 221(1), pp. 3–12. doi: 10.1002/path.2697.Autophagy.

Gogvadze, V., Zhivotovsky, B. and Orrenius, S. (2010) 'The Warburg effect and mitochondrial stability in cancer cells', *Molecular Aspects of Medicine*. Elsevier Ltd, 31(1), pp. 60–74. doi: 10.1016/j.mam.2009.12.004.

Günther, H. (2013) *NMR Spectroscopy: Basic Principles, Concepts and Applications in Chemistry*. 3rd Editio. Weinheim: Wiley-VCH.

Guo, Q. *et al.* (2018) 'Rheumatoid arthritis: Pathological mechanisms and modern pharmacologic therapies', *Bone Research*. Springer US. doi: 10.1038/s41413-018-0016-9.

Vander Heiden, M. G., Cantley, L. C. and Thompson, C. B. (2009) 'The Metabolic Requirements of Cell Proliferation', *Science*, 324(5930), pp. 1029–1033. doi: 10.1126/science.1160809.

Hradilkova, K. *et al.* (2019) 'Regulation of Fatty Acid Oxidation by Twist 1 in the Metabolic Adaptation of T Helper Lymphocytes to Chronic Inflammation', *Arthritis and Rheumatology*, 71(10), pp. 1756–1765. doi: 10.1002/art.40939.

Klein, K., Karouzakis, E. and Gay, S. (2018) 'Rheumatoid Arthritis and Epigenetics', in *The Epigenetics of Autoimmunity*, pp. 149–166. doi: 10.1016/B978-0-12-809912-4.00007-6.

Klocke, K., Holmdahl, R. and Wing, K. (2017a) 'CTLA-4 expressed by FOXP3+ regulatory T cells prevents inflammatory tissue attack and not T-cell priming in arthritis', *Immunology*, 152(1), pp. 125–137. doi: 10.1111/imm.12754.

Klocke, K., Holmdahl, R. and Wing, K. (2017b) 'CTLA-4 expressed by FOXP3+ regulatory T cells prevents inflammatory tissue attack and not T-cell priming in

arthritis', *Immunology*, 152(1), pp. 125–137. doi: 10.1111/imm.12754.

Konkel, J. E. *et al.* (2010) 'PD-1 signalling in CD4+ T cells restrains their clonal expansion to an immunogenic stimulus, but is not critically required for peptide-induced tolerance', *Immunology*, 130(1), pp. 92–102. doi: 10.1111/j.1365-2567.2009.03216.x.

Liberti, M. V. and Locasale, J. W. (2016) 'The Warburg Effect: How Does it Benefit Cancer Cells?', *Trends in Biochemical Sciences*. Elsevier Ltd, 41(3), pp. 211–218. doi: 10.1016/j.tibs.2015.12.001.

Lubberts, E. (2010) 'Th17 cytokines and arthritis', *Seminars in Immunopathology*, pp. 43–53. doi: 10.1007/s00281-009-0189-9.

Luckheeram, R. V. *et al.* (2012) 'CD4 +T cells: Differentiation and functions', *Clinical and Developmental Immunology*, 2012. doi: 10.1155/2012/925135.

Lunt, S. Y. and Vander Heiden, M. G. (2011) 'Aerobic Glycolysis: Meeting the Metabolic Requirements of Cell Proliferation', *Annual Review of Cell and Developmental Biology*, 27(1), pp. 441–464. doi: 10.1146/annurev-cellbio-092910-154237.

MacLeod, M. K. L. *et al.* (2009) 'CD4 memory T cells: what are they and what can they do?', *Semin Immunollogy*, 21(2), pp. 53–61. doi: doi:10.1016/j.smim.2009.02.006.

McInnes, I. B. and Schett, G. (2017) 'Pathogenetic insights from the treatment of rheumatoid arthritis', *The Lancet*. Elsevier Ltd, pp. 2328–2337. doi: 10.1016/S0140-6736(17)31472-1.

Murphy, K. and Weaver, C. (2017) *Janeway's Immunobiology*. 9th Editio. New York and London: Garland Science.

Natoli, G. and Ostuni, R. (2019) 'Adaptation and memory in immune responses', *Nature Immunology*. Springer US, 20(7), pp. 783–792. doi: 10.1038/s41590-019-0399-9.

Negre-Salvayre, A. *et al.* (2010) 'Pathological aspects of lipid peroxidation', *Free Radical Research*, 44(10), pp. 1125–1171. doi: 10.3109/10715762.2010.498478.

Nelson, D. L. and Cox, M. M. (2009) *Lehninger Principles of Biochemistry*. 6th Editio. New York: W. H. Freeman and Company.

Ota, Y. *et al.* (2016) 'Effect of nutrient starvation on proliferation and cytokine secretion of peripheral blood lymphocytes', *Molecular and Clinical Oncology*, 4(4), pp. 607–610. doi: 10.3892/mco.2016.763.

Otto Warburg, B., Wind, F. and Negelein, N. (1926) 'The metabolism of tumours in the body.', *Biochem. Z. Biochem. Z. Biochem. Z.. Biol. Chem*, 309(2), pp. 397–519. Available at: https://www.ncbi.nlm.nih.gov/pmc/articles/PMC2140820/pdf/519.pdf.

Ouyang, W. *et al.* (2011) 'Regulation and Functions of the IL-10 Family of Cytokines in Inflammation and Disease', *Annual Review of Immunology*, 29(1), pp. 71–109. doi: 10.1146/annurev-immunol-031210-101312.

Owen, J. *et al.* (2012) *Kuby Immunology*. 7th Editio. New York: W. H. Freeman and Company. doi: 10.1007/s13398-014-0173-7.2.

Parkin, J. and Cohen, B. (2001) 'An overview of the immune system', *The Lancet*, 357, pp. 1777–1789. doi: 10.1016/S0140-6736(00)04904-7.

Pearce, E. L. *et al.* (2013) 'Fueling immunity: Insights into metabolism and lymphocyte function', *Science*, 342(6155). doi: 10.1126/science.1242454.

Quintin, J. *et al.* (2014) 'Innate immune memory: Towards a better understanding of host defense mechanisms', *Current Opinion in Immunology*. Elsevier Ltd, 29(1), pp. 1–7. doi: 10.1016/j.coi.2014.02.006.

Rajeshkumar, N. V. *et al.* (2014) 'Therapeutic targeting of the Warburg effect in pancreatic cancer relies on an absence of p53 function', *Cancer Research*, 75(16), pp. 3355–3364. doi: doi:10.1158/0008-5472.CAN-15-0108.

Reader, J. R. *et al.* (2003) 'Interleukin-9 induces mucous cell metaplasia independent of inflammation', *American Journal of Respiratory Cell and Molecular Biology*, 28(6), pp. 664–672. doi: 10.1165/rcmb.2002-0207OC.

Renner, K. *et al.* (2015) 'Metabolic plasticity of human T cells: Preserved cytokine production under glucose deprivation or mitochondrial restriction, but 2-deoxy-glucose affects effector functions', *European Journal of Immunology*, 45(9), pp. 2504–2516. doi: 10.1002/eji.201545473.

Reuschenbach, M., Von Knebel Doeberitz, M. and Wentzensen, N. (2009) 'A systematic review of humoral immune responses against tumor antigens', *Cancer Immunology, Immunotherapy*, 58(10), pp. 1535–1544. doi: 10.1007/s00262-009-0733-4.

Rodeghero, R. *et al.* (2013) 'Location of CD4+ T cell Priming Regulates the Differentiation of Th1 and Th17 cells and their Contribution to Arthritis', *Journal Immunology*, 190(11), pp. 1–7. doi: 10.4049/jimmunol.1203045.

Sakaguchi, S. *et al.* (2010) 'FOXP3 + regulatory T cells in the human immune system', *Nature Reviews Immunology*. Nature Publishing Group, 10(7), pp. 490–500. doi: 10.1038/nri2785.

Salvador, G. *et al.* (2005) 'P53 Expression in Rheumatoid and Psoriatic Arthritis Synovial Tissue and Association With Joint Damage', *Annals of the Rheumatic Diseases*, 64(2), pp. 183–187. doi: 10.1136/ard.2004.024430.

Souto-Carneiro, M. *et al.* (2020) 'Proinflammatory profile of autoimmune CD8+ T cells relies on increased LDHA activity and aerobic glycolysis', Arthritis and Rheumatology (in press). doi: 10.1002/art.41420.

Sun, L., Fu, J. and Zhou, Y. (2017) 'Metabolism controls the balance of Th17/T-regulatory cells', *Frontiers in Immunology*, 8(NOV), pp. 1–12. doi: 10.3389/fimmu.2017.01632.

Tobón, G. J., Izquierdo, J. H. and Canas, C. A. (2013) 'B lymphocytes: Development, tolerance, and their role in autoimmunity - Focus on systemic lupus erythematosus',

*Autoimmune Diseases*, 2013((Tobon, Izquierdo, Canas) Department of Internal Medicine, Division of Rheumatology, ICESI University School of Medicine, Cra 98 No. 18-49, Cali, Colombia), p. 827254. doi: 10.1155/2013/827254.

Tripmacher, R. *et al.* (2008) 'Human CD4+ T cells maintain specific functions even under conditions of extremely restricted ATP production', *European Journal of Immunology*, 38(6), pp. 1631–1642. doi: 10.1002/eji.200738047.

Tsokos, G. C. (2016) 'Metabolic control of arthritis: Switch pathways to treat', *Science Translational Medicine*, 8(331), pp. 8–11. doi: 10.1126/scitranslmed.aaf4953.

Wahl, D. R. *et al.* (2010) 'Characterization of the metabolic phenotype of chronically activated lymphocytes', *Lupus*, 19(13), pp. 1492–1501. doi: 10.1177/0961203310373109.

Weyand, C. M. and Goronzy, J. J. (2017) 'Immunometabolism in early and late stages of rheumatoid arthritis', *Nature Reviews Rheumatology*. Nature Publishing Group, 13(5), pp. 1–11. doi: 10.1038/nrrheum.2017.49.

Weyand, C. M. and Goronzy, J. J. (2018) 'A Mitochondrial Checkpoint in Autoimmune Disease', *Cell Metabolism*, 28(2), pp. 185–186. doi: 10.1016/j.cmet.2018.07.014.

Weyand, C. M., Shen, Y. and Goronzy, J. J. (2018) 'Redox-sensitive signaling in inflammatory T cells and in autoimmune disease', *Free Radical Biology and Medicine*. Elsevier B.V., 125, pp. 36–43. doi: 10.1016/j.freeradbiomed.2018.03.004.

Weyand, C. M., Zeisbrich, M. and Goronzy, J. J. (2017) 'Metabolic signatures of T-cells and macrophages in rheumatoid arthritis', *Current Opinion in Immunology*, 46, pp. 112–120. doi: 10.1016/j.coi.2017.04.010.

World Health Organization (2020) *Arthritic preponderance*. Available at: who.int/chp/topics/rheumatic/en (Accessed: 2 April 2020).

Wynn, T. A. (2003) 'IL-13 Effector functions', *Annual Review of Immunology*, 21(1), pp. 425–456. doi: 10.1146/annurev.immunol.21.120601.141142.

Yanes, R. E. and Goronzy, J. J. (2016) 'Regulation of metabolic pathways in CD4 T memory cell responses of older individuals', *The Journal of Immunology*, 196(1), p. 204.4. Available at: http://www.jimmunol.org/content/196/1_Supplement/204.4.abstract.

Yang, Z. *et al.* (2013) 'Phosphofructokinase deficiency impairs atp generation, autophagy, and redox balance in rheumatoid arthritis T cells', *Journal of Experimental Medicine*, 210(10), pp. 2119–2134. doi: 10.1084/jem.20130252.

Yang, Z. *et al.* (2016) 'Restoring oxidant signaling suppresses proarthritogenic T cell effector functions in rheumatoid arthritis', *Science Translational Medicine*, 8(331), pp. 1–14. doi: 10.1126/scitranslmed.aad7151.

Yatim, K. M. and Lakkis, F. G. (2015) 'A brief journey through the immune system', *Clinical Journal of the American Society of Nephrology*, 10(7), pp. 1274–1281. doi:

10.2215/CJN.10031014.

Zhang, J.-M. and An, J. (2007) ‘Cytokines, Inflammation and Pain’, *Int Anesthesiol Clin.*, 45(2), pp. 27–37. doi: 10.1097/AIA.0b013e318034194e.

Zhu, J. and Paul, W. E. (2009) ‘CD4 T cells : fates , functions , and faults ASH 50th anniversary review CD4 T cells : fates , functions , and faults’, *Immunobiology*, 112(5), pp. 1557–1569. doi: 10.1182/blood-2008-05-078154.

Zu, X. L. and Guppy, M. (2004) ‘Cancer metabolism: Facts, fantasy, and fiction’, *Biochemical and Biophysical Research Communications*, 313(3), pp. 459–465. doi: 10.1016/j.bbrc.2003.11.136.